technische universität
dortmund

2020

SCIENTIFIC HIGHLIGHTS

Annual Report

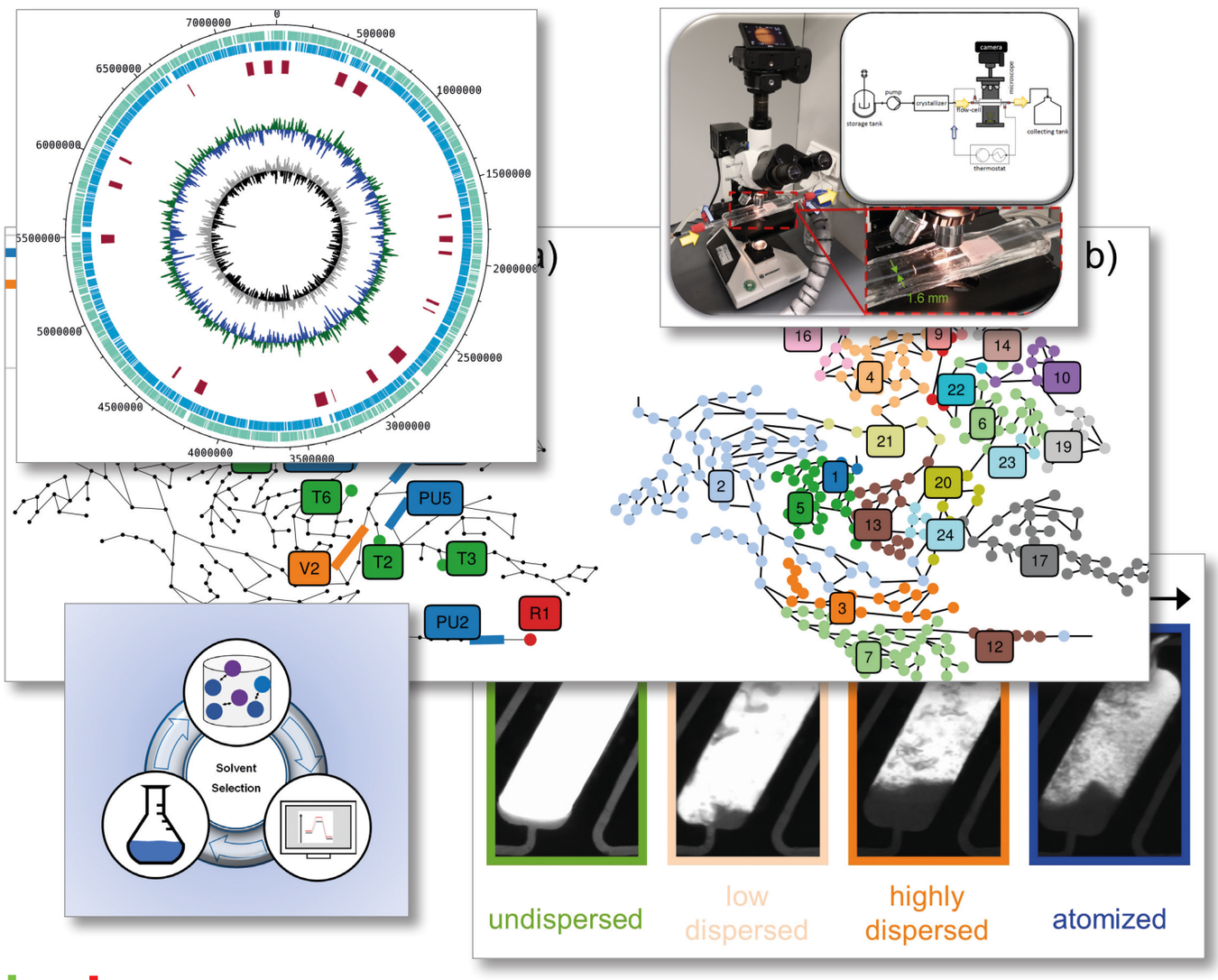

Fakultät Bio- und
Chemieingenieurwesen

Content

Content

Department of BCI

Preface

Dear Reader,

I proudly present the 11th volume of the annual Scientific Highlights of the Department of Bio- and Chemical Engineering of the TU Dortmund University. It has become a more or less loved tradition to present our annual “greatest hits” in this format. The here presented excellent scientific achievements of our various research groups are particularly remarkable since they have been realized under the difficult conditions of the COVID 19 epidemic. Due to combined efforts of all students, technicians and teachers, we have been successful in keeping up the teaching and researching program. The present Scientific Highlights are evidence for this. This year has also given us substantial reinforcement in our scientific manpower. We welcome our new colleague Sergio Lucia as Professor for Process Automation Systems and wish him and us a fruitful and cooperative joint future.
As always, I’d like to express my hope that reading these Highlights will be of interest not only to the members of our faculty but also to our present and maybe future collaboration partners in academia and industry.

Enjoy the reading

Prof. Joerg Tiller

Equipment Design (AD)

Micro-Computed Tomography for the 3D Investigation of Multiphase Flow in Capillaries

CNN-based image analysis approach allows for 3D imaging of droplet formation

Julia Schuler, Laura Maria Neuendorf, Kai Petersen, Norbert Kockmann

In the chemical and pharmaceutical industry, droplet-based microfluidics is known to be advantageous, especially when it comes to smaller production quantities or highly specialized products. Processes performed in microfluidic apparatuses benefit from laminar flow regimes and high surface to volume ratios, which makes processes safer and easier to predict and control. To increase the physical understanding of droplet generation, X-ray based micro-computed tomography is applied. Micro-computed tomography (CT) is a 3D, non-invasive imaging approach offering high spatial resolutions.

For a full CT-scan, acquiring X-ray projection images of the sample from different angular positions, at least covering an angle range of 180°, is necessary. Furthermore, successful reconstruction of a set of X-ray projections to a 3D volume requires static samples, as the movement of the sample leads to undesired artifacts. A scanning protocol based on post-acquisition synchronization is used to apply micro-computed tomography for the investigation of periodic droplet formation. Multiple projections are acquired for each angular position, instead of one. In the next step, only one particular X-ray projection for each angular position is selected resulting in a set of projection images showing the emerging droplet in a quasi-static state. The selection of the particular X-ray projection per angular position is based on image segmentation using a convolutional neural network (CNN). Following this, reconstruction of the X-ray projections to a 3D volume and extraction of the droplet/PDMS interface at different times is possible, see Figure1.

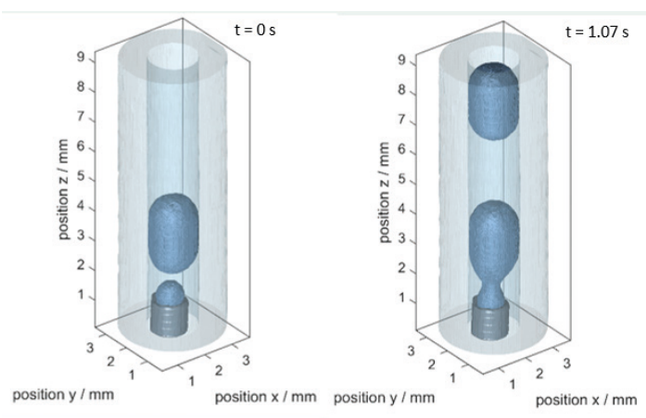

Figure 1: Surface representation of an emerging droplet and detached droplet for a volume flow rate ratio ($\Phi = \frac{\dot{V}_{water}}{\dot{V}_{PDMS}} = 0.67$) and Capillary number ($Ca = \frac{\mu_{PDMS} u_{PDMS}}{\sigma_{PDMS,water}} = 8.6 \cdot 10^{-4}$) at different times (cf.[1]).

3D scans are performed for water droplets in silicone oil (PDMS) generated in a co-flow configuration. Viscosity of the continuous phase and volume flow rates are varied to investigate the effect of Capillary number and volume flow rate ratio (V-water/V-PDMS) on droplet formation and final droplet sizes. It was found that final droplet size increases with increasing flow rate ratio and decreasing capillary number, see Figure 2.

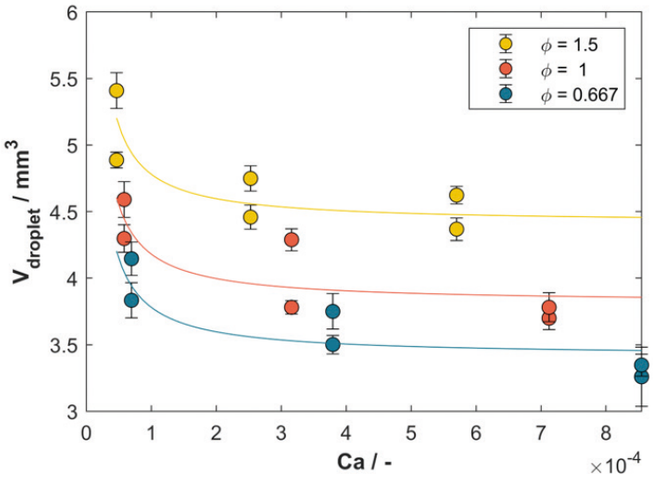

Figure 2: Resulting droplet volume as a function of Φ and *Ca* (cf.[1]).

Contact:
julia.schuler@tu-dortmund.de
norbert.kockmann@tu-dortmund.de

Publications:
[1] J. Schuler, L.M. Neuendorf, K. Petersen, N. Kockmann, AIChE J 67, e17111 (2020).
[2] J. Schuler, L.M. Neuendorf, K. Petersen, N. Kockmann, I*CNMM*2020-1061, vol. 2020, p. V001T16A004 (2020).

Design of an Automated Reagent-Dispensing System for Reaction Screening and Validation

Customized lab robot performs DNA-tagged multi-component reaction

Jens Bobers, Mateja Klika Škopić, Robin Dinter, Piriyanth Sakthithasan, Laura Neukirch, Christian Gramse, Ralf Weberskirch, Andreas Brunschweiger, Norbert Kockmann

Lab automation strategies have a vast potential for accelerating discovery of active pharmaceutical ingredients. Automating repetitive procedures can support chemists in optimizing reaction conditions. Particularly, the technology of DNA-encoded libraries (DELs) may benefit from automation techniques, since translation of chemical reactions to DNA-tagged reactants often requires screening and evaluation of large numbers of reactants. Here, we describe a portable, automated system for reagent dispensing that was designed from open-source materials. The performance of a micelle-mediated Povarov reaction to DNA-tagged hexahydropyrroloquinolines shows the potential of the robotic system for high throughput experimentation.

The basic design of the **A**utomated **D**osage **S**ystem (ADoS) was adapted from an open-source 3D printer design, whose original printer head was substituted by a custom injection unit consisting of a gas chromatograph (GC) syringe moved by a stepper motor. For connectors and more complex parts of the robot 3D printing was utilized. Figure 1 presents the final design of the robotic system (A) and the modularized workspace (B), in which standardized operation plates can be placed in. These operation plates represent different tasks performed by the robot as continuous syringe cleaning (a), storage of stock solutions (b), and performing reactions in 96-well plates (c). The GC syringe was calibrated to ensure accurate and precise dispensing volumes from 1 µL up to 50 µL.

The ADoS was applied to pipetting reactants for a Povarov three-component reaction from DNA-tagged aldehydes, olefins, and anilines to DNA-tagged hexahydropyrroloquinolines. A surface-active polymer was used to mediate the reaction between DNA-tagged aldehydes, the hydrophobic anilines, and the olefin. Decreasing polymer concentration from 140 µM to 3.5 µM resulted in product yield dropping from 46 % to 15 %, which reveals reaction progress even for concentration near by the critical micelle concentration of 1 µM. The results confirmed that the ADoS reproduced the manually pipetted reactions faithfully and reached yields above 90 % with a polymer concentration of 500 µM for all investigated co-solvents.

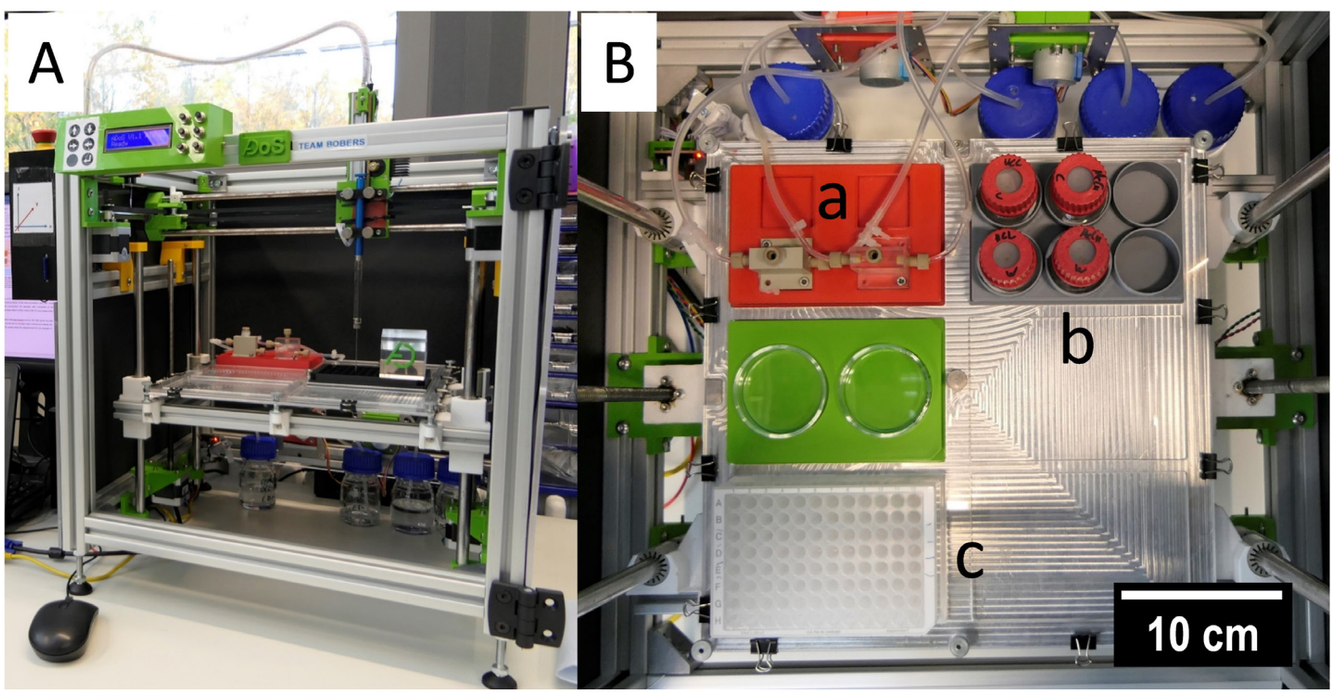

Figure 1: Setup of the ADoS (A) and modular workspace (B) consisting of continuous cleaning station (a), big flasks for stock solutions (b), and 96-well plate (c).

Publications:
J. Bobers, M. Klika Škopić, R. Dinter, P. Sakthithasan, L. Neukirch, C. Gramse, R. Weberskirch, A. Brunschweiger, N. Kockmann, ACS Comb. Sci. 22, 101 - 108 (2020).

Contact:
jens.bobers@tu-dortmund.de
norbert.kockmann@tu-dortmund.de
andreas.brunschweiger@tu-dortmund.de

Equipment Element Design Assisted by Topology Optimization

Light-weigth and stress-optimized apparatuses with optimized geometries

Daniel Becker, Norbert Kockmann

The use of lightweight structures with bionic designs have made their way into the fields of architecture and aeronautics. The high potential in material efficiency and cost reduction makes these designs interesting for chemical equipment design, too. Particularly mobile pressure vessels or plate structures can benefit from lower weight with less fuel consumption during transporting. Establishing bionic structures in the field of pressure vessel design a new manufacturing process is needed together with novel bionic design concepts.

A well-known bionic optimization approach is the topology optimization which is inspired by the growth behavior of bone structures. The topology optimization uses loads which are known from a reference model on a broad installation space. The material in this installation space is distributed according to the loads of the reference model. In this optimization the SIMP (solid isotropic material with Penalization) method is used. The SIMP method maximizes the stiffness of a component by utilizing a density depended modulus of elasticity.

As a reference model support structures are used which are designed by the AD2000 code. In Figure 1 an example for a support saddle is shown which is designed by AD2000 code S2/3. New design approaches developed by topology optimization can reach same strength values with lower mass. An example for an optimized support saddle is shown in Figure 1 right side. The mass of the new design is reduced by 30 % in comparison to the reference model. Further examples are the support structure of pressure vessels in Figure 2.

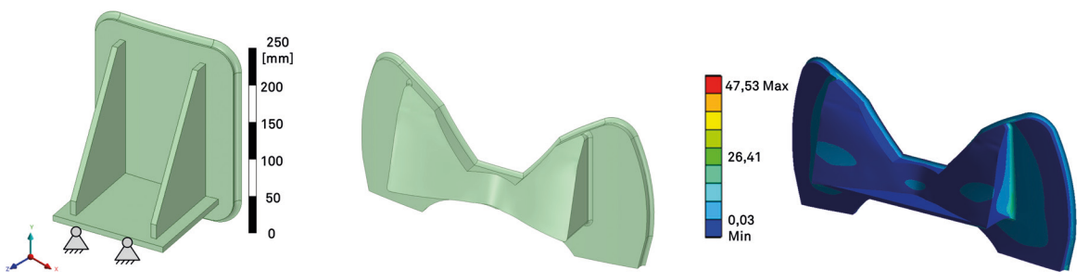

Figure 1: Reference model of support saddle designed by AD2000 code on the left side, Topology optimised design of support saddle in the midlle and the resultus of an FEM simulation on the right side.

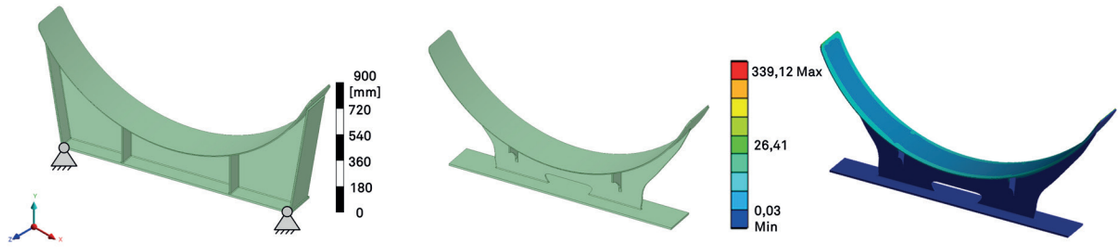

Figure 2: Reference model of support claw designed by AD2000 code on the left side, Topology optimised design of support saddle in the midlle and the resultus of an FEM simulation on the right side.

Contact:
daniel4.becker@tu-dortmund.de
norbert.kockmann@tu-dortmund.de

Publications:
D. Becker, I. Fiedler, N. Nikbin, N. Kockmann, Bionic optimization of pressure vessel support structures, Poster price at PAAT-Jahrestagung, Münster, 9.-10. November 2020.

Mass Transfer and Selectivity of Gas-Liquid Reactions

Investigations on chemical and biochemical reactions in capillaries

Julia Grühn, Waldemar Krieger, Norbert Kockmann

Microreactors are characterized by a large specific surface area and are therefore of interest for many applications in research and development. Because of the resulting enhanced heat and mass transfer, microreactors provide a great potential for process intensification and process control. The focus of this work lies on gas-liquid reactions. These are of great importance in the chemical and biochemical industry and subject of current research. The implementation of traditional sensors is a drawback when investigating mass transfer phenomena within microstructured devices, since they disturb the flow and reactor characteristics.

An Arduino based slider setup is developed, which is equipped with a computer-vision system to track single slugs of gas-liquid slug flow. This setup is combined with an optical analytical method utilizing the consecutive oxidation of leuco-indigo carmine in order to study flow structure, selectivity and mass transfer phenomena in gas-liquid slug flow with high temporal and spatial resolution. Mass transfer was investigated for varying flow rates and gas/liquid ratios. The experimental work is complemented with numerical simulations, where the complex process of combining advection, diffusion, and chemical reaction for slug flow was successful resulting in a fair match between experimental and numerical data for the reactant and fully oxidized product (Figure 1).

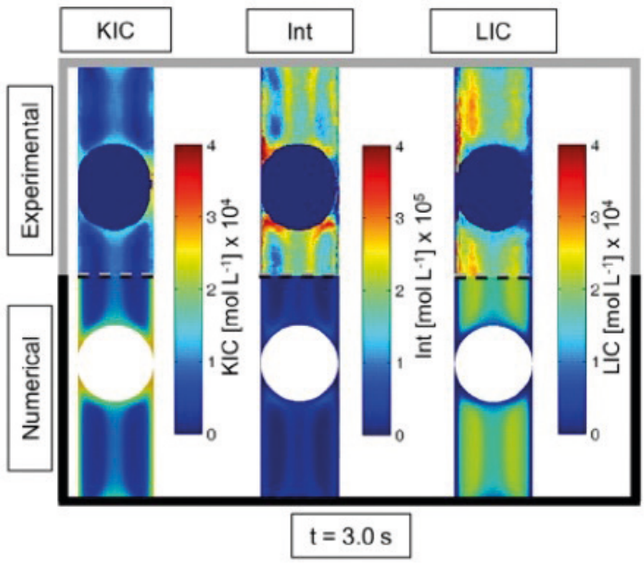

Figure 1: Experimental and numerical concentration profiles of the three indigo carmine species: keto-indigo carmine (KIC), radical intermediate (Int), leuco-indigo carmine (LIC) at time step t = 3.0. Numerical concentration profiles are integrated over the cross-section. Total volumetric flow rate = 4 ml min−1, gas/liquid ratio = 0.5, Re = 48.

In order to obtain information about the interaction between reaction and fluid mechanics by performing a parallel reaction, a bio-catalytically gas-liquid reaction system was tested for suitability. The selected enzyme is Laccase and the tested chromogenic substrates are ABTS (2,2´-azino-bis(3-ethylbenzothiazoline-6-sulphonic acid)), SAz (syringaldazine) and OPD (o-phenylene-diamine). The reaction times and Michaelis-Menten kinetic of the single reactions indicate that ABTS, SAz, and Laccase (Figure 2) are compatible reaction systems to perform a parallel reaction and are therefore the most promising reaction systems for investigating the relationship between fluid mechanics and selectivity.

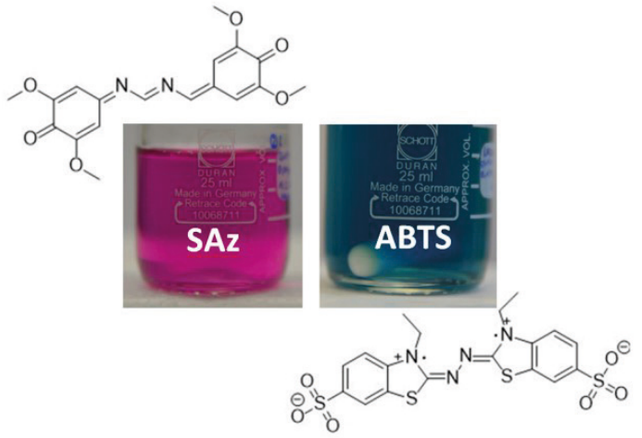

Figure 2: SAz and ABTS are suitable for parallel reaction that enables investigations on selectivity and mass transfer.

Publications:
W. Krieger, E. Bayraktar, O. Mierka, L. Kaiser, R. Dinter, J. Hennekes, S. Turek, N. Kockmann, AIChE J., 66(6), e16953 (2020).
J. Grühn, I. Burke, N. Neuhaus, N. Kockmann, Chem. Ing. Technik, 92(5), 624-628 (2020).

Contact:
julia.gruehn@tu-dortmund.de
norbert.kockmann@tu-dortmund.de

Temperature-Controlled Mini-Channel Flow-Cell for Non-Invasive Particle Measurements in Solid-Liquid Flow

Optical particle measurement with inline cell under light microscope with digital camera

Mira Schmalenberg, Fabian Sallamon, Christian Haas, Norbert Kockmann

The observation and analysis of particles, their size, morphology, and agglomerate formation is important for a good knowledge of processes with solids. Particularly, crystallization depends on ensuring sufficient analytics not only for the process itself, but also for characterizing apparatuses and products. Image analysis in particular is suitable for characterizing particles and crystals, in addition to the many other analytical methods.

Solid-liquid suspension flow is often involved in the production of pharmaceuticals and fine chemicals. In these fields, working with continuous small-scale equipment in order to save costs and resources is of increasing interest. Therefore, it is also important to enable process control for small-scale apparatus, which requires the development of new concepts to observe and control crystallization processes in mini-channel equipment. The particles and crystals should be detected and measured with as low impact as possible because contact between process medium and the sensors can often lead to the incrustation of the sensor, disturb the particle size and shape, or contaminate the system.

For the observation of crystallizing processes in mini-channel crystallizers, a non-invasive, temperature-controlled flow-cell is designed in this work. In particular, this flow cell has been designed to examine crystals in a fluorinated ethylene propylene (FEP) tube with an inner diameter of 1.6 mm. Crystals can be investigated using a standard optical camera and microscope. An image processing routine enables the evaluation of crystal size. The algorithms were implemented in a graphical user interface. A defined quantity (1 w.-%) of tracer crystals (L-alanine) of the sieve fractions 90 – 125 µm and 125 – 180 µm were used to investigate the sufficiency of the image analysis method. It could be shown that the particle size distribution is sufficiently well described in comparison with a conventional sedimentation method.

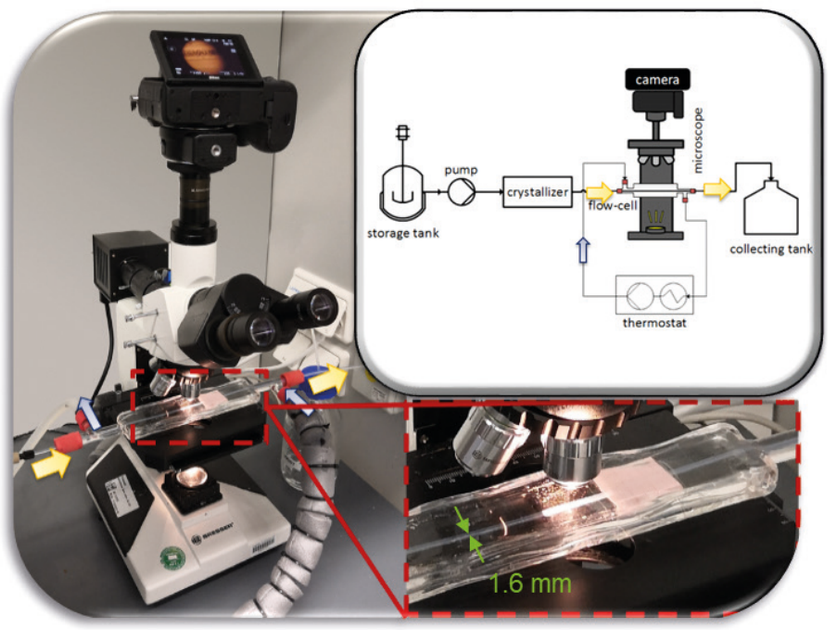

Figure 1: Coiled tube with homogeneous suspension flow; photo (left), schematic (right).

Contact:
mira.schmalenberg@tu-dortmund.de
norbert.kockmann@tu-dortmund.de

Publications:
M. Schmalenberg, F. Sallamon, C. Haas, N. Kockmann, ASME 2020 18th ICNMM, ICNMM2020-1062, V001T16A005, https://doi.org/10.1115/ICNMM2020-1062.

Efficient Shortcut Method for Determining the Process Window in Stirred Pulsed Extraction Columns

Mira Schmalenberg, Timothy Aljoscha Frede, Christopher Mathias, Norbert Kockmann

Recent studies showed the superior separation performance of stirred-pulsed columns of different diameters in liquid-liquid extraction processes. Here, an efficient shortcut method will be presented, which is time and resource-efficient as well as cost-effective to determine the operational window of these columns for industrial separation tasks. Savings in time of less experiments and costs of materials consumption can be estimated with up to 30 %. The presented method is particularly suitable before the application of new chemical systems, which are particularly cost-intensive and scarce in material supply.

A practical shortcut method is presented for the application of industrial chemical systems in stirred-pulsed extraction columns to achieve reasonable results in short time with low effort. For this purpose, the industrial system containing salts, impurities, and expensive products is replaced by model component systems in a first step. By using the model systems, the flooding and hydrodynamic behavior is investigated in a DN15 stirred pulsed measurement cell (see Figure 1) and a DN15 stirred-pulsed extraction column. These investigations help finding the optimal operation window for complex industrial chemical systems in a resource-efficient manner. Therefore, flooding points of the industrial systems are estimated based on hydrodynamic studies of a reduced form of the industrial system, the so-called model system. A schematic representation of the shortcut method is shown and compared to the conventional method in Figure 2.

For testing the applicability of the shortcut method, the difference between the flooding loadings of model and industrial system is evaluated. Since the difference in flooding loadings between the model and the industrial system remains constant at different stirrer speeds and specific pulsation frequency, material savings of up to 34 % can be achieved using this method.

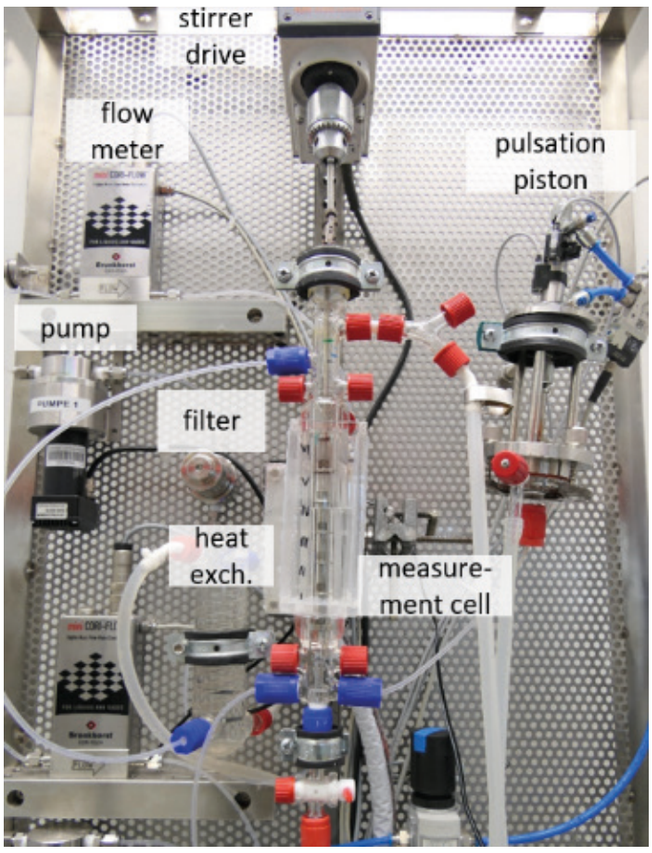

Figure 1: DN15 stirred-pulsed extraction measurement cell.

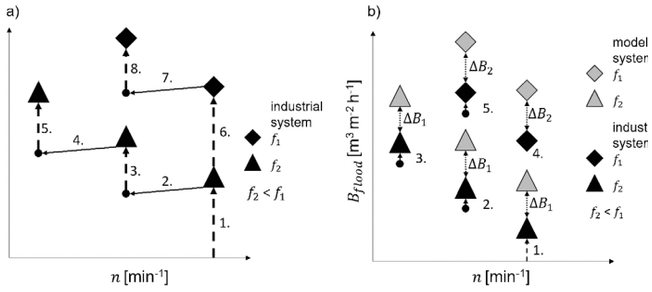

Figure 2: a) Schematic representation of the conventional method. b) Schematic representation of the shortcut method.

Publications:
M. Schmalenberg, T. A. Frede, C. Mathias, N. Kockmann, Chem. Ing. Tech. 93, 2021, doi.org/10.1002/cite.202000066.
Received: April 01, 2020; accepted: December 18, 2020, First published: 21 January 2021.

Contact:
mira.schmalenberg@tu-dortmund.de
timothy.frede@tu-dortmund.de
norbert.kockmann@tu-dortmund.de

Automated Kinetic Data Acquisition and Reaction Optimization with Microreactors

Optical particle measurement with inline cell under light microscope with digital camera

Verena Fath, Thorsten Röder, Norbert Kockmann

In chemical process development, efficient kinetic data acquisition is essential and can greatly benefit from model prediction tools. Continuous flow microreactors are particularly well suited for rapid data generation with low substance consumption. This research highlight includes also inline FT-IR spectroscopy combined with self-modeling curve resolution for self-optimising processes and real-time optimisation of organic syntheses using Nelder–Mead and design of experiment methods.

This work presents an approach to obtain and model kinetic data in combining a microreactor setup and real-time process monitoring through inline FT-IR spectroscopy and self-modeling curve resolution (SMCR). Two model reactions - imine synthesis of benzaldehyde with benzylamine and deprotonation reaction with n-butyllithium - serve as proof of concept and additionally demonstrate the method's broad range of application, which includes simple reactions as well as complex mechanisms.
The self-optimisation of a chemical reaction multi-variate and multi-objective optimisations in real-time is performed in a modular, autonomous platform that performs. To demonstrate its flexibility (which extends to industrial production settings), the performances (in terms of identifying optimal reaction conditions) of two common optimisation strategies, modified simplex algorithm and model-free design of experiments, are subsequently compared. Simultaneously, kinetic data are collected to gain further insights into the involved chemical processes. Further, the system is also capable of providing real-time responses to disturbances to the chemical process.
Subsequent replications of the model reactions with collection and modeling of kinetic data using dynamic-state conditions and spectra evaluation indicate that the presented approach possesses higher time-efficiency compared to batch or steady-state studies. If quick estimates are needed with only analyzing the elementary reaction mechanism, research labs may achieve significant time and cost savings through applying the outlined approach.

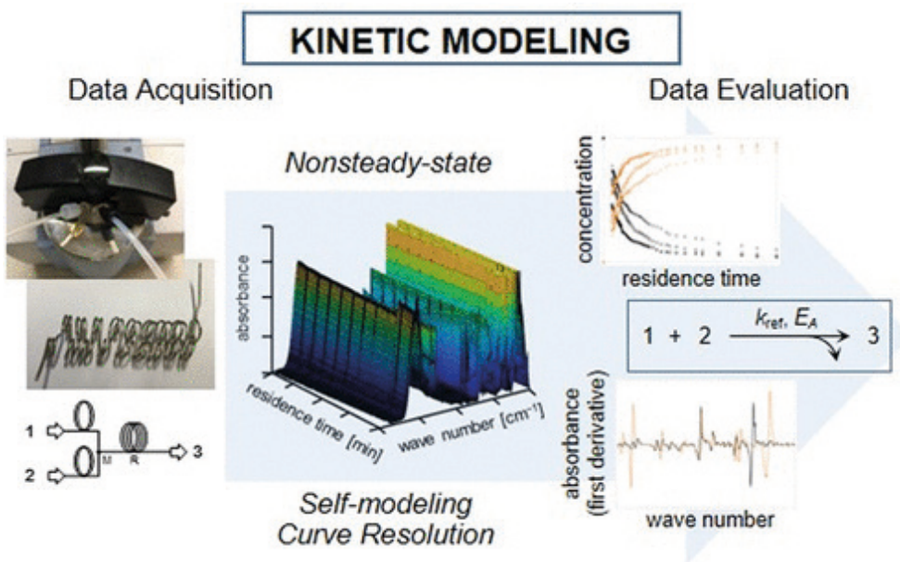

Figure 1: Data acquisition in a capillary microreactor with inline FT-IR sensor, data analysis and kinetic modelling and optimization.

Contact:
t.roeder@hs-mannheim.de
norbert.kockmann@tu-dortmund.de

Publications:
V. Fath, P. Lau, C. Greve, N. Kockmann, T. Röder, Efficient Kinetic Data Acquisition and Model Prediction in Continuous Flow Microreactors using Inline FT-IR Spectroscopy combined with SMCR Technique, Org. Proc. R&D, 24(10), 1955-1969, 2020, doi.org/10.1021/acs.oprd.0c00037.

V. Fath, N. Kockmann, J. Otto, T. Röder, Self-Optimising Processes and Real-Time-Optimisation of Organic Syntheses in a Microreactor System using Nelder-Mead and Design of Experiments, Reaction Chemistry & Engineering, 5(7), 1281-1299, 2020, doi.org/10.1039/D0RE00081G.

Publications 2020 - 2018

2020

Peer Reviewed Journal Papers

- M.M. Awad, D. Attinger, A. Bejan, A. Beskok, G.P. Celata, S. Colin, V.K. Dhir, P. Di Marco, S.V. Ekkad, S. Garimella, M. Kawaji, M.R. King, N. Kockmann, J. Kriegel, S.K. Mitra, S. Moghaddam, Y.S. Muzychka, V. Narayanan, G. Ribatski, S.A. Sherif, M. Shoji, P. Stephan, J.R. Thomé, P.B. Weisensee
  Professor Satish G. Kandlikar on His 70th Birthday
  J. Therm. Sci.&Eng. Appl., 12, 060301-1 - 3, 2020, doi.org/10.1115/1.4048813

- N. Kockmann
  Der Schnellstart in die digitale Lehre unter Corona-Randbedingungen
  Chem. Ing. Technik, 92(12), 1877-1886, 2020, doi.org/10.1002/cite.202000206

- J. Bobers, J. Grühn, S. Höving, T. Pyka, N. Kockmann
  Two-phase Flow in Coiled Flow Inverter – Process Development and Scale-out From Batch to Continuous Flow
  Org. Proc. R&D, 24(10), 2094-2105, 2020, doi.org/10.1021/acs.oprd.0c00152

- V. Fath, P. Lau, C. Greve, N. Kockmann, T. Röder
  Efficient Kinetic Data Acquisition and Model Prediction in Continuous Flow Microreactors using Inline FT-IR Spectroscopy combined with SMCR Technique
  Org. Proc. R&D, 24(10), 1955-1969, 2020, doi.org/10.1021/acs.oprd.0c00037

- J. Schuler, L.M. Neuendorf, K. Petersen, N. Kockmann
  Micro-Computed Tomography for the 3D Time-Resolved Investigation of Monodisperse Droplet Generation in a Co-Flow Setup
  AIChE J., 67(2) e17111, 2021, doi.org/10.1002/aic.17111

- V. Fath, N. Kockmann, J. Otto, T. Röder
  Self-Optimising Processes and Real-Time-Optimisation of Organic Syntheses in a Microreactor System using Nelder-Mead and Design of Experiments
  Reac. Chem. & Eng., 5(7), 1281-1299, 2020, doi.org/10.1039/D0RE00081G

- N. Kockmann
  Gewusst wie! Entwurf und Betrieb eines Rohrreaktors mit enger Verweilzeitverteilung
  Chem. Ing. Technik, 92(6), 685-691, 2020, doi.org/10.1002/cite.202000028

- C.V. Benzin, N. Kockmann, T. Röder
  Lab-Scale Microreactor Plant for the Study of Methylations with Liquid Chloromethane
  Chem. Eng. & Technol., 43(9), 1733-1740, 2020, doi.org/10.1002/ceat.202000011

- W. Krieger, E. Bayraktar, O. Mierka, L. Kaiser, R. Dinter, J. Hennekes, S. Turek, N. Kockmann
  Arduino based slider setup for gas-liquid mass transfer investigation
  AIChE J., 66(6), e16953, 2020, doi.org/10.1002/aic.16953

- J. Bobers, M. Klika Škopić, R. Dinter, P. Sakthithasan, L. Neukirch, C. Gramse, R. Weberskirch, A. Brunschweiger, N. Kockmann
  Design of an Automated Reagent-Dispensing System for Reaction Screening and Validation with DNA-tagged Substrates
  ACS Combinatorial Science, 22(3), 101-108, 2020, doi.org/10.1021/acscombsci.9b00207

- J. Grühn, I. Burke, N. Neuhaus, N. Kockmann
  Investigations on selectivity of gas-liquid reactions in capillaries
  Chem. Ing. Technik, 92(5), 624-628, 2020, doi.org/10.1002/cite.201900144

- N. Steinfeldt, N. Kockmann
  Experimental and Numerical Characterization of Transport Phenomena in a Falling-film Microreactor with Gas-Liquid Reaction
  Ind. Eng. Chem. Res., 59(9), 4033-4047, 2020, doi.org/10.1021/acs.iecr.9b04154

- J. Schuler, N. Kockmann
  Micro-Computed Tomography for the investigation of stationary liquid/liquid and liquid/gas interfaces in capillaries
  AIChE J., 66(4), e16890, 2020, doi.org/10.1002/aic.16890

- M. Schmalenberg, A. Nokon, N. Kockmann
  Design and Hydrodynamic Characterization of a Lab-scale Draft Tube Baffle Crystallizer
  Chem. Ing. Technik, 92(3), 288-294, 2020; doi.org/10.1002/cite.201900078

- A. Bamberg, M. Bortz, N. Kockmann, S. Bröcker, L. Urbas
  Was den digitalen Zwilling zum genialen Kompagnon macht
  Chem. Ing. Technik, 92(3), 192-198, 2020, doi.org/10.1002/cite.201900168

Peer-Reviewed Conference Papers

- M. Schmalenberg, F. Sallamon, C. Haas, N. Kockmann
  Temperature-Controlled Minichannel Flow-Cell for Non-Invasive Particle Measurements in Solid-Liquid Flow
  ICNMM2020, Orlando, USA, 17. July 2020

- J. Schuler, L.M. Neuendorf, K. Petersen, N. Kockmann
  3D Investigation of Droplet Generation in a Miniaturized Coflowing Device Using Micro-Computed Tomography
  ICNMM2020, Orlando, USA, 17. July 2020

Conference Presentations and Posters

- N. Kockmann
  Ontologie und Metadaten-Standards für die Katalyse und Prozesstechnik
  NFDI4Cat, Vortrag, NFDI4Ing Ontologien, Darmstadt, 30. November 2020

- N. Kockmann, P. Pelz
  NFDI-Initiative – Forschungsdaten für Chemiker und Ingenieure
  Plenar-Vortrag, PAAT, Münster, 9.-10. November 2020

- A. Schindel, M. Schmalenberg, M. Polyakova, M. Grünewald, N. Kockmann
  Matching matrix for the selection of continuous crystallization technologies exemplified by the CFI-crystallizer
  Vortrag, PAAT-Jahrestagung, Münster, 9.-10. November 2020

- L. Bittorf, A. Marschand, K. Pathak, H. Weinhold, K. Wekenborg, N. Kockmann
  Vacuum FEA integration for a modular laboratory distillation column and advantages of small-scale equipment
  Vortrag, PAAT-Jahrestagung, Münster, 9.-10. November 2020

- T.A. Frede, I. Burke, N. Kockmann
  Seebeck Element Reaction Calorimeter with Commercially Available Microreactors
  Posterbeitrag, PAAT-Jahrestagung, Münster, 9.-10. November 2020

Publications 2020 - 2018

- D. Becker, I. Fiedler, N. Nikbin, N. Kockmann
  Bionic optimization of pressure vessel support structures
  Posterbeitrag, PAAT-Jahrestagung, Münster, 9.-10. November 2020

- P. Sakthithasan, M. Venhuis, N. Kockmann
  Fully automated pulsation system module for high-pressure processes
  Posterbeitrag, PAAT-Jahrestagung, Münster, 9.-10. November 2020

- J. Grühn, T. Eroglu, M. Oruc, T. Pyka, N. Kockmann
  Vom Labor- in den Produktionsmaßstab: Untersuchung einer enzymkatalysierten gas/flüssig-Reaktion
  Posterbeitrag, PAAT-Jahrestagung, Münster, 9.-10. November 2020

- A. Klose, K. Stark, T. Schenk, L. Bittorf, M. Hoernicke, A. Stutz, S. Merkelbach, M. Maurmaier, M. Eckert, A. Menschner, P. Santos, T. Scherwietes, N. Kockmann, S. Unland, L. Urbas
  Service-Design im Engineering modularer Anlagen
  Vortrag, PAAT-Jahrestagung, Münster, 9.-10. November 2020

- D. Becker, A. Behr, N. Kockmann
  Optimierung von Wärmeübertragern mit Hilfe von bionischen Prinzipien und evolutionären Algorithmen
  Vortrag, NAFEMS-Jahrestagung, online, 13.-14. Oktober 2020

- J. Grühn, T. Pyka, N. Kockmann
  Biocatalytic gas-liquid reactions in coiled capillaries
  Posterbeitrag ProcessNet Jahrestagung Aachen, 21.-24. September 2020

- A. Frede, D. Sürig, N. Kockmann
  Isothermal Reaction Calorimetry using Peltier Elements for Exothermic Reactions in Microreactors
  Posterbeitrag ProcessNet Jahrestagung Aachen, 21.-24. September 2020

- J. Bobers, M. Klika Škopić, R. Dinter, P. Sakthithasan, L. Neukirch, C. Gramse, R. Weberskirch, A. Brunschweiger, N. Kockmann
  Design of an Automated Reagent-Dispensing System for Reaction Screening and Validation with DNA-tagged Substrates
  Posterbeitrag ProcessNet Jahrestagung Aachen, 21.-24. September 2020

- J. Bobers, E. Forys, B. Oldach, N. Kockmann
  Characterization of Mixing Quality in Polyimide-based Microreactors by UV/Vis-Online Monitoring of DMP Hydrolysis
  Posterbeitrag ProcessNet Jahrestagung Aachen, 21.-24. September 2020

- L. Bittorf, J. Oeing, T. Kock, N. Kockmann
  Modular process development in the laboratory – Plug & Research
  Vortrag ProcessNet Jahrestagung Aachen, September 2020

- P. Sakthithasan, N. Kaufhold, L. Orth, N. Kockmann
  Design of a stirred-pulsed liquid-liquid extraction for high-pressure processes
  Posterbeitrag ProcessNet Jahrestagung Aachen, 21.-24. September 2020

- N. Kockmann, M. Dittmann
  Ausbildung mit modularen verfahrenstechnischen Anlagen
  Posterbeitrag ProcessNet Jahrestagung Aachen, 21.-24. September 2020

- V. Fath, P. Lau, C. Greve, N. Kockmann, T. Röder
  Self-Optimising Processes: Optimisation of organic syntheses in an automated-flow microreactor system using Nelder-Mead and Design of Experiments
  Posterbeitrag ProcessNet Jahrestagung Aachen, 21.-24. September 2020

- T. Klement, T. Röder, N. Kockmann
  Kinetic measurements of acrylic acid polymerization with respect to highly exothermal behavior
  Posterbeitrag ProcessNet Jahrestagung Aachen, 21.-24. September 2020

- J. Grühn, N. Kockmann
  Biocatalytic gas-liquid reactions in coiled capillaries
  Posterbeitrag ProcessNet Jahrestagung Aachen, 21.-24. September 2020

- K. Dadhe, L. Urbas, M. Bortz, N. Kockmann
  Begreifbare KI-Anwendungen in der Prozessindustrie
  Keynote-Vortrag ProcessNet Jahrestagung Aachen, 21.-24. September 2020

- J. Schuler, L.M. Neuendorf, K. Petersen, N. Kockmann
  Micro-Computed Tomography for the 3-Dimensional Investigation of Liquid/Liquid-Slug-Flow Generation
  4th International Symposium on Multiscale Multiphase Process Engineering (MMPE), Berlin, 30.8. – 2.9. 2020

- T. Klement, N. Kockmann, T. Röder
  Kinetic measurements of acrylic acid polymerization with respect to highly exothermal behavior
  Jahrestagung ProcessNet FG-Reaktionstechnik, Würzburg, 18.5.2020

- C. Benzin, N. Kockmann, T. Röder
  Methylation with chloromethane in a microreactor – kinetic studies and modelling
  Jahrestagung ProcessNet FG-Reaktionstechnik, Würzburg, 18.5.2020

- V. Fath, S. Szmais, P. Lau, C. Greve, N. Kockmann, T. Röder
  Real-Time-Optimisation of Organic Syntheses in a Microreactor System combined with Online Analytics using Nelder-Mead and Design of Experiments
  Jahrestagung ProcessNet FG-Reaktionstechnik, Würzburg, 18.5.2020

- J. Bobers, E. Forys, B. Oldach, N. Kockmann
  Characterization of Mixing Quality in Polyimide-based Microreactors by UV/Vis-Online Monitoring of DMP Hydrolysis
  Jahrestagung ProcessNet FG-Reaktionstechnik, Würzburg, 18.5.2020

- T.A. Frede, F. Reichmann, T. Piontek, D. Sürig, N. Kockmann
  Reactor Temperature Control of Microreactors in a Reaction Calorimeter using Peltier Elements
  Jahrestagung ProcessNet FG-Reaktionstechnik, Würzburg, 18.5.2020

- L. Kaiser, W. Krieger, B. Oldach, G. Wiese, N. Kockmann
  Ultrasonic sensors for noninvasive flow rate and particle measurement
  Posterbeitrag Jahrestagung ProcessNet FG-Kristallisation, Dortmund, 17.-18. März 2020

- M. Schmalenberg, S. Lindemann, L. Mensing, N. Kockmann
  Investigations on Start-up Behavior of a Miniaturized Draft Tube Baffle Crystallizer for Continuous Operation
  Vortrag, Jahrestagung ProcessNet FG-Kristallisation, Dortmund, 17.-18. März 2020

- J. Schuler, L.M. Neuendorf, K. Petersen, N. Kockmann
  Micro-computed tomography for the 3D investigation of liquid-liquid slug flow in a thin polymer tube
  Vortrag, Jahrestagung ProcessNet FG Mehrphasenströmung, Paderborn, 17.-18. März 2020

- J. Schuler, F. Buthmann, J. Herath, J. Ernst, N. Kockmann
  Investigations on single and multiphase mass transfer of iodine in miniaturized equipment using micro-computed tomography
  Poster, Jahrestagung ProcessNet FG-Wärme- und Stoffübertragung, Erfurt, 12.-13. März 2020

Publications 2020 - 2018

- N. Kockmann
  Solids handling in micro flow
  Keynote Flow Chemistry Conference, Cambridge, March 9-10, 2020

- N. Kockmann
  Smart Process Equipment im Labor – neue Möglichkeiten und Ansätze
  M2Aind Symposium, Mannheim, Keynote, 4. Februar 2020

2019

Peer Reviewed Journal Papers

- V. Fath, S. Smaisz, P. Lau, N. Kockmann, T. Röder
  Model-based Scale-up Predictions: From Micro- to Millireactors using Inline FT-IR Spectroscopy
  Org. Proc. R&D, 23(9), 2020-2030, 2019; doi.org/10.1021/acs.oprd.9b00265

- A. Klose, S. Merkelbach, A. Menschner, S. Hensel, S. Heinze, L.Bittorf, N. Kockmann, C. Schäfer, S. Szmais, M. Eckert, T. Rüde, T. Scherwietes, P. da Silva Santos, F. Stenger, T. Holm, W. Welscher, N. Krink, T. Schenk, A. Stutz, M. Maurmaier, K. Stark, M. Hoernicke, S. Unland, S. Erben, F. Keßler, F. Apitz, L. Urbas
  Orchestration Requirements for Modular Process Plants in Chemical and Pharmaceutical Industries
  Chem. Eng. & Technol., 42(11), 2282-2291, 2019; doi.org/10.1002/ceat.201900298

- W. Krieger, M. Hörbelt, S. Schuster, J. Hennekes, N. Kockmann
  Kinetic study of leuco-indigo carmine oxidation and investigation of Taylor and Dean flow superposition in a coiled flow inverter
  Chem. Eng. & Technol., 42(10), 2052-2060, 2019; DOI: 10.1002/ceat.201900120

- V. Fath, N. Kockmann, T. Röder
  In-situ Reaction Monitoring of Unstable Lithiated Intermediates through Inline FT-IR Spectroscopy: A Mechanistic Investigation
  Chem. Eng. & Technol., 42(10), 2095-2104, 2019; DOI: 10.1002/ceat.201900120

- L. Bittorf, F. Reichmann, M. Schmalenberg, S. Soboll, N. Kockmann
  Equipment and Separation Units for Flow Chemistry Applications and Process Development
  Chem. Eng. & Technol., 42(10), 1985-1995, 2019; DOI: doi.org/10.1002/ceat.201900120

- N. Kockmann
  Digital methods and tools for chemical equipment and plants
  Reac. Chem. & Eng., 4, 1522-1529, 2019; DOI: 10.1039/C9RE00017H

- C.V. Miguel, C. Moreira, M.A. Alves, J.B.L.M. Campos, J. Glassey, E. Schaer, N. Kockmann, A. Porjazoska Kujundziski, M. Polakovic, L.M. Madeira
  Developing a Framework for Assessing Teaching Effectiveness in Higher Education
  Edu. Chem. Eng., 29(10), 21-28, 2019; doi.org/10.1016/j.ece.2019.06.001

- N. Kockmann
  A brief history of chemical reactor and reaction technology
  Chemie Ingenieur Technik, 91(6), 941-952 2019; doi.org/10.1002/cite.201900001

- N. Kockmann
  50 Jahre Chemietechnik und BCI in Dortmund – ein kurzer Abriss aus Lehre und Forschung
  Chemie Ingenieur Technik, 91(6), 695-698, 2019; doi.org/10.1002/cite.201970066

- T. Klement, N. Kockmann, T. Röder
  Reactor Concept for Contactless Kinetic Measurement in Oscillating Droplets via Raman Spectroscopy
  Chemie Ingenieur Technik, 91(5), 651-656, 2019; doi.org/10.1002/cite.201800199

- M. Schmalenberg, W. Krieger, N. Kockmann
  Modular Coiled Flow Inverter with Narrow Residence Time Distribution for Process Development and Production
  Chemie Ingenieur Technik, 91(5), 567-575, 2019; doi.org/10.1002/cite.201800172

- F. Reichmann, K. Vennemann, T.A. Frede, N. Kockmann
  Mixing time scale determination in microchannels using reaction calorimetry
  Chemie Ingenieur Technik, 91(5), 622-631, 2019; doi.org/10.1002/cite.201800169

- L. Hoehr, F. Reichmann, M. Berndt, J. Sackmann, N. Kockmann, W.K. Schomburg
  Ultrasonic fabrication of polymer plate reactors with a surface coating
  Chem. Eng. & Technol., 42(5), 971-979, 2019; DOI: 10.1002/ceat.201800333

- S. Schwolow, B. Mutsch, N. Kockmann, T. Röder
  Model-based scale-up and reactor design for solvent-free synthesis of an ionic liquid in a millistructured flow reactor
  Reac. Chem. & Eng., 4(3), 523-536, 2019; DOI: 10.1039/C8RE00148K

- L. Hohmann, M. Schmalenberg, M. Prasanna, M. Matuschek, N. Kockmann
  Suspension Flow Behavior and Particle Residence Time Distribution in Helical Tube
  Chem. Eng. J., 360, 1371-1389, 2019; doi.org/10.1016/j.cej.2018.10.166

Peer-Reviewed Conference Papers

- J. Bobers, N. Kockmann
  Development of a Manufacturing Process For Polyimide-based Microstructured Devices Using Reactive Ion Etching
  ASME-ICNMM2019-4208, St. John´s, Canada, June 23-26, 2019

- J. Bobers, N. Kockmann
  Non-invasive Temperature Measurement For Polyimide-based Microstructured Devices
  ASME-ICNMM2019-4207, St. John´s, Canada, June 23-26, 2019

- N. Kockmann, W. Krieger, M. Schmalenberg
  Design and Scale-up of Modular Capillary-Flow Inverter Reactors with Narrow Residence Time Distribution
  ASME-ICNMM2019-4237, St. John´s, Canada, June 23-26, 2019

- J. Schuler, N. Kockmann
  Investigation of multiphase interfaces in small channels using micro CT
  ASME-ICNMM2019-4203, St. John´s, Canada, June 23-26, 2019

Publications 2020 - 2018

2018

Peer Reviewed Journal Papers

- N. Kockmann
  100 % Digital in der Prozessindustrie – Eindrücke und Ergebnisse vom Tutzing-Symposion 2018
  Chem. Ing. Technik, 90 (11), 1621-1627, 2018; DOI: 10.1002/cite.201800135

- N. Kockmann, L. Bittorf, W. Krieger, F. Reichmann, M. Schmalenberg, S. Soboll
  Smart Equipment – A Perspective Paper
  Chem. Ing. Technik, 90 (11), 1806-1822, 2018; DOI: 10.1002/cite.201800020

- S. Soboll, N. Kockmann
  Hydrodynamics and mass transfer in a lab-scale, stirred-pulsed extraction column
  Chem. Eng. & Technol., 41(9), 1847-1856, 2018; DOI: 10.1002/ceat.201800283

- L. Hohmann, L. Löbnitz, C. Menke, B. Santhirakumaran, P. Stier, F. Stenger, F. Dufour, G. Wiese, S. zur Horst-Meyer, B. Kusserow, W. Zang, H. Nirschl, N. Kockmann
  Continuous Downstream Processing of Amino Acids in a Modular Miniplant
  Chem. Eng. & Technol., 41(6), 1152-1164, 2018; DOI: 10.1002/ceat.201700657

- L. Hohmann, T. Greinert, O. Mierka, S. Turek, G. Schembecker, E. Bayraktar, K. Wohlgemuth, N. Kockmann
  Analysis of Crystal Size Dispersion Effects in a Continuous Coiled Tubular Crystallizer: Experiments and Modelling
  Cryst. Growth & Design., 18 (3), 1459–1473, 2018; DOI: 10.1021/acs.cgd.7b01383

- S. Soboll, L. Bittorf, N. Kockmann
  Axial backmixing and residence time distributions in a stirred-pulsed, miniaturized extraction column
  Chem. Eng. & Technol., 41(1) 134-142, 2018; DOI: 10.1002/ceat.201700152

Peer Reviewed Conference Papers

- F. Reichmann, Y. Jirmann, N. Kockmann
  Mixing Time Scale Measurement with Fast Exothermic Reactions Using Microchannel Reaction Calorimetry
  Proc. ASME-ICNMM2018-7627, Dubrovnik, June 11-13, 2018

- F. Reichmann, N. Kockmann
  Mass Transfer Studies During Bubble Breakup Behind Micronozzles in Laminar and Turbulent Breakup Regime
  Proc. ASME-ICNMM2018-7630, Dubrovnik, June 11-13, 2018

- W. Krieger, R. Dinter, G. Wiese, S. zur Horst-Meyer, N. Kockmann
  Active sensors for gas-liquid mass transfer studies in capillaries
  Proc. ASME-ICNMM2018-7659, Dubrovnik, June 11-13, 2018

- M. Schmalenberg, N. Kockmann
  Miniaturized Tubular Cooling Crystallizer with Solid-Liquid Flow for Process Development
  Proc. ASME-ICNMM2018-7660, Dubrovnik, June 11-13, 2018

Book Chapters

- N. Kockmann
  Historischer Abriss zur Entstehung und Entwicklung der Chemischen Reaktionstechnik
  in W. Reschetilowski, (Ed), Handbuch chemische Reaktoren, Springer Reference, November 2018

- S. Falß, N. Kloye, M. Holtkamp, A. Prokofyeva, T. Bieringer, N. Kockmann
  Process Intensification through Continuous Manufacturing: Implications for Unit Operation and Process Design
  in A.A. Lapkin (Ed.) Handbook of Green Chemistry: Vol. 12: Green Chemical Engineering, Wiley-VCH, Weinheim, July 2018

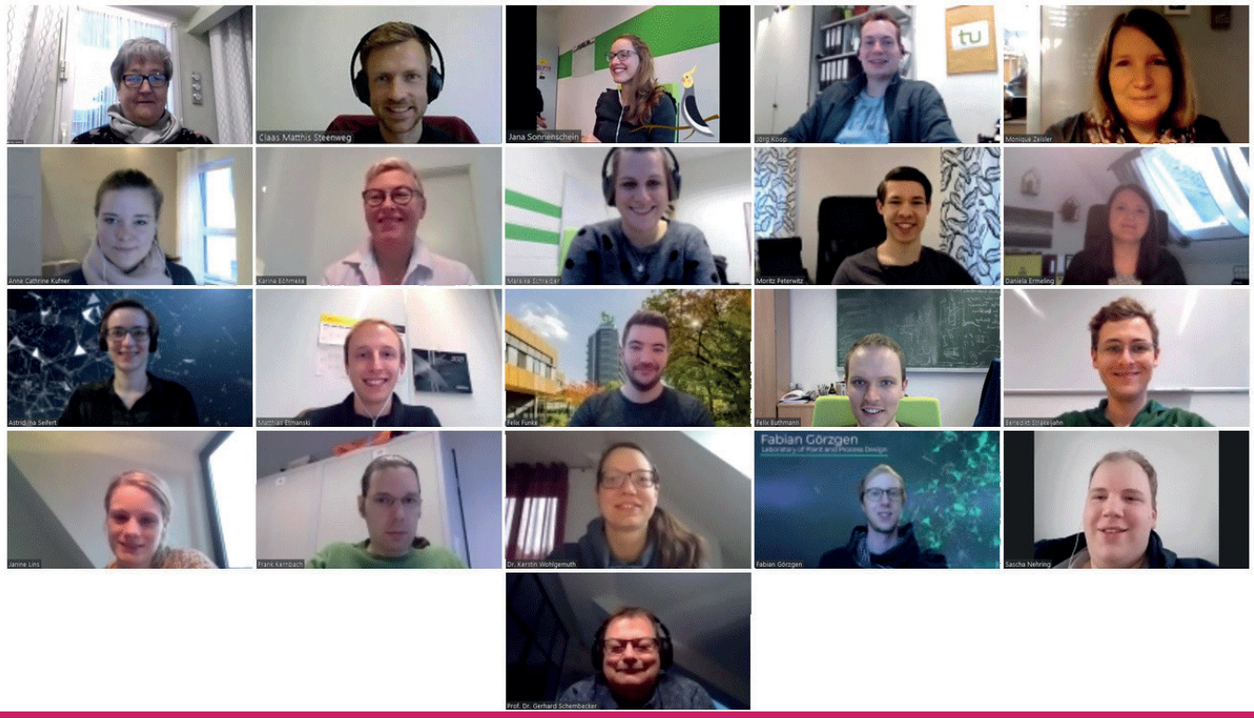

Plant and Process Design (APT)

Contribution of Secondary Structure Changes to the Surface Activity of Proteins

Essential for interface stabilization or overestimated gimmick?

Jörg Koop, Juliane Merz, Clemens Pietzsch, Gerhard Schembecker

Structural change of proteins at interfaces is often reported, but the impact of these changes on surface activity is rarely investigated. Thus, this study aims to clarify the relationship between the actual change of secondary structure of proteins at the interface and the macroscopic surface activity determined in foaming experiments. The result was that although some proteins exhibited structural changes at the interface, no general correlation could be found. Additionally, the changes detected were too slow to impact the quick process of adsorption and stabilization during the foaming experiments. However, it was shown that the ability to quickly increase the surface pressure at the interface while maintaining a native-like conformation correlates with the macroscopic surface activity of proteins.

The so-called surface activity is an intrinsic property of proteins, enabling them to adsorb at and stabilize gas-liquid interfaces. That process on molecular level leads to the formation of foam in protein solutions sparged with gas on macroscopic level, which, for instance, can occur in gassed bioreactors.

The fact that proteins are capable of changing their structure at air-water interfaces is well known. This study aims to investigate the impact of the secondary structure change on proteins' macroscopic surface-activity. However, the surface activity of proteins also depends on their environment, especially pH and ionic strength of the solution in which they are dissolved. Those parameters were adjusted for each protein investigated to ensure maximum surface activity.

Thus, we analyzed 5 model proteins in foaming experiments and ranked them according to their surface activity. Additionally, Infrared Reflection Absorption Spectroscopy (IRRAS) was applied to the protein solutions. It is a spectroscopic technology, with that the secondary structure of proteins at the air-water interface can be analyzed (see Figure 1). The different types of secondary structure elements (α-helices (α), β-sheets (β), β-sheets in aggregated structures (β#), and random coils (rc)) appear at different wavenumbers in the so-called amide-I band. Thus, from the shape of the amide-I band, the amount of secondary structure elements at the air-water interface can be estimated. The proteins were analyzed in bulk liquid with Fourier Transform Infrared (FTIR) spectroscopy as well. That was done to check for quick structural changes directly upon the adsorption at the air-water interface (see Figure 1). Those would not be detectible by IRRAS alone since one measurement takes about 3 minutes.

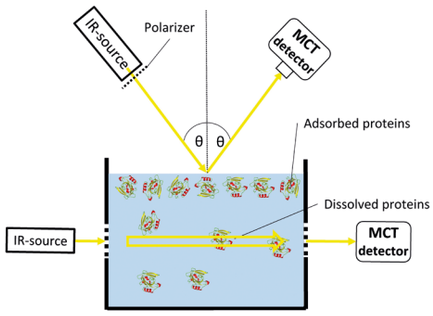

Figure 1: Principle of IRRAS and FTIR: IRRAS analyzing proteins adsorbed at the interface, FTIR analyzing proteins in bulk liquid.

Contact:
joerg.koop@tu-dortmund.de
gerhard.schembecker@tu-dortmund.de

Some proteins, for instance, α-lactalbumin, exhibited no structural change at the interface at all (see Figure 2). Myoglobin, on the other hand, changed its secondary structure by forming β-sheets. That was quite apparent since, in native state, myoglobin does not contain any β-sheets, which agrees with the FTIR measurement we performed. Thus, the β-sheets were formed after the adsorption at the interface. However, the interfacial changes happened on a timescale of hours, indicating that they are way too slow to increase surface activity during foam formation and stabilization, considering that the latter occurs on the timescale of seconds.

Furthermore, it was shown that α-lactalbumin and myoglobin had a native-like structure at the beginning of the adsorption like almost all other proteins investigated. The only exception was the low surface-active papain.

From the results obtained, it could be concluded that the secondary structure change at the air-water interface is no requirement for high surface activity. No correlation could be found between surface activity and the structure itself or the change of the structure. However, from surface pressure measurements, it could be concluded that the capability to increase the surface pressure quickly correlates with the surface activity determined in foam fractionation experiments.

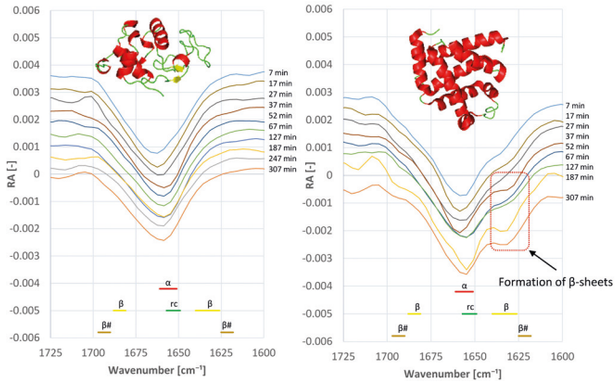

Figure 2: Comparison of IRRA spectra in the amide-I region of two surface-active proteins: α-lactalbumin exhibiting no structural change (left) and myoglobin slowly forming β-sheets.

Publications:
J. Koop, J. Merz, C. Pietzsch, G. Schembecker, Contribution of Secondary Structure Changes to the Surface Activity of Proteins, Journal of Biotechnology 323, 208-220 (2020).

Correlating Mobile Phase Dispersion in Centrifugal Partition Chromatography

New insights into flow regimes forming within this innovative chromatographic technology

Angela Fromme, Colin Fischer, Kristina Keine, Gerhard Schembecker

Accurate knowledge of the flow regime within the Centrifugal Partition Chromatography (CPC) is crucial for designing an efficient separation process. The fact that the direct analysis of the flow regime in apparatuses of industrial dimensions is impossible due to their stacked rotor construction is a fundamental challenge. Thus, valid correlations are needed to determine the flow regime inside the CPC based on the properties of the solvent system and operational parameters.

The separation efficiency in CPC is significantly affected by the size of the interfacial area between both liquid phases. Consequently, it is advantageous that the mobile phase is finely dispersed in the stationary phase. The degree of dispersion is classified into four different flow regimes: undispersed, low dispersed, highly dispersed, and atomized.

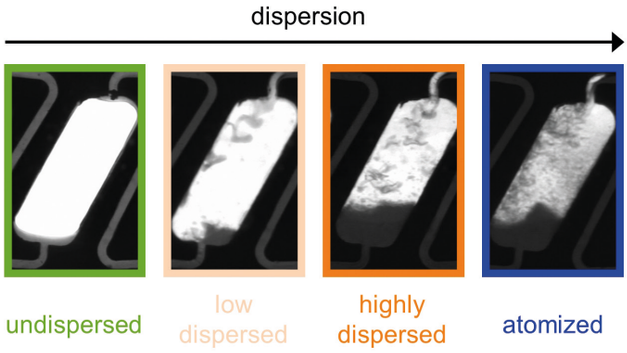

Figure 1: Different flow regimes within the CPC.

Those states described in Figure 1 are influenced by the physical properties of the solvent system and the operating parameters. A dimensional analysis was performed to correlate these parameters with the state of dispersion, resulting in three different dimensionless numbers:

1) The Ohnesorge number (Oh_{CPC}) describing the ratio of viscous forces to surface stress forces.

2) The Eötvös number (Eo_{CPC}) expressing the ratio of gravity forces to surface stress or capillary forces.

3) The Weber number describing the ratio of inertia forces to surface stress (We_{CPC}).

Subsequently, the correlation between the dimensionless numbers and the flow regime was investigated. The flow regime of various aqueous-organic solvent systems was analyzed inside a single-rotor setup using a monochromatic highspeed camera. Additionally, the mobile phase volume flow and the rotational speed were varied. The flow regime for each set of parameters was determined by eye, and the results are shown in Figure 2:

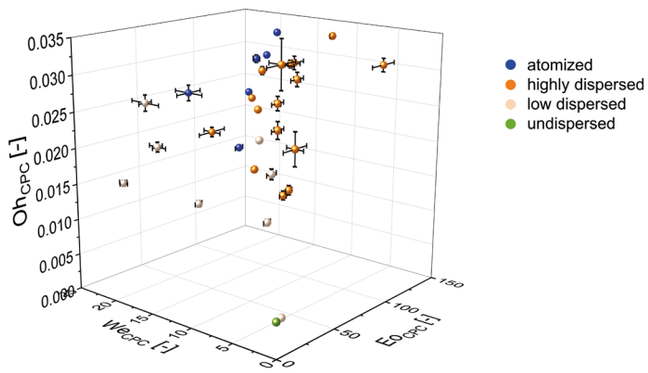

Figure 2: States of mobile phase dispersion in dependency of the Weber number, the Eötvös number, and the Ohnesorge number in descending mode at 25 °C.

It can be seen that each flow regime occurs in a discrete volume element inside the three-dimensional diagram. Hence, with the three dimensionless numbers used in this study, it is possible to predict the dispersion inside of a CPC chamber.

If the aim is to increase the interfacial area in the CPC chamber, some general heuristics can be derived from the results obtained. With increasing dimensionless numbers, the degree of dispersion also increases. Regarding the physical properties of the phases, a high viscosity of the mobile phase leads to a higher Ohnesorge number. The density difference should be increased as well since it leads to a high Eötvös number. As all dimensionless numbers increase with decreasing interfacial tension, the latter should be low to achieve a good dispersion inside the CPC chamber.

Those results decisively simplify the selection of phase system and operating point when designing a separation task.

Publications:
A. Fromme, C. Fischer, K. Keine, G. Schembecker, J CHROMATOGR A. 1620, 2440-2451 (2020).

Contact:
felix.buthmann@tu-dortmund.de
gerhard.schembecker@tu-dortmund.de

Publications 2020 - 2018

2020

Peer-Reviewed Journal Papers

- J. Koop, J. Merz, C. Pietzsch, G. Schembecker
  Contribution of Secondary Structure Changes to the Surface Activity of Proteins
  Journal of Biotechnology 323, 208-220 (2020)

- I. Lukin, I. Wingartz, G. Schembecker
  Application of rotating packed bed for in-line aroma stripping from cell slurry
  Journal of Chemical Technology & Biotechnology 95 (11), 2834-2841 (2020)

- M. Peterwitz, R. Loll, J. Jodwirschat, G. Schembecker
  Evaluating the potential of adjusting axial back mixing in continuous manufacturing of solid oral dosage forms
  Chemie Ingenieur Technik 92 (9), 1162-1162 (2020)

- J. Koop, J. Merz, R. Wilmshöfer, R. Winter, G. Schembecker
  Influence of thermally induced structure changes in diluted β-lactoglobulin solutions on their surface activity and behavior in foam fractionation
  Journal of Biotechnology 319, 61-68 (2020)

- I. Lukin, L. Pietzka, K. Groß, A. Górak, G. Schembecker
  Economic evaluation of rotating packed bed use for aroma absorption from bioreactor off-gas
  Chemical Engineering and Processing-Process Intensification 154, 108011 (2020)

- A. Fromme, C. Fischer, D. Klump, G. Schembecker
  Correlating the phase settling behavior of aqueous-organic solvent systems in a centrifugal partition chromatograph
  Journal of Chromatography A 1620, 461005 (2020)

- A. Fromme, C. Fischer, K. Keine, G. Schembecker
  Characterization and correlation of mobile phase dispersion of aqueous-organic solvent systems in centrifugal partition chromatography
  Journal of Chromatography A 1620, 460990 (2020)

- L. David, P. Schwan, M. Lobedann, S.O. Borchert, B. Budde, M. Temming
  Side-by-side comparability of batch and continuous downstream for the production of monoclonal antibodies
  Biotechnology and bioengineering 117 (4), 1024-1036 (2020)

- L. David, M.P. Bayer, M. Lobedann, G. Schembecker
  Simulation of continuous low pH viral inactivation inside a coiled flow inverter
  Biotechnology and bioengineering 117 (4), 1048-1062 (2020)

- A. Fromme, F. Funke, J. Merz, G. Schembecker
  Correlating physical properties of aqueous-organic solvent systems and stationary phase retention in a centrifugal partition chromatograph in descending mode
  Journal of Chromatography A 1615, 460742 (2020)

- L. David, L.M. Waldschmidt, M. Lobedann, G. Schembecker
  Simulation of pH level distribution inside a coiled flow inverter for continuous low pH viral inactivation
  Biotechnology and bioengineering 117 (2), 429-437 (2020)

- C. Post, N. Wentingmann, C. Bramsiepe, G. Schembecker
  Using design spaces for more accurate cost estimation during early engineering phases
  Chemical Engineering Research and Design 153, 592-602 (2020)

Publications 2020 - 2018

2019

Peer-Reviewed Journal Papers

- A. Fromme, F. Funke, J. Merz, G. Schembecker
  Correlating physical properties of aqueous-organic solvent systems and stationary phase retention in a centrifugal partition chromatograph in descending mode
  Journal of Chromatography A (2019) 1615 - DOI: 10.1016/j.chroma.2019.460742

- D. Wetzel, A. Barbian, V. Jenzelewski, G. Schembecker, J. Merz, M. Piontek
  Bioprocess optimization for purification of chimeric VLP displaying BVDV E2 antigens produced in yeast Hansenula polymorpha
  (2019) Journal of Biotechnology, 306, pp. 203-212, DOI: 10.1016/j.jbiotec.2019.10.008

- I. Lukin, G. Jach, I. Wingartz, P. Welters, G. Schembecker
  Recovery of Natural α-Ionone from Fermentation Broth
  (2019) Journal of Agricultural and Food Chemistry, 67 (49), pp. 13412-13419, DOI: 10.1021/acs.jafc.8b07270

- I. Kaplanow, F. Goerzgen, J. Merz, G. Schembecker
  Mass Transfer of Proteins in Aqueous Two-Phase Systems
  (2019) Scientific Reports, 9 (1), art. no. 3692, DOI: 10.1038/s41598-019-39797-9

- L. David, J. Niklas, B. Budde, M. Lobedann, G. Schembecker
  Continuous viral filtration for the production of monoclonal antibodies
  (2019) Chemical Engineering Research and Design, 152, pp. 336-347, DOI: 10.1016/j.cherd.2019.09.040

- M. Termühlen, B. Strakeljahn, G. Schembecker, K. Wohlgemuth
  Characterization of slug formation towards the performance of air-liquid segmented flow
  (2019) Chemical Engineering Science, 207, pp. 1288-1298, DOI: 10.1016/j.ces.2019.07.033

- M. Eilermann, C. Schach, P. Sander, C. Bramsiepe, G. Schembecker
  Generation of an equipment module database — A maximum coverage problem
  (2019) Chemical Engineering Research and Design, 148, pp. 164-168, DOI: 10.1016/j.cherd.2019.05.055

- H. Radatz, M. Schröder, C. Becker, C. Bramsiepe, G. Schembecker
  Selection of equipment modules for a flexible modular production plant by a multi-objective evolutionary algorithm
  (2019) Computers and Chemical Engineering, 123, pp. 196-221, DOI: 10.1016/j.compchemeng.2018.12.009

- L. David, B. Maiser, M. Lobedann, P. Schwan, M. Lasse, H. Ruppach, G. Schembecker
  Virus study for continuous low pH viral inactivation inside a coiled flow inverter
  (2019) Biotechnology and Bioengineering, 116 (4), pp. 857-869, DOI: 10.1002/bit.26872

- H. Radatz, K. Kühne, C. Bramsiepe, G. Schembecker
  Comparison of capacity expansion strategies for chemical production plants
  (2019) Chemical Engineering Research and Design, 143, pp. 56-78, DOI: 10.1016/j.cherd.2018.12.018

- S. Heisel, J. Ernst, A. Emshoff, G. Schembecker, K. Wohlgemuth
  Shape-independent particle classification for discrimination of single crystals and agglomerates
  (2019) Powder Technology, 345, pp. 425-437, DOI: 10.1016/j.powtec.2019.01.018

- D. Wetzel, J.-A. Chan, M. Suckow, A. Barbian, M. Weniger, V. Jenzelewski, L. Reiling, J.S. Richards, D.A. Anderson, B. Kouskousis, C. Palmer, E. Hanssen, G. Schembecker, J. Merz, J.G. Beeson, M. Piontek
  Display of malaria transmission-blocking antigens on chimeric duck hepatitis B virus-derived virus-like particles produced in Hansenula polymorpha
  (2019) PLoS ONE, 14 (9), art. no. e0221394, DOI: 10.1371/journal.pone.0221394

- S. Heisel, J. Holtkötter, K. Wohlgemuth
  Measurement of agglomeration during crystallization: Is the differentiation of aggregates and agglomerates via ultrasonic irradiation possible?
  (2019) Chemical Engineering Science, 210, art. no. 115214, DOI: 10.1016/j.ces.2019.115214

Publications 2020 - 2018

2018

Peer-Reviewed Journal Papers

- M.-C. Lührmann, J. Timmermann, G. Schembecker, K. Wohlgemuth
  Enhanced Product Quality Control through Separation of Crystallization Phenomena in a Four-Stage MSMPR Cascade
  Crystal Growth & Design 18 (2018) 7323-7334

- M. Eilermann, A. Tebbe, D. Schwarz, S. Leufke, C. Bramsiepe, G. Schembecker
  Approach for the characterization of industrial process tasks as basis for the generation and application of an equipment module database
  Chemical Engineering Science 191 (2018) 42-55

- M. Eilermann, C. Post, H. Radatz, C. Bramsiepe, G. Schembecker
  A general approach to module-based plant design
  Chemical Engineering Research and Design 137 (2018) 125-140

- I. Kaplanow, J. Stecker, G. Schembecker, J. Merz
  Multistage Processing of Tunable Aqueous Polymer Phase Impregnated Resins (TAPPIR®)
  Chemical Engineering and Technology 41 (2018) 1324-1330

- I. Lukin, J. Merz, G. Schembecker
  Techniques for the recovery of volatile aroma compounds from biochemical broth: A review
  Flavour and Fragrance Journal 33 (2018) 203-216

- D. Wetzel, T. Rolf, M. Suckow, T. Rolf, M. Suckow, A. Kranz, A. Barbian, J-A. Chan, J. Leitsch, M. Weniger, V. Jenzelewski, B. Kouskousis, C. Palmer, J.G. Beeson, J. Merz, M. Piontek
  Establishment of a yeast-based VLP platform for antigen presentation
  Microbial Cell Factories 17 (2018) 17

- M.- C. Lührmann, M. Termühlen, J.Timmermann, G. Schembecker, K. Wohlgemuth
  Induced nucleation by gassing and its monitoring for the design and operation of an MSMPR cascade
  Chemical Engineering Science 192 (2018) 840-849

- T. Kleetz, R. Scheel, G. Schembecker, K. Wohlgemuth
  Cooling Crystallization: Does Gassing Compete with Seeding?
  Crystal Growth & Design 18 (2018) 4906-4910

- S. Heisel, M. Rolfes, K. Wohlgemuth
  Discrimination between Single Crystals and Agglomerates during the Crystallization Process
  Chemical Engineering and Technology 41 (2018) 1218-1225

- M.-C. Ostermann, M. Termühlen, G. Schembecker, K. Wohlgemuth
  Growth Rate Measurements of Organic Crystals in a Cone-Shaped Fluidized-Bed Cell
  Chemical Engineering and Technology 41 (2018) 1165-1172

- L. Hohmann, T. Greinert, O. Mierka, S. Turek, G. Schembecker, E. Bayraktar, K. Wohlgemuth, N. Kockmann
  Analysis of Crystal Size Dispersion Effects in a Continuous Coiled Tubular Crystallizer: Experiments and Modelling
  Crystal Growth & Design 18 (2018) 1459–1473

- I. Kaplanow, M. Schmalenberg, I. Borgmann, G. Schembecker, J. Merz
  Tunable Aqueous Polymer Phase Impregnated Resins (TAPPIR®): Investigation of the impregnation stability
  Separation and Purification Technology 190 (2018) 1-8

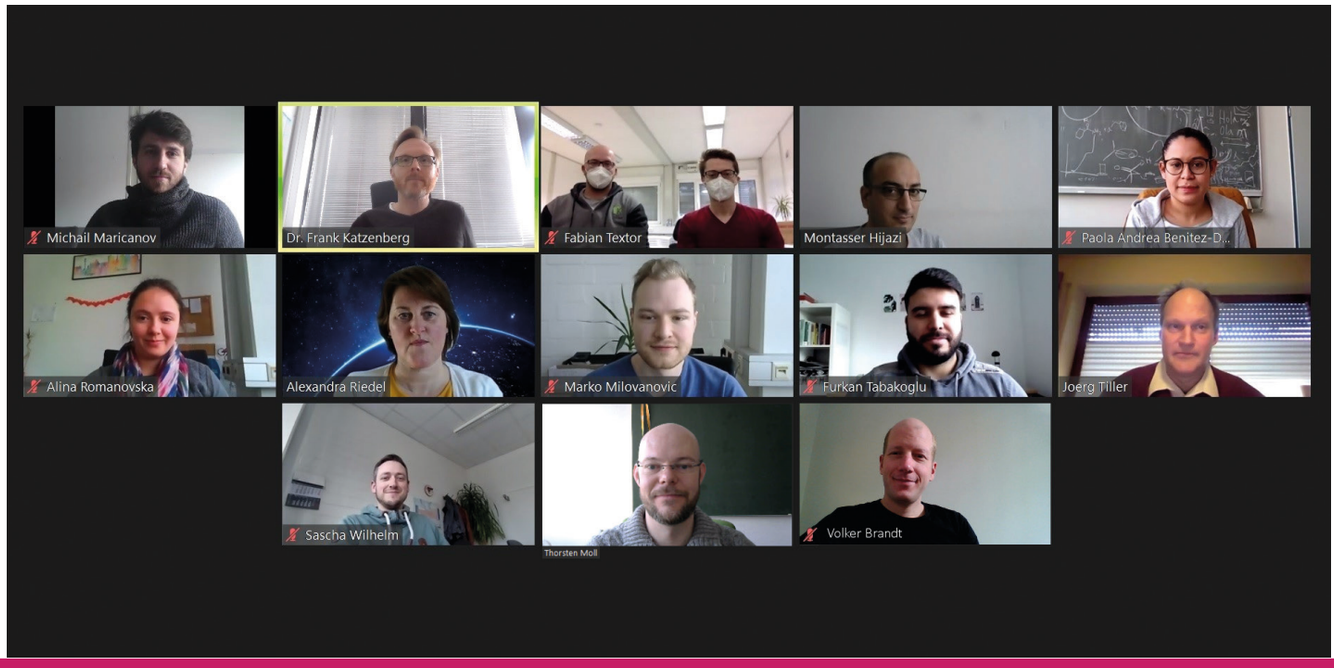

Biomaterials and Polymer Science (BMP)

X-Ray Analysis Reveals the Dynamic Changes of Inner Structure of APCNs During Swelling

Nanostructured amphiphilic polymer conetworks (APCNs) change their inner structure during swelling depending on their topology

Lena Benski, Ismail Viran, Frank Katzenberg, Joerg C. Tiller

Amphiphilic polymer conetworks (APCNs) are transparent nanomaterials that are best known as soft contact lenses, but have also importance in other fields of medicine and can be used as separation membranes and as carrier material for catalysts and biocatalysts. So far APCNs are considered as materials that contain two polymer phases that can be swollen independently in orthogonal solvents. This is the basis of their many applications. In this study, we could show for the first time that this is not the case and the phases change their nanostructure depeding on the molecular composition of the polymer networks - their topology.

The aim of this study was to gain a better insight into the structure of the nanophases of APCNs swollen in a solvent that is selective to one phase. To this end, APCNs based on hydrophilic PMOx (30 repeating units) acting as the crosslinker and hydrophobic 2-ethylhexyl acrylate (EhAc) acting as the polymer phase were prepared (see Figure 1) and analyzed using small-angle X-ray scattering (SAXS) in order to gain information on the swollen state of the nanophases in water and toluene.

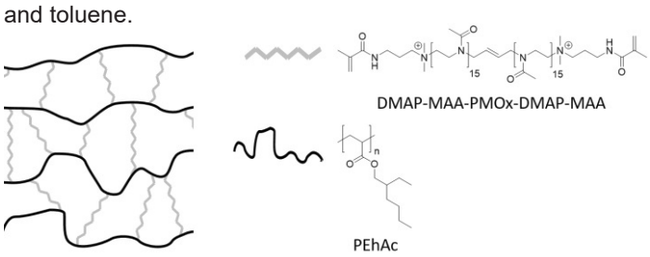

Figure 1: Schematic overview of the prepared APCNs with the hydrophilic N-[3-(Dimethylamino)-propyl]-methacrylamide (DMAP-MAA) terminated poly(2-methyl-2-oxazoline) (PMOx) acting as macrocrosslinker and the hydrophobic poly(2-ethylhexyl acrylate) (PEhAc) acting as polymer phase.

The SAXS measurements on APCNs swollen in orthogonal indicate revealed that structural change upon swelling is strongly dependent on the topology of the APCN (Figure 2).

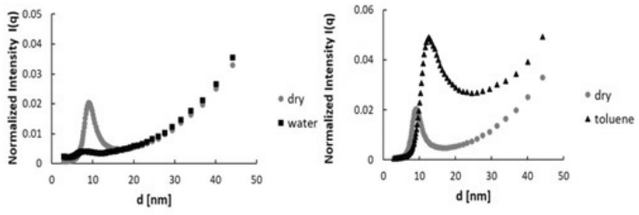

Figure 2: SAXS profiles obtained from PEhAc-l-PMOx conetworks with a PMOx content of 70 wt% that were swollen in water (left) or toluene (right). Intensities were accumulated over 4 h and normalized to the overall counts of the respective measurement.

As exemplarily shown in Figure 2, the regular nanophases indicated by the narrow peak at 10 nm in the dry sample is increasing in size by swelling in toluene retaining the overall regular nanostructure of the material (Figure 2, right). In contrast, swelling in water leads to a loss in regular structure (Figure 2, left).

Contact:
lena.benski@tu-dortmund.de
frank.katzenberg@tu-dortmund.de
joerg.tiller@tu-dortmund.de

The nanophase separation shown by AFM and the swelling data of these APCNs suggest a homogeneous swelling of each individual polymer phase with a respective selective solvent over a broad range of compositions. SAXS data revealed that this is not true for both phases, but the crosslinker phase is more isolated than visible in the AFM images and the selective solvent is not fully swelling this phase excluding isolated non-swollen regions. The model of the topologically dependent swelling is shown in Figure 3 suggests that the topologically isolated cross-linker phase cannot swell without changing its nanostructure.

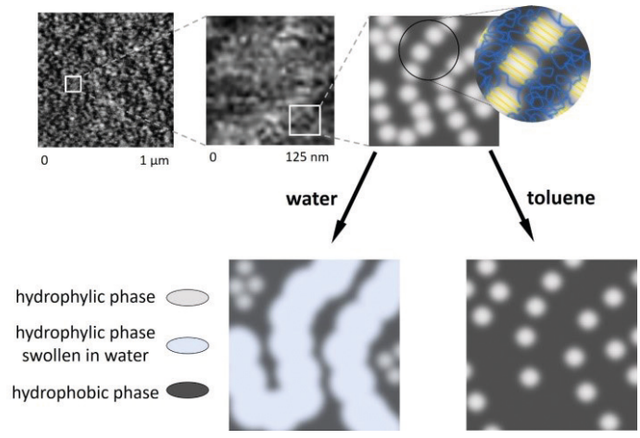

Figure 3: AFM image of the dry APCN PEhAc-l-PMOx(70) 1 x 1 µm (top, left) and schematic illustrations of the magnified image in dry (top, right) and the swollen phases in water (bottom, left) and in toluene (bottom, right).

This finding is of importance for the applications of APCNs particularly in fields of drug delivery. Further, the present study shows that it might be useful to investigate APCNs more thoroughly with scattering methods to better reveal their true swelling behavior.

Publications:
L. Benski, I. Viran, F. Katzenberg, J.C. Tiller, Small-Angle X-Ray Scattering Measurements on Amphiphilic Polymer Conetworks Swollen in Orthogonal Solvents. Macromol. Chem. Phys. 2021, 222, 2000292.

Thermal ON/OFF Switches for Enzymes

Enzymes fully inhibited by LCST polymers with an enzyme inhibitor end group recover their activity at higher temperatures

Montasser Hijazi, Esra Türkmen, Joerg C. Tiller

Great efforts have been made to control the activity of enzymes, which is an important issue in biomedical and analytical applications. Several examples in the literature describe enzyme inhibitors that can be switched by temperature or light. However, these inhibitors can either not fully inhibit the enzyme activity or cannot fully recover it. In the present study, we designed enzyme inhibitors by terminating LCST poly(2-oxazoline)s (POx) with an IDA group, which are able to fully inhibit the enzyme laccase and horse radish peroxidase. Increasing the temperature leads to full recovery of the enzyme activity. This is the first example of full ON/OFF switch of biocatalysts.

Several approaches in the literature attach enzyme inhibitors to the side chains of thermo-responsive polymers. Although they collapse at a certain temperature, the inhibitors are still at the surface of the collapsed coils. We propose that this can be circumvented by using enzyme inhibitors attached to the terminal of a thermo-sensitive polymer (Figure 1). A macromolecule designed this way should be able to “hide” the inhibitor inside the coil after thermally induced phase transition, which should enable a full ON and OFF switching of the enzyme activity.

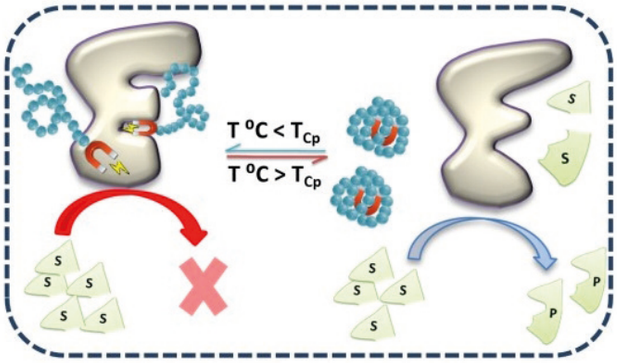

Figure 1: Concept of a thermal ON/OFF switch of enzyme activity by an inhibitor terminated LCST polymer.

We have previously reported on POx with an iminodiacetic acid (IDA) end group (POx-IDA) as a very efficient enzyme inhibitor. In order to render POx-IDA into a thermo-switchable enzyme inhibitor, a number of different POx with a lower critical solution temperature (LCST) was synthesized by polymerizing various 2-alkyl-2-oxazolines (e.g. 2-ethyl-2-oxazoline (EtOx) and 2-butyl-2-oxazoline (BuOx)) as homopolymers and statistical copolymers that are known as LCST polymers followed by terminating them with an IDA group. The transition temperature (cloud point, T_{cp}) at which the different POx-IDA go from the soluble to the insoluble state can be varied between 4 and 48°C. The transition starts at a temperature ($T_{cp,\ on}$), where the enzyme is fully inhibited and ends at a temperature ($T_{cp,\ off}$), where the enzyme activity is fully recovered. As shown exemplarily for laccase, the enzyme can be switched with temperature (Figure 2). This process is fully reversible and can be repeated several times. The same is true for horse radish peroxidase. Further, POx-IDA can be removed from the mixture above T_{cp} by filtration.

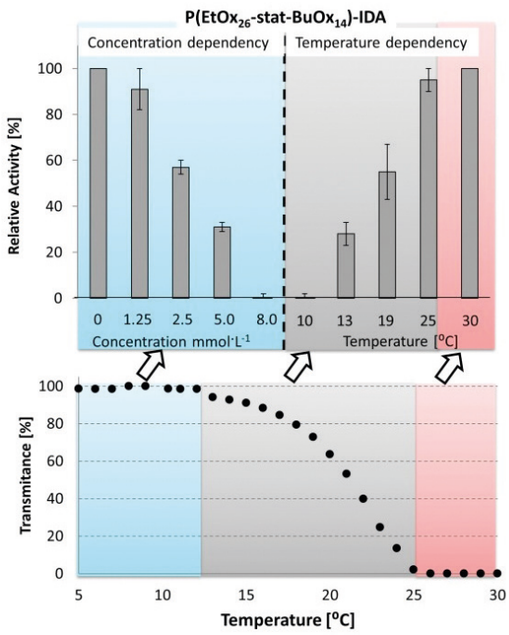

Figure 2: Top Left: Change in activity of laccase at 10 °C as function of the concentration of P($EtOx_{26}$-stat-$BuOx_{14}$)-IDA; Top Right: Change in activity of laccase at different temperatures in the presence of 8 mM P($EtOx_{26}$-stat-$BuOx_{14}$)-IDA. Bottom: Turbidity curve of P($EtOx_{26}$-stat-$BuOx^{14}$)-IDA in aqueous acetate buffer (100 mM, pH 5.0) + 2.8 mM 2,4-Dimethylphenol (DMP). The laccase assay was performed in acetate buffer with DMP as substrate.

The here presented approach will likely be applicable for a broad range of temperature-controllable enzymatic processes. The selectivity of some of the here shown inhibitors might be used to temperature control the activity of enzymes in multi-enzyme systems.

Publications:
M. Hijazi, E. Türkmen, J.C. Tiller
Chemistry – A European Journal 2020, 26(59):13367-13371.

Contact:
montasser.hijazi@tu-dortmund.de
joerg.tiller@tu-dortmund.de

How can Stable Amorphous $CaCO_3$ (ACC) Nanoparticles be Formed within a Hydrogel?

The positive site of glyphosate as stabilizer for ACC

Marko Milovanovic, Joerg C. Tiller

$CaCO_3$ is mostly found in nature as crystalline material. It is originally formed as amorphous $CaCO_3$ (ACC), which is very unstable and crystallizes quickly. Living organisms can stabilize ACC and can thus use it to form very stable exoskeletons in fantastic shapes, e.g. in corals. So far, stabilizing ACC in matrix materials was not possible, thus, artificially mimicking structures similar to the ones found in nature was hardly possible. We found that the enzyme-induced formation of calcium carbonate within hydrogels results in stable ACC nanoparticles in the presence of the infamous pesticide glyphosate.

Enzyme-induced mineralization with $CaCO_3$ is possible by soaking a urease containing hydrogel in an aqueous solution of $CaCl_2$ and urea. The enzyme urease hydrolyzes urea to form carbonate ions, which then bind to the Ca^{2+} ions resulting in the precipitation of $CaCO_3$. The salt is first amorphous (ACC), but quickly forms the crystal modifications aragonite and/or calcite (Figure 1). We explored numerous known crystallization inhibitors for calcium carbonate in free suspension, regarding their ability to stabilize the ACC in the hydrogels. However, none of those suppressed the crystallization of amorphous particles in hydrogel phases.

Figure 1: Schematic representation of hydrogel calcification. Absence of crystallization inhibitors leads to the formation of crystalline $CaCO_3$, while the presence of inhibitors should lead to stabilization of amorphous phases.

By looking for analogs of natural crystallization inhibitors for ACC, we found that the infamous molecule *N*-(phosphonomethyl)glycine, also known as glyphosate, can stabilize amorphous calcium carbonate for several weeks in water swollen hydrogels and for several months in dry state. Furthermore, the calcification in the presence of glyphosate ensures a homogeneous distribution of the precipitated amorphous inorganic material, as depicted in Figure 2. The stabilization of ACC was found to be due to the presence of glyphosate in combination with the confinement within the hydrogel, which is independent on the chemical nature of the polymeric material.

By increasing the calcification temperature and adding Mg^{2+} ions, the precipitated amount of ACC in the hydrogel can be increased. Different concentrations of glyphosate and Mg^{2+} ions can be synergistically used to selectively precipitate most of the commonly known $CaCO_3$ modifications.

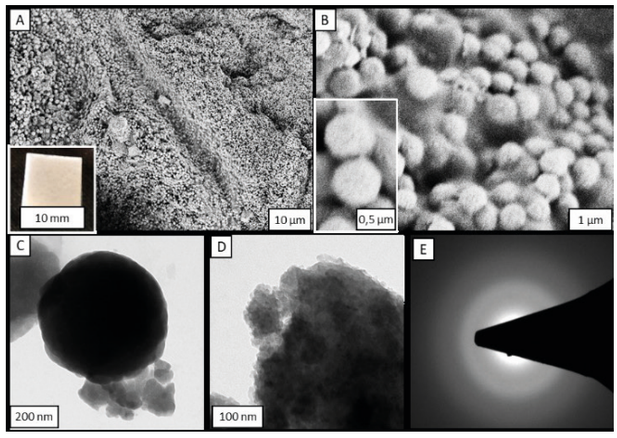

Figure 2: SEM-images and exemplary TEM-SAED-Image of a mineralized PDMA-l-TEG after calcification in the presence of *N*-(phosphonomethyl)glycine (glyphosate 1 g l^{-1}) at 20 °C for 24 h.

It is possible to isolate calcium carbonate particles of different modifications from the hydrogel by thermal degradation at different temperatures. Further, during storage of the ACC containing hydrogels in water, a calcite layer is formed at the surface of the hydrogel, which linearly grows in thickness over time. This offers the possibility to build an intrinsically scratch resistant surface on hydrogels.

Controlling the mineralization and crystallization as well as varying the hydrogel might lead to a wide variety of composite materials with different properties, such as improved mechanical performance.

Contact:
marko.milovanovic@tu-dortmund.de
joerg.tiller@tu-dortmund.de

Publications:
M. Milovanovic, T. Unruh, V. Brandt, J.C. Tiller, Forming amorphous calcium carbonate within hydrogels by enzyme-induced mineralization in the presence of *N*-(phosphonomethyl)glycine. Journal of Colloid and Interface Science 2020, 579, 357-368.

Realizing a Shape-Memory Effect for Synthetic Rubber (IR)

New exceptional shape-memory polymers

Dominik Segiet, Laura M. Neuendorf, Joerg C. Tiller, Frank Katzenberg

Lightly crosslinked natural rubber (NR) offers an exceptional shape memory effect (SME) with huge strain and energy storage capacity and tunable trigger temperature near body temperature. Unfortunately, this SME, referred to as shape memory natural rubber (SMNR), is not suitable for biomedical applications due to a content of some proteins that can cause anaphylactic shock by a hypersensitivity of the immune system. However, networks of protein-free industrial rubber (IR), the synthetic analog of NR, are also unsuitable for such applications, since their trigger temperatures are far below room temperature. We demonstrate that additivation with stearic acid (StA) as well as poly(2-ethyl-2-oxazoline) (PEtOx) is an efficient tool for solving this problem and realizing an SME for IR networks with properties comparable with those of SMNR.

The objective of this work was to realize a biocompatible shape-memory polymer (SMP) similar to SMNR based on protein-free industrial rubber. To this end, synthetic rubber IR SKI-3 (IR) was chosen and two different approaches were followed. Firstly, we explored the influence of stearic acid (StA) on the 'intrinsic' shape-memory effect (SME) of IR. Secondly, we blended IR with the biocompatible poly(2-ethyl-2-oxazoline) (PEtOx) prior to crosslinking to obtain an 'extrinsic' SME. We found that by addition of less than 10 wt% StA the melting temperature of the strain-fixing poly(cis-1,4-isoprene) crystals and thus the trigger temperature of cold- and hot-programmed IR can be efficiently increased up to 26.2 °C and 33.5 °C, respectively. Figure 1 shows the T_{trig} of cold-programmed IR-networks. While the shape-memory parameters stay nearly uninfluenced, the width of the trigger range becomes broader by addition of StA).

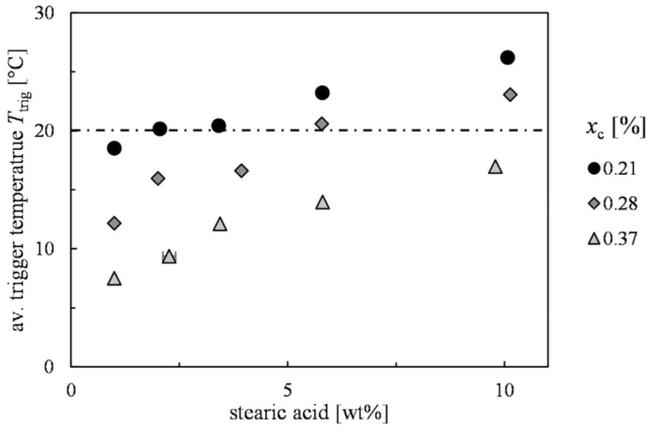

Figure 1: Trigger temperatures of cold-programmed IR-SKI-3 networks in dependence on the StA concentration.

As a second approach, we blended IR with the amorphous amphiphilic high polymer poly(2-ethyl-2-oxazoline) (PEtOx) to obtain an extrinsic glass transition-based SME with trigger temperature above RT and another benefit; the triggerability by polar solvents such as water. We found for IR/PEtOx networks with PEtOx concentrations up to 30 wt% that the intrinsic shape-memory effect of IR is dominant and that PEtOx effectively increases the melting/trigger temperature of the poly(cis-1,4-isoprene) crystals. At higher concentrations, the networks show a decreasing T_{trig} up to a concentration of 50 wt% PEtOx. Networks with compositions in this intermediate region are stabilized by both, the crystals of IR and the high T_g nanophases of PEtOx, see Figure 2.

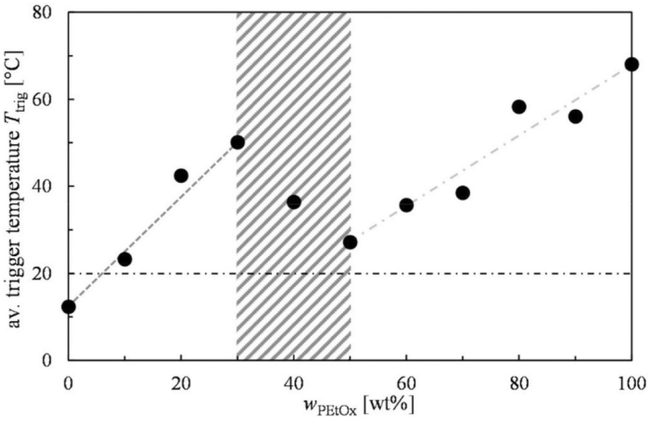

Figure 2: Trigger temperatures of IR-SKI-3/PEtOx conetworks in dependence on PEtOx concentration.

At high PEtOx concentrations above 60 wt%, no IR crystals were observed anymore and the extrinsic shape-memory effect based on PEtOx is the only shape stabilizing effect. Depending on composition, the trigger temperatures range from 18 °C (100 % IR) to 68 °C (100 % PEtOx) and maximum storable strains vary from 1000 % (100 % IR) to 240 % (100 % PEtOx), respectively. Besides heat, we found that water as well as acetone and DMF are capable of triggering all programmed IR-PEtOx networks with more than 40 wt% of PEtOx, while toluene and p-xylene were found to trigger all IR/PEtOx networks with IR contents above 30 %. Furthermore, the as-prepared IR/PEtOx networks are the first example of nanophase-separated APCNs prepared by crosslinking of a polymer blend in bulk.

Concluding, both methods have the potential of making IR a protein-free and efficient, and in the case of IR/PEtOx also water-triggerable SMP that can be applied for biomedical purposes.

Contact:
frank.katzenberg@tu-dortmund.de

Publications:
D. Segiet, L. M. Neuendorf, J. C. Tiller, F. Katzenberg,
Polymer 2020, 203, 122788.

Thermo-Responsive Volume-Changes of PEtOx Hydrogels

New insights into the LCST behavior of hydrogels

Dominik Segiet, Robert Jerusalem, Frank Katzenberg, Joerg C. Tiller

Hydrogels that react with dimension changes triggered by temperature are important smart materials for medical applications, such as drug delivery at body temperature, or engineering designs, e.g. temperature-dependent opening and closing of flow channels in microfluidic devices. Although hydrogels composed of poly(N-isopropylacrylamide) (PNiPAM) are well understood, little is known about thermo-responsive hydrogels based on other polymers. Such knowledge is important to broaden the application of smart hydrogels to other temperature ranges and to be able to use polymers that can bear more functionalities and/or are less toxic than PNiPAM. The present study reveals fundamental structure/property relations that might be useful to generally predict the behavior of thermo-responsive hydrogels.

In this work, thermo-responsive hydrogels based on poly-2-ethyl-2-oxazoline (PEtOx) were prepared by cross-linking the commercially available high polymer. PEtOx shows a lower critical solution temperature (LCST) in water, i.e., it is water-soluble at low temperatures and precipitates above LCST. When using this behavior in a hydrogel, the material would shrink with higher temperature. In contrast to the LCST polymer PNiPAM, the transition temperature T_{cp} of PEtOx from soluble to insoluble state is concentration dependent, which might play a role for the hydrogel as well. We found that the degree of swelling S of the PEtOx hydrogels linearly decreases with higher temperatures and all differently cross-linked hydrogels converge in a so called “break point temperature” T_{BP} for a certain polymer/solvent system. While the T_{BP} of hydrogels prepared from PEtOx with a low molecular weight of 10 kg mol^{-1} were found at 72 °C, the T_{BP} of hydrogels based on PEtOx with a high molecular weight of 122 kg mol^{-1} was found at 66 °C. The T_{BP} of the hydrogels increased further to 79 °C when adding 8 wt% ethanol to the water. Thus, it could be shown that the T_{BP} of the synthesized PEtOx hydrogels correlates with the LCST of the respective starting PEtOx.

The net chain molecular weight M_c only affects the maximum degree of swelling and, thus, the swelling-deswelling rate dS/dT of the hydrogel. It was found that the full temperature-induced transition occurs below LCST and the transition range is broad and nearly linear in contrast to other reported LCST hydrogels (see Figure 1a). The hydrogels do not cloud during the experiments, as seen in Figure 1b and c.

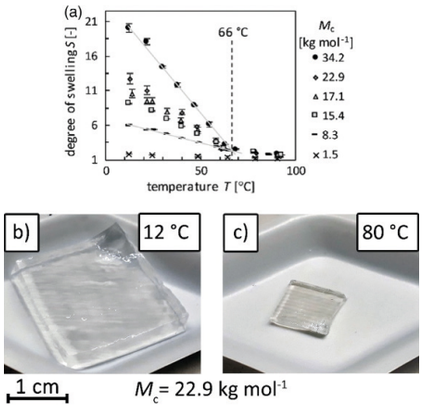

Figure 1: a) Temperature-dependent swelling curves of PEtOx hydrogels. b) PEtOx hydrogel below T_{BP}, c) PEtOx hydrogel above T_{BP}.

Contact:
joerg.tiller@tu-dortmund.de

Considering that due to entropic reasons polymer chains cannot aggregate in a polymer network as opposed to linear chains in a solution, it is reasonable to assume that the swelling behavior of a hydrogel correlates to the hydrodynamic radius R_h of a polymer in solution measured via light scattering. This assumption fits well with light scattering experiments of highly diluted, narrowly distributed, high molecular weight PNiPAM by Wu et al., who showed that S and R_h truly correlate (see Figure 2). Thus, instead of performing light scattering experiments, the S versus T curve can be considered to obtain information about the coil-to-globule transition of a polymer in a solution.

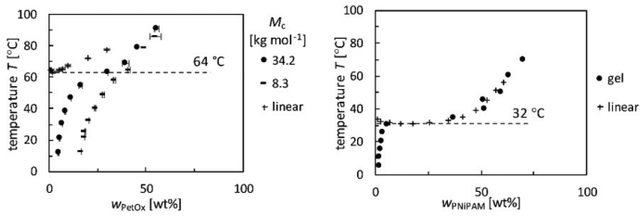

Figure 2: Phase diagrams containing the cloud point temperature T_{cp} of the starting left) PEtOx and right) PNiPAM and the swelling curves of the respective cross-linked networks in water.

Further, we found that for estimating the transition range of LCST hyrogels, the concentration-dependent T_{cp} curve can be considered, since only polymers that have practically no temperature-dependent T_{cp} are promising candidates for LCST hydrogels with a narrow swelling transition.

Although PEtOx hydrogels show no narrow transition range, they are interesting candidates for membranes with continuously adjustable permeability, shown in previous work on the example of thermo-sensitive amphiphilic polymer conetworks. Accordingly, dS/dT, the maximum degree of swelling S, as well as T_{BP}, below which the thermo-responsiveness of a PEtOx hydrogel is amplified by solvation, can be tailored as well as adapted to the requirements of a potential application.

Publications:
D. Segiet, R. Jerusalem, F. Katzenberg, J.C. Tiller,
J. Polym.Sci, Part B: Polym. Phys. 2020, 58, 747-755.

Publications 2020 - 2018

2020

Peer Reviewed Articles

- M. Milovanovic, M. T. Unruh, V. Brandt, J. C. Tiller
  Forming amorphous calcium carbonate within hydrogels by enzyme-induced mineralization in the presence of N-(phosphonomethyl) glycine
  Journal of Colloid and Interface Science 579, 357-368 (2020)

- M. Hijazi, E. Tuerkmen, J. C. Tiller
  Poly(2-oxazoline)s with a 2,2′- Iminodiacetate End Group Inhibit and Stabilize Laccase
  ChemBioChem 21, 874-882 (2020)

- D. Segiet, R. Jerusalem, F. Katzenberg, J. C. Tiller
  Investigation of the Swelling Behavior of Hydrogels Derived from High Molecular Weight Poly(2-Ethyl-2-Oxazoline)
  Journal Polymer Science, Part B: Polymer Physics 58, 747–755 (2020)

- M. Breisch, K. Loza, K. Pappert, A. Rostek, C. Rurainsky, K. Tschulik, M. Heggen, M. Epple, J. C. Tiller, T. A. Schildhauer, M. Köller, C. Sengstock
  Enhanced dissolution of silver nanoparticles in a physical mixture with platinum nanoparticles based on the sacrificial anode effect
  Nanotechnology 31, 055703 (2020)

- C. Krumm, S. Trump, L. Benski, J. Wilken, F. Oberhaus, M. Köller, J. C. Tiller
  Fast-Acting Antibacterial, Self-Deactivating Polyionene Esters
  ACS Applied Materials Interfaces 12, 21201–21209 (2020)

- D. Segiet, L. M. Neuendorf, J. C. Tiller, F. Katzenberg
  Realizing a shape-memory effect for synthetic rubber (IR)
  Polymer 203, 122788 (2020)

- M.Hijazi, E. Tuerkmen, J. C. Tiller
  Full Thermal Switching of Enzymes by Thermoresponsive Poly(2-oxazoline)-Based Enzyme Inhibitors
  Chemistry A European Journal 26, 13367-13371 (2020)

2019

Peer Reviewed Articles

- L. Benski, J. C. Tiller
  Telechelic biocidal poly(2-oxazoline)s and polycations
  European Polymer Journal 2019, 120, 109233

- M. Breisch, V. Grasmik, K. Loza, K. Pappert, A. Rostek, N. Ziegler, A. Ludwig, M. Heggen, M. Epple, J. C. Tiller, T. A. Schildhauer, M. Köller, C. Sengstock
  Bimetallic silver–platinum nanoparticles with combined osteo-promotive and antimicrobial activity
  Nanotechnology 2019, 30, 305101

- M. Breisch, K. Loza, K. Pappert, A. Rostek, C. Rurainsky, K. Tschulik, M. Heggen, M. Epple, J. C. Tiller, T. A. Schildhauer, M. Köller, C. Sengstock
  Enhanced dissolution of silver nanoparticles in a physical mixture with platinum nanoparticles based on the sacrificial anode effect
  Nanotechnology 2019, 31, 055703

- M. Hijazi, P. Spiekermann, C. Krumm, J. C. Tiller
  Poly(2-oxazoline)s terminated with 2,2′-imino diacetic acid form noncovalent polymer–enzyme conjugates that are highly active in organic solvents
  Biotechnol. Bioeng. 2019, 116, 272-282

- T. Raidt, P. Santhirasegaran, R. Hoeher, J. C. Tiller, F. Katzenberg
  Shock- and Energy-Absorption Capability of Cold-Programmable Shape Memory Polymers
  Macromol. *Chem. Phys. 2019, 220, 1800274*

- D. Segiet, T. Raidt, H. Özdem, S. Weckes, J. C. Tiller, F. Katzenberg
  Thermo-/moisture-responsive shape-memory effect of poly(2-ethyl-2-oxazoline) networks
  Journal of Polymer Science Part B: Polymer Physics 2019, 57, 1053-1061

- W. Tillmann, L. Hagen, D. Stangier, M. Krabiell, P. Schröder, J. C. Tiller, C. Krumm, C. Sternemann, M. Paulus, M. Elbers
  Influence of etching-pretreatment on nano-grained WC-Co surfaces and properties of PVD/HVOF duplex coatings
  Surface and Coatings Technology 2019, 374, 32-43

Publications 2020 - 2018

2018

Peer Reviewed Articles

- N. Rauner, C. Mueller, S. Ring, S. Boehle, A. Strassburg, C. Schoeneweiss, M. Wasner, J. C. Tiller
  A Coating that Combines Lotus-Effect and Contact-Active Antimicrobial Properties on Silicone
  Advanced Functional Materials 28 (29) 1801248 (2018)

- M. Leurs, B. Dorn, S. Wilhelm, M. Manisegaran, J. C. Tiller
  Multicore Artificial Metalloenzymes Derived from Acylated Proteins as Catalysts for the Enantioselective Dihydroxylation and Epoxidation of Styrene Derivatives
  Chemistry 24 (42) 10859 -10867 (2018)

- M. Schmidt, A. Romanovska, Y. Wolf, T. - D. Nguyen, A. Krupp, H. L. Tumbrink, J. Lategahn, J. Volmer, D. Rauh, S. Luetz, C. Krumm, J. C. Tiller
  Insights into the Kinetics of the Resistance Formation of Bacteria against Ciprofloxacin Poly(2-methyl-2-oxazoline) Conjugates
  Bioconjugate Chemistry 29 (8), 2671-2678 (2018)

- L. Richter, M. Hijazi, F. Arfeen, C. Krumm, J. C. Tiller
  Telechelic, Antimicrobial Hydrophilic Polycations with Two Modes of Action
  Macromolecular Bioscience 18 (4), 1700389 (2018)

- M. Hijazi, C. Krumm, S. Cinar, L. Arns, W. Alachraf, W. Hiller, W. Schrader, R. Winter, J. C. Tiller
  Entropically driven Polymeric Enzyme Inhibitors by End-Group directed Conjugation
  Chemistry A European Journal 24 (18), 4523-4527 (2018)

- T. Raidt, M. Schmidt, J. C. Tiller, F. Katzenberg
  Cross-Linking of Semi-Aromatic Polyesters Towards High Temperature Shape Memory Polymers with Full Recovery
  Macromolecular Rapid Communications 39 (6), 1700768 (2018)

- D. E. Apostolides, C. S. Patrickios, T. Sakai, M. Guerre, G. Lopez, B. Ame´duri, V. Ladmiral, M. Simon, M. Gradzielski, D. Clemens, C. Krumm, J. C. Tiller, B. Ernould, J. - F. Gohy
  Near-Model Amphiphilic Polymer Conetworks Based on Four-Arm Stars of Poly(vinylidene fluoride) and Poly(ethylene glycol): Synthesis and Characterization
  Macromolecules 51 (7), 2476-2488 (2018)

Bioprocess Engineering (BPT)

Activating the Silent Potential of Microorganisms

Triaging of Culture Conditions for Enhanced Secondary Metabolite Diversity from Different Bacteria

Jenny Schwarz, Georg Hubmann, Katrin Rosenthal, Stephan Lütz

Secondary metabolites (SMs) are a chemically diverse and large group of biomolecules with complex structures. Approximately 300,000 secondary metabolites are characterized and many SMs are biologically active. They possess antibiotic, cytostatic, or other relevant activities. Therefore, SMs are of high interest for pharmaceutical research and drug discovery. Today, the number of freely available fully sequenced bacterial genomes made genomic information more accessible for genome mining to find the enzymes involved in microbial SM biosynthesis. Most often, the activation of these enzymes and the SM synthesis have been achieved by perturbing culture conditions. The culture-condition induced approach is commonly known as the One Strain, Many Compounds (OSMAC) approach to enable the discovery of many compounds produced by one microbial source. Here, we explored the biosynthetic potential of several bacteria, using genome mining, various OSMAC conditions and SM detection based on high performance liquid chromatography-mass spectrometry (HPLC-MS).

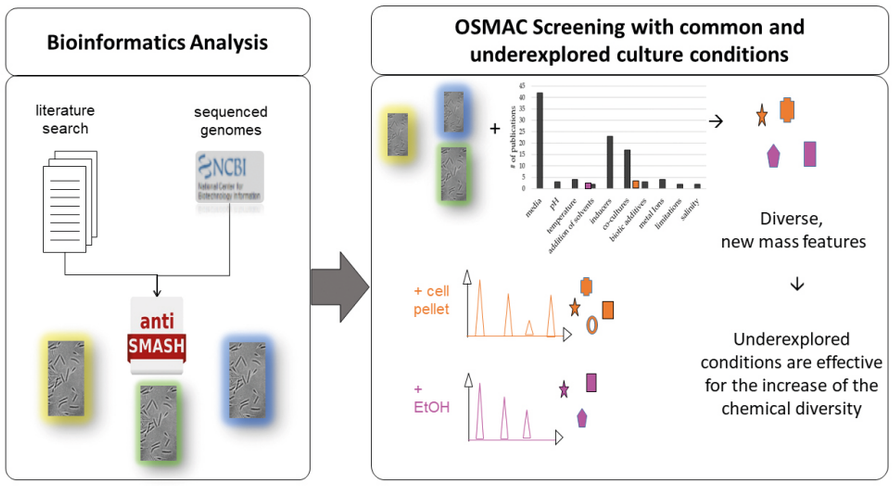

Figure 1: Exploring secondary metabolite diversity in bacteria as a source of new drugs.

Over the past decade, the One Strain Many Compounds (OSMAC) approach has been established for activation of biosynthetic gene clusters (BGCs), which mainly encode the enzymes of secondary metabolite (SM) biosynthesis pathways. These BGCs were successfully activated by altering various culture conditions, such as aeration rate, temperature, and nutrient composition. Here, we determined the biosynthetic potential of 43 bacteria using the genome mining tool antiSMASH. Based on the number of BGCs, the biological safety, availability of deposited cultures, and literature coverage, we selected five promising candidates: *Bacillus amyloliquefaciens, Corallococcus coralloides, Pyxidicoccus fallax, Rhodococcus jostii,* and *Streptomyces griseochromogenes*. The bacteria were cultivated under a broad range of OSMAC conditions (nutrient-rich media, minimal media, nutrient-limited media, addition of organic solvents, addition of biotic additives, type of culture vessel) to fully assess the biosynthetic potential. In particular, we investigated so far scarcely applied OSMAC conditions to enhance the diversity of SMs. We detected the four predicted compounds bacillibactin, desferrioxamine B, myxochelin A, and surfactin. In total, 590 novel mass features were detected in a broad range of investigated OSMAC conditions, which outnumber the predicted gene clusters for all investigated bacteria by far. Interestingly, we detected mass features of the bioactive compounds cyclo-(Tyr-Pro) and nocardamin, so far not reported in OSMAC screenings. Remarkably, the infrequently applied OSMAC conditions in defined medium with and without nutrient limitation were demonstrated to be very effective for BGC activation and for SM discovery.

Contact:
jenny.schwarz@tu-dortmund.de
stephan.luetz@tu-dortmund.de

Publications:
J. Schwarz, G. Hubmann, K. Rosenthal, S. Lütz, Biomolecules 11(2),193 (2021).

Environmental Assessment of Enzyme Production and Purification

How green are biocatalysts?

Martin Becker, Stephan Lütz, Katrin Rosenthal

The importance of bioprocesses has increased during the last decades, as they are considered to be more sustainable than chemical processes in many cases. The sustainability of processes can be estimated with E *factors, which are easy-to-calculate values applicable for an initial assessment. However, the contribution of biocatalyst preparation, namely enzyme synthesis and purification, is usually neglected. We therefore determined the simple* E *factor (g waste per g product), the complete* E *factor (additionally includes water consumption) and the* E^+ *factor (additionally includes water consumption and* CO_2 *emission) for biocatalyst production and purification. The calculated complete* E *factor is 37.835* $g_{waste} \cdot g_{enzyme}^{-1}$*, which shows that the contribution of enzyme production and purification should not be neglected for sustainability assessment of bioprocesses.*

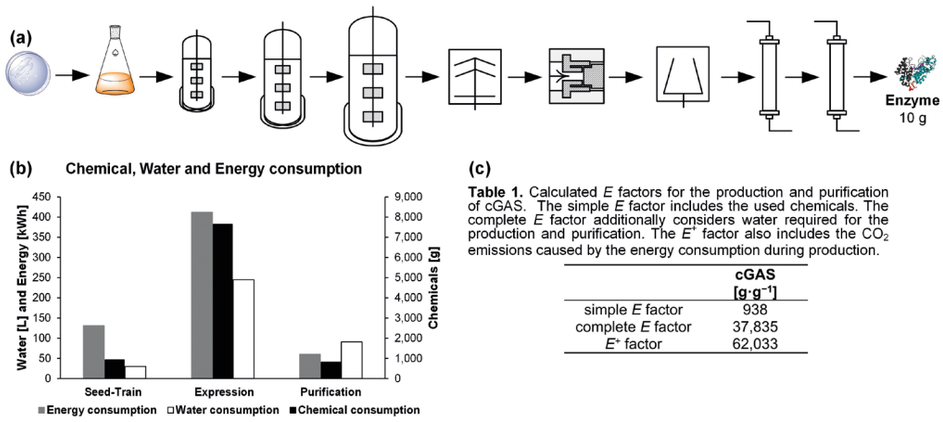

Table 1. Calculated *E* factors for the production and purification of cGAS. The simple *E* factor includes the used chemicals. The complete *E* factor additionally considers water required for the production and purification. The E^+ factor also includes the CO_2 emissions caused by the energy consumption during production.

	cGAS [$g \cdot g^{-1}$]
simple *E* factor	938
complete *E* factor	37,835
E^+ factor	62,033

Figure 1: Overview of cGAS production and calculated results: (a) Scheme of production and purification of 10 g enzyme; (b) Chemicals, water and energy consumption during seed-train, expression as well as purification of 10 g enzyme; (c) Table with calculated *E* factors for the production of enzyme.

The *E* factor was calculated for the production of 10 gram of the model enzyme cyclic GMP-AMP synthase (cGAS). With available laboratory data, a process for production and purification was designed. Cultivation, enzyme expression and purification were taken into account. Figure 1 summarizes all individual steps. Based on this process, the required chemicals and water as well as energy consumption were calculated. In total, 9.39 kg of chemicals, 2.92 kg of solvents, 367.25 L of water, and 412.2 kWh of energy are required to produce 10 g cGAS. Especially, the expression step represents the greatest potential for savings. Water consumption could be reduced by achieving higher cell densities during fermentation resulting in smaller reactor volumes. Based on these results, it was possible to calculate the *E* factors, which are summarized in Table 1. The simple *E* factor includes the chemicals needed to produce one gram of enzyme and is 938 g waste per g cGAS. Since the simple *E* factor does not take into account the consumption of solvents and water, which leave the process contaminated, the complete *E* factor should rather be considered, which is 37,835 g of waste per g of cGAS. The E^+ factor, which also takes the energy consumption in the production of the enzyme into account, is 62,033 g of waste per g of purified cGAS.

By this approach, significant steps to reduce the *E* factor can be identified easily and quickly. The results show that the enzyme production, especially the expression step, has a significant impact on the economic and ecological assessment of bioprocesses. These values can be transferred to similar processes in order to estimate the contribution of biocatalyst synthesis to a bioprocess.

Publications:
M. Becker, S. Lütz, K. Rosenthal. Molecules 26(3), 573 (2021).

Contact:
martin4.becker@tu-dortmund.de
stephan.luetz@tu-dortmund.de
katrin.rosenthal@tu-dortmund.de

Publications 2020 - 2018

2020

Journal Papers

- K. Rosenthal, M. Becker, J. Rolf, R. Siedentop, M. Hillen, M. Nett, S. Lütz
  Catalytic promiscuity of cGAS: A facile enzymatic synthesis of 2'- 3' linked cyclic dinucleotides
  ChemBioChem, 21(22), 3225-3228 (2020)

- S. Lütz, A. Liese
  30 Jahre sichere Gentechnik in Deutschland
  Angewandte Chemie, 132, 2-4 (2020)

- J. Schwarz, K. Rosenthal, R. Snajdrova, M. Kittelmann, S. Lütz
  The Development of Biocatalysis as a Tool for Drug Discovery
  CHIMIA, 74(5), 368-377 (2020)

- J. Rolf, M. Julsing, K. Rosenthal, S. Lütz
  A Gram-Scale Limonene Production Process with Engineered *Escherichia coli*
  Molecules, 2020, 25(8), 1881 (2020)

- A. Sester, K. Stüer-Patowsky, W. Hiller, F. Kloss, S. Lütz, M. Nett
  Biosynthetic Plasticity Enables Production of Fluorinated Aurachins
  ChemBioChem 21(16), 2268-2273 (2020)

Presentations & Poster

- K. Rosenthal, J. Rolf, M. Becker, R. Siedentop, S. Lütz
  Cell-free synthesis of enzymes for the production of pharmaceutically relevant molecules
  ProcessNet-Jahrestagung, 21. - 24. September 2020, online

- K. Rosenthal
  Microbioreactors for Biotransformations and Whole Cell Biocatalysis
  (invited lecture)
  µTAS 2020 (24th International Conference on miniaturized Systems for Chemistry and Life Science), 3. - 4. October 2020, online

2019

Journal Papers

- L.M. Schmitz, J. Schäper, K. Rosenthal, S. Lütz
  Accessing the biocatalytic potential for C-H-activation by targeted genome mining and screening
  ChemCatChem 11, 5766-5777 (2019)

- L.M. Schmitz, K. Rosenthal, S. Lütz
  Recent Advances in Heme Biocatalysis Engineering
  Biotechnology and Bioengineering 116, 3469-3475 (2019)

- J. Rolf, K. Rosenthal, S. Lütz
  Application of Cell-Free Protein Synthesis for Faster Biocatalyst Development
  Catalysts, 9(2):190 (2019)

Presentations & Poster

- K. Rosenthal, M. Becker, M. Nett, S. Lütz
  Enzymatic synthesis of cyclic dinucleotides – Exploiting a human enzyme with broad substrate scope
  GDCh-Wissenschaftsforum Chemie, 15-18 September 2019, Aachen, Germany

- K. Rosenthal, M. Becker, J. Rolf, M. Nett, S. Lütz
  Enzymatic synthesis of cyclic dinucleotides – Exploring the catalytic potential of human cGAS
  (Best poster award) Trends in Enzymology and Biocatalysis, 27-31 May 2019, Rome, Italy

- L.M. Schmitz, J. Schäper, S. Lütz
  Genome mining combined with high throughput screening revealed novel biocatalysts for hydroxylation reactions
  Trends in Enzymology and Biocatalysis, 27-31 May 2019, Rome, Italy

- J. Rolf, K. Hildebrand, K. Rosenthal, S. Lütz
  Protein synthesis without cells: Engineering a high-throughput platform for enzyme screening
  German Conference on Synthetic Biology, 12-13 September 2019, Aachen, Germany

- K. Rosenthal, J. Rolf, S. Lütz
  Cell-free protein synthesis: Accelerating biocatalyst development
  German Conference on Synthetic Biology, 12- 13 September 2019, Aachen, Germany

- L.M. Schmitz, J. Schäper, K. Rosenthal, S. Lütz
  Identification of novel microbial P450s as drug-metabolizing enzymes
  Basellife, 9-12 September 2019, Basel, Switzerland

- J. Schwarz, S. Lütz
  Targeting the potential for new bioactive molecules
  14th International Symposium on the Genetics of Industrial Microorganisms, 08-11 September 2019, Pisa, Italy

Publications 2020 - 2018

2018

Journal Papers

- K. Rosenthal, S. Lütz
  Recent developments and challenges of biocatalytic processes in the pharmaceutical industry
  Current Opinion in Green and Sustainable Chemistry 11, 58-64 (2018)

- A. Worsch, F. K. Eggimann, M. Girhard, C. J. von Bühler, F. Tieves, R. Czaja, A. Vogel, C. Grumaz, K. Sohn, S. Lütz, M. Kittelmann, V.B. Urlacher
  A novel cytochrome P450 monooxygenase from *Streptomyces platensis* resembles activities of human drug metabolizing P450s
  Biotechnology & Bioengineering 115 (9), 2156-2166 (2018)

- M. Schmidt, A. Romanovska, Y. Wolf, T. - D. Nguyen, A. Krupp, H. Tumbrink, J. Lathgahn, J. Volmer, D. Rauh, S. Lütz, C. Krumm, J. C. Tiller
  Insights into the kinetics of the resistance formation of bacteria against ciprofloxacin poly(2-methyl-2-oxazoline) conjugates
  Bioconjugate Chemistry 29 (8), 2671-2678 (2018)

Book Chapter

- J. Schwarz, J. Volmer, S. Lütz
  Enzyme in der chemischen und pharmazeutischen Industrie
  In: K.E. Jäger, A. Liese, C. Syldatk (eds), Einführung in die Enzymtechnologie. Springer Spektrum, Berlin, Heidelberg (2018)

Presentations & Poster

- J. Schwarz, S. Lütz
  Influence of Nutrient Limitation on the Production Profile of Bacteria with High Biosynthetic Potential
  European Conference on Natural Products, 02-05 September 2018, Frankfurt am Main, Germany

- K. Rosenthal, M. Becker, J. Rolf, S. Lütz
  Enzymatic synthesis of cyclic dinucleotides
  Emerging Trends in Natural Product Biotechnology, 20-21 September 2018, Dortmund, Germany

- A. Steinmann, C. Dickmeis, A. Kohl, D. Decembrino, S. Wohlgemuth, M. Girhard, S. Lütz
  Development of an Analytical Method for Metabolic Profiling of Monolignol- and Lignan-Producing *Escherichia coli*
  Emerging Trends in Natural Product Biotechnology, 20-21 September 2018, Dortmund, Germany

- J. Rolf, M. Julsing, S. Lütz
  Biotechnological monoterpene production in *Escherichia coli*
  ProcessNet-Jahrestagung, 10-13 September 2018, Aachen, Germany

- K. Rosenthal, M. Becker, J. Rolf, S. Lütz
  Enzymatic synthesis of cyclic dinucleotides
  ProcessNet-Jahrestagung, 10-13 September 2018, Aachen, Germany

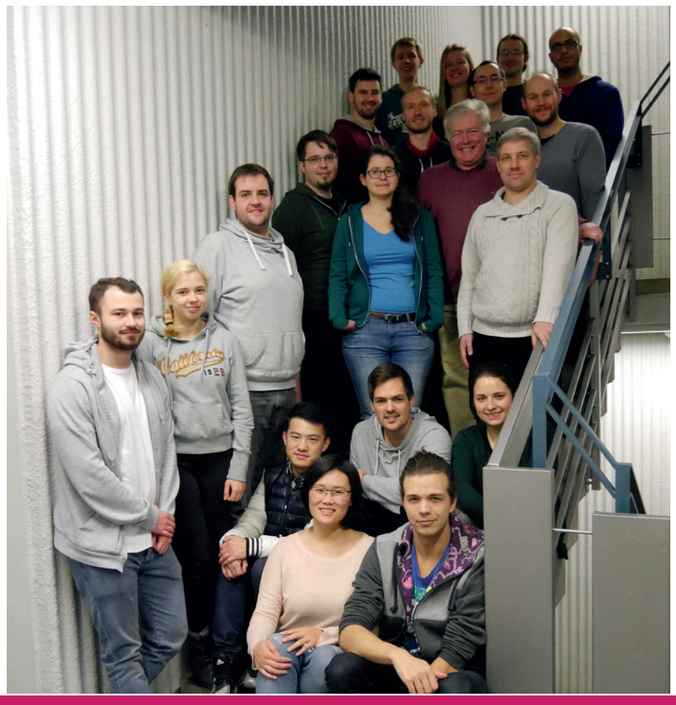

Chemical Reaction Engineering (CVT)

Direct Air Capture of Carbon Dioxide

Energy Efficiency and Moisture Balance

Carsten Drechsler, David W. Agar

According to the International Panel on Climate Change (IPCC), the primary objective of the Paris Conference on Climate Change in 2015: to limit the increase in global temperature to 2 °C and preferably less than 1.5 °C, can now only be achieved with the help of negative emission technologies (NET) to reduce the atmospheric concentrations of greenhouse gases. Natural measures for CO_2 removal, from air, such as reforestation, exhibit both short- and long-term drawbacks and can have unintended ecological consequences. Artificially separating CO_2 at a concentration of 400 ppm from the atmosphere – the so-called direct air capture (DAC) – is a technically challenging task, especially if it is to be implemented at the large-scale required. The technology of choice – chemically enhanced adsorption – has been demonstrated successfully at a small-scale for amounts of around 1,000 t p.a., but two challenges must still be surmounted: the highly efficient use of the energy source and the negative impact of non-selective moisture adsorption on the energy requirement. Furthermore, the final fate of the CO_2 recovered remains to be resolved.

The underlying principle of our research is to exploit the heat liberated in the hydrogenation of carbon dioxide to methane in the Power-to-Gas (PtG) Sabatier reaction in order to thermally regenerate the adsorbent. This requires both a source of CO_2-free hydrogen – generated either from water electrolysis or methane pyrolysis - and a high degree of heat recovery between heating up and cooling down the adsorbent. The methane thus produced is carbon-neutral. If it is pyrolysed, the overall process represents a carbon-negative anthropogenic coalification. Unfortunately, the immobilised amines used to adsorb low concentrations of CO_2 also tend to take up the considerable amounts of moisture present in the air. So far, we have been unable to modify this hydrophilic behaviour of the adsorbent without impairing its CO_2-adsorption capacity and kinetics. Alternative engineering strategies to prevent the ad- and desorption of water vapour overwhelming the energy demand, such as impeded desorption and vapor recompression, have been investigated and shown to cut the moisture energy penalty by almost 50 %. Additionally, both hybrid regeneration processes with combined temperature and vacuum swing contributions together with alternative configurations of the methanisation reactor have been examined in order to minimise the total energy consumption over the entire DAC-PtG system (Figure 1).

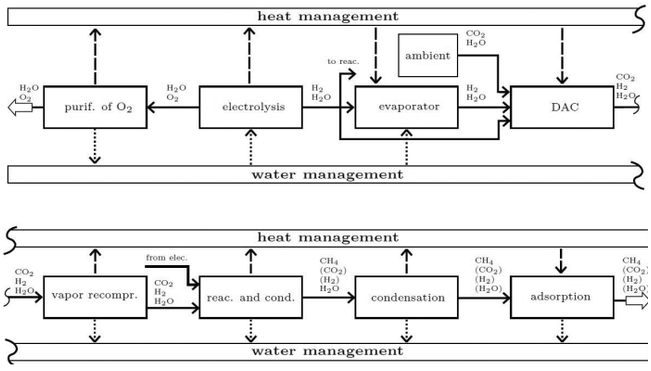

Figure 1: Flowsheet of the DAC-PfG process network (modified from *).

Contact:
carsten.drechsler@tu-dortmund.de
david.agar@ tu-dortmund.de

A novel coveyor belt adsorber arrangement (Figure 2) has been devised to reconcile the conflicting demands of elutive desorption, regenerative-recuperative heat exchange, low pressure drop and high mass transfer, and its performance characteristics assessed with the help of detailed simulations. More than 95 % of the sensible heat expended to heat the adsorbent from the adsorption (25 °C) to the desorption (100 °C) temperature can be recovered in this manner.

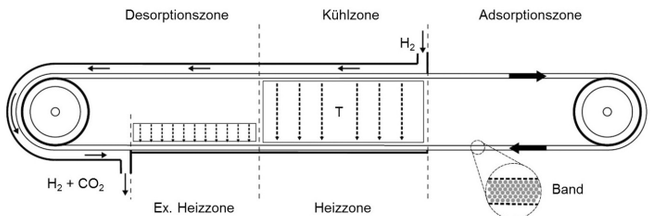

Figure 2: Scheme of the conveyor belt adsorber developed for direct air capture of CO_2. (modified from **).

Publications:
C. Drechsler, D.W. Agar, Computers & Chemical Engineering, 126:520-534 (2019).
C. Drechsler, D. W. Agar, Chemie-Ingenieur-Technik, 92(3):282-287 (2020)**.
C. Drechsler, D. W. Agar, Int. J. of greenhouse gas control, 105:105230 (2021)*.

Publications 2020 - 2018

2020

Peer-reviewed Publications

- L. Arsenjuk, M. Wiesehahn, E. Morales Zimmermann, W. Katschan, D.W. Agar
  Capacitative determination of wall-thickness in liquid-liquid slug flow and its application as a non-invasive microfluidic viscosity sensor
  Sensors and Actuators A: Physical 315:112342 (2020)

- D. Hellmann, I. de Oliviera-Gonclaves, D.W. Agar
  Coxaial flow contactors as alternative to double T-contactors for triphasic slug flow generation
  Chemie-Ingenieur-Technik, 92(5):532-539 (2020)

- C. Drechsler, D.W. Agar
  Comparison of highly heat integrated adsorber concepts for use in direct air capture processes
  Chemie-Ingenieur-Technik, 92(3):282-287 (2020)

- C. Drechsler, D.W. Agar
  Intensified integrated direct air capture – power-to-gas process based on H_2O and CO_2 from ambient air
  Applied Energy 273:115076 (2020)

- N. von Vietinghoff, D. Hellmann, J. Priebe, D.W. Agar
  Intermediate gas feed in bi- or triphasic gas-liquid(-liquid) segmented slug flow capillary reactors
  Symmetry 12(12):2092 (2020)

- N. von Vietinghoff, W. Lungrin, R. Schulzke, J. Tilly, D.W. Agar
  Photoelectric sensor for fast and low-proced determination of bi- and triphasic segmented slug flow parameters
  Sensors 20(23):6948 (2020)

- L. Arsenjuk, M. Asshoff, J. Kleinheider, D.W. Agar
  A device fro continuous and flexible adjustment of liquid-liquid slug size in microchannels
  J. of flow chemistry 10:409-422 (2020)

- C. Drechsler, D.W. Agar
  Invesitgation of water co-adsorption on the energy balance of solid sorbent based direct air capture processes
  Energy 192:116587 (2020)

Presentations

- N. Antweiler, D.W. Agar
  Hydrogen from methane pyrolysis
  VDMA Webinar 08.12.2020

2019

- D. Hellmann, D.W. Agar
  Modeling of Slug Velocity and Pressure Drop in Gas-Liquid-Liquid Slug Flow
  Chemical Engineering and Technology 42(10), pp. 2138-2145 (2019)

- C. Drechsler, D.W. Agar
  Simulation and optimization of a novel moving belt adsorber concept for the direct air capture of carbon
  Computers and Chemical Engineering 126, pp. 520-534 (2019)

- M. Wiesehahn, L. Buzilowski, T. Kembügler, M. Moghaddam, D.W. Agar
  Selective Partial Oxidation of Hydrogen Sulfide by the BrOx Cycle
  Chemie-Ingenieur-Technik 91(5), pp. 663-667 (2019)

- C. Drechsler, A.M. Dashliborun, S.M. Taghavi, D.W. Agar, F. Larachi
  Bubble Behavior in Marine Applications of Bubble Columns: Case of Ellipsoidal Bubbles in Slanted and Rolling Columns
  Industrial and Engineering Chemistry Research 58(6), pp. 2343-2355 (2019)

2018

Proceedings & Book Chapters

- J. González Rebordinos, F. Saki, F. Matulla, D. W. Agar
  Experimental Study on Thermal and Catalytic Hydrogen Bromide Oxidation
  Industrial & Engineering Chemistry Research 2018, 57, 50, 17111-17118

- J. González Rebordinos, R. Tian, N. Robert, D. W. Agar
  Carbon retrieval and purification in the BrOx cycle for CO2-free energy
  Chemical Engineering Research & Design 2018, 140, 283-291

- M. Hussainy, D. W. Agar
  Modeling and optimization of the cyclic steady state operation of adsorptive reactors
  Chinese Journal of Chemical Engineering 2018, 26(6), 1321-1329

- A. A. Munera Parra, C. Asmanoglo, D. W. Agar
  Modelling and Optimization of a Moving-Bed Adsorptive Reactor for the Reverse Water-Gas Shift Reaction
  Computers & Chemical Engineering 2018, 109, 203–215

- M. G. Gelhausen, D. Lenz, F. Krull, V. Korkmaz, D. W. Agar
  3D Printing for Chemical Process Laboratories II: Measuring Liquid-Solid Mass Transfer Coefficients
  Chemical Engineering Technology 2018, 41(4), 798–805

- M. G. Gelhausen, T. Feuerbach, A. Schubert, D. W. Agar
  3D Printing for Chemical Process Laboratories I: Materials and Connection Principles
  Chemical Engineering Technology 2018, 41(3), 618–627

Presentations & Poster

- C. Drechsler, J. M. Alava, D. W. Agar
  MATLAB Unit Operation potential improvements for academic use
  CAPE-OPEN 2018 annual meeting, Ludwigshafen, Germany, October 2018

- C. Asmanoglo, D. W. Agar
  Entwicklung wärmeintegrierter Adsorber/Desorber-Konzepte für eine Anwendung in Direct Air Capture (DAC) Technologien
  1. Statuskonferenz zur BMBF Fördermaßnahme CO2Plus, Berlin, Germany, April 2018

- C. Schwarz, D. W. Agar
  Reduzierung räumlicher Diskretisierungsfehler in der Volume-of-Fluid-Methode durch analytische Integration der Grenzflächenformfunktion
  Jahrestreffen Bremen der ProcessNet-Fachgruppen MPH & WSUE & CFD, HTT & AuW, KRI, PMT, Bremen, Germany, März 2018

- D. Hellmann, T. Krell, D. W. Agar
  Calculation of slug velocity and pressure drop in multiphase Slug Flow
  International Conference on Micro Reaction Technology - IMRET, Karlsruhe, Germany, Oktober 2018

- D. Hellmann, I. de Oliveira-Goncalves, A. Thierfelder, D. W. Agar
  Generation of uniform gas-liquid-liquid slug flow for micro suspension catalysis
  9th Workshop "Chemical and Biological Micro Laboratory Technology", Ilmenau, Germany, Februar 2018

- M. Wiesehahn, D. W. Agar
  Selective partial oxidation via the BrOx cycle
  Jahrestreffen Reaktionstechnik, Würzburg, Germany Mai, 2018

Process Dynamics and Operations (DYN)

Efficient Operation of Blast Furnaces through a Neural Net Model-Based Optimizing Control Scheme

Pourya Azadi, Sebastian Engell

The daily operation of blast furnaces in the steel industry is challenging due to the long-term effect of the actions of the operators, which may lead to an oversupply of carbon-based fuels, causing surplus production of carbon monoxide and an inefficient operation. The steel industry has a strong interest in better support for the operators or even better in full automation for a more energy-efficient stable operation of blast furnaces. Model-based control schemes are promising candidates for achieving this. The spatial extension, the lack of precise mechanistic knowledge about the physio-chemical phenomena, and the presence of unmeasured disturbances make the application of first principles-based models in the operation of blast furnaces difficult. Therefore, we developed an optimizing control scheme based on a dynamic neural net model that maximizes the carbon monoxide efficiency in the iron oxide reduction reactions and thus reduces the total carbon supply and CO_2 emissions.

An industrial blast furnace (BF) is an extremely energy-intensive gas-solid reactor in which iron ore, charged from the top, and hot blast air, injected through the tuyeres at the bottom, undergo a large number of complex chemical reactions to produce liquid iron. Due to the utilization of carbon-based fossil fuels (coke and pulverized coal), the BF has a large environmental impact with an annual total CO_2 emission of more than 7 million tons. In the blast furnace, carbon-based materials produce carbon monoxide (CO) as the main reducing agent for the reduction of iron ore. In the daily operation of BFs, it is often the case that the operators apply an excess amount of carbon-based fuels to improve the thermal stability of the process, which however causes fluctuations in the conversion profile by the surplus production of CO. To ensure an efficient use of CO in the reduction reactions and thus to prevent an excessive use of carbon-based fuels, we propose a model-based dynamic optimization scheme that mitigates the unexploited excess of CO while keeping process productivity and safety constraints. It comprises a surrogate model that represents the conversion of the iron-oxide reduction reaction (γ) as a function of the ratio of the CO to CO_2 concentrations (CO/CO_2) in the outgoing gas on top of the BF. The scheme uses a black-box model that characterizes the BF operation status in terms of the temperature of the outgoing gas (TG), the pressure drop between the tuyere level and the top of the furnace (DP), and the gas utilization factor ($\eta_{CO}=CO_2/(CO+CO_2)$).

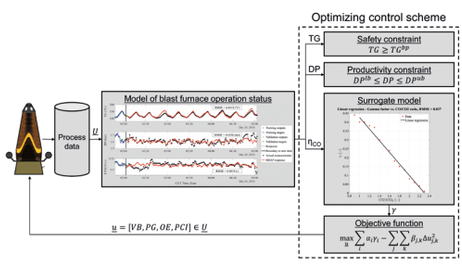

Figure 1: Flowchart of the dynamic black-box model-based optimizing control scheme.

Figure 1 shows the flowchart of the proposed control scheme. Using real plant measurements of the large-scale BF Schwelgern 2 of thyssenkrupp Steel Europe, a nonlinear autoregressive neural network with exogenous inputs (NARX) was developed for the multistep ahead prediction (MSAP) of TG, DP, and η_{CO}, based upon a set of fast and slow dynamic input variables ($\underline{U}$). The fast dynamic variables describe the gas phase, while the slow dynamic variables are related to the solid phase. TG and DP are related to safety and productivity constraints. Top gas temperatures less than the boiling point of water (T^{bp}) impede the evaporation of the moisture in the solid feed materials and increase the risk of process abnormalities due to wet raw materials. If DP is less than its lower threshold (DP^{lb}), the driving force for pushing the gas through the solid bed is diminished, resulting in less productivity. When DP exceeds the maximum threshold (DP^{ub}), the burden descent is hindered and the productivity will also decrease. The degree of the higher oxide (Fe_2O_3 and Fe_3O_4) reduction reactions (γ) can be defined by the amount of oxygen that is removed from the iron ore. The reduction of Fe_2O_3 to Fe_3O_4 lowers the mole ratio of oxygen to iron (O/Fe) from 1.5 to 1.33, and by the reduction of Fe_3O_4 to FeO, O/Fe further drops to 1.06. The γ factor can be identified from η_{CO}, the CO/CO_2 ratio.

The proposed control scheme was simulated with real plant measurements for a time interval of one hour. The control scheme suggests corrective actions by the hot blast flowrate (VB), the oxygen enrichment (OE), the pulverized coal injection (PCI), and the top pressure (PG) such that the process conditions favor a better use of CO. The simulation results show 3 % saving in the total carbon supply thanks to optimal control input trajectories (see Figure 2).

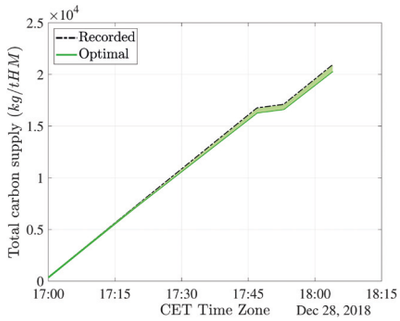

Figure 2: Total carbon supply before and after optimization.

Contact:
pourya.azadi@tu-dortmund.de
sebastian.engell@tu-dortmund.de

Publications:
P. Azadi, S. Ahangari Minaabad, H. Bartusch, R. Klock, S. Engell, Nonlinear prediction model of blast furnace operation status, Computer Aided Chemical Engineering, 48, 217-222 (2020).

P. Azadi, R. Klock, S. Engell, Efficient utilization of active carbon in a blast furnace through a black-box model-based optimizing control scheme, accepted for the 11th IFAC symposium on advanced control of chemical processes (ADCHEM) (2021).

Model Predictive Control for Switching Nonlinear Systems

Taher Ebrahim, Sebastian Engell

In many technical systems, discrete switches occur either because the actuators are discrete (a pump is switched on or off) or because the behavior of the system itself changes abruptly between different modes of operation, as e.g. heating up of a liquid and evaporation at the boiling temperature. Control schemes for such systems are usually designed heuristically, combining classical continuous control and a fixed switching logic. While model predictive control is increasingly used to increase the performance of systems with continuous dynamics, to apply this principle to switching systems is significantly more demanding. The main reason for this is that the optimization problem which must be solved during the operation of the system, within fixed sampling intervals, becomes much more complex due to the presence of the discrete variables (also known as the combinatorial explosion). This work proposes a computationally efficient MPC scheme which manipulates both the discrete and the continuous degrees of freedom together in an optimal manner to achieve the desired control goals.

Figure 1 illustrates a supermarket refrigeration system, which consists of several display cases where the goods are presented to the customers, and a central compressor rack that consists of several compressors. Each display case is equipped with an on/off expansion valve by which the temperature inside the case is controlled, and the compressors can be either switched on or off.

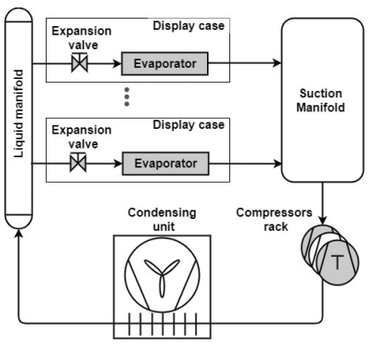

Figure 1: Simplified illustration of a supermarket refrigeration system adapted from Sonntag et al. (2009).

The main goal of the control system is to keep the temperature of the goods within a narrow range in the presence of disturbances such as ambient temperature and the mass of the goods. While realizing the required cooling temperature, the suction pressure must be kept within certain bounds in order to limit the variations of the refrigerant evaporation temperature. Furthermore, the energy consumption of the compressors along with their switching frequency should be minimized in order to prolong their life span. If the system is not considered as a whole but the temperatures in the display cases are regulated locally and the compressors are switched to maintain the suction pressure, there is a tendency of the expansion valves to synchronize their switching signals, since they are exposed to almost the same operating conditions. This leads to large variations in the suction pressure and frequent switching of the compressors, which unnecessarily shorten their lifetime and increase the energy consumption. By an optimizing control scheme, the different goals can be achieved simultaneously, while avoiding synchronization of the switching of the expansion valves.

Publications:
T. Ebrahim, S. Subramanian, S. Engell, (2018), Hybrid NMPC for switching systems applied to a supermarket refrigeration system. In Proceedings European Control Conference (ECC), IEEE, 813-818.

T. Ebrahim, S. Engell, A bi-level approach to MPC for switching nonlinear systems, In Proceedings IFAC World Congress 2020, Berlin.

References:
C. Sonntag, M. Kölling, S. Engell, Sensitivity-based Predictive Control of a Large-scale Supermarket Refrigeration System. IFAC Proceedings Volumes, Volume 42, Issue 11, 2009, Pages 345-350.

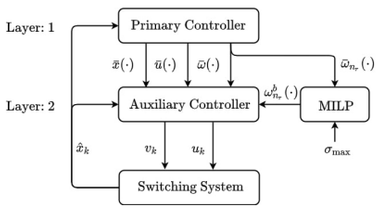

Figure 2: MPC scheme for switching nonlinear systems.

As a consequence of the presence of the discrete degrees of freedom within the optimization problem, a mixed integer optimal control problem (MIOCP) has to be solved which is very computationally intensive specially for nonlinear systems. In our work, an efficient MPC scheme for switching systems (Figure 2) which replaces the computationally intensive direct solution of the MIOCP by two simpler nonlinear optimization problems (NLP) and one mixed integer linear problem (MILP) has been developed. The upper layer solves a relaxed version of the MIOCP and submits the resulting optimal solution with relaxed trajectories of the discrete degrees of freedom to the lower layer. On the lower layer, the discrete degrees of freedom are computed as the closest switching approximation to the input trajectories from the upper-layer and the switching times are then optimized by the auxiliary controller to minimize the deviation from the result of the upper-layer optimization.

The proposed scheme was tested by simulations of a supermarket refrigeration system with three display cases and a central compressor rack with three identical on/off compressors. Figure 3 shows the resulting closed-loop trajectories of the relevant variables together with the number of active compressors for two hours of daytime conditions followed by two hours with different operating parameters for nighttime conditions. It can be noticed that all the variables are kept within the bounds with tight tracking of the reference signals for the goods temperature (3.5 °C for the day and 4.0 °C for the night), and the switching frequency of the compressors is significantly reduced since the suction pressure occupies its complete allowed band. Moreover, the synchronization problem of the expansion valves was resolved as result of using optimizing central control scheme. Only two compressors are found to be necessary to realize the desired pressure and the average computational time for one MPC iteration is less than 10 % of the sampling interval, which enables online usage within MPC algorithm.

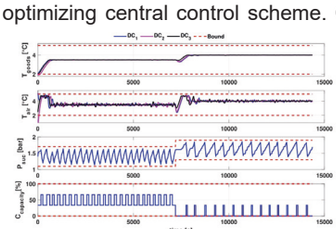

Figure 3: Closed-loop trajectories of the process using the proposed MPC approach.

Contact:
taher.ebrahim@tu-dortmund.de
sebastian.engell@tu-dortmund.de

Economic Multi-Stage NMPC for large Scale Plants: eNMPC of the Tennessee Eastman Challenge Process

Alexandru Tatulea-Codrean, Sebastian Engell

The goal of this work is to demonstrate the design and implementation of a robust nonlinear model predictive control (NMPC) scheme for a large-scale plant-wide control problem. Our approach implements robust economics optimizing control for the Tennessee Eastman Challenge (TEC) process, taking into account plant-model mismatch and external disturbances. This represents the first NMPC implementation for this process where only economic criteria are used. The results obtained demonstrate the feasibility of plant-wide economics optimizing NMPC

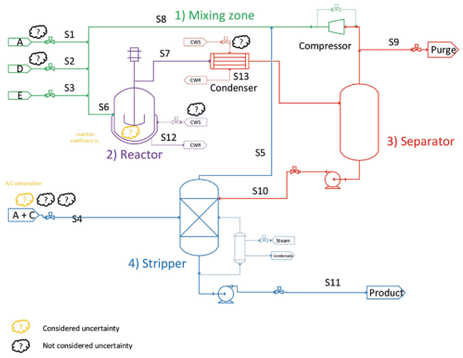

Figure 1: Simplified flow-sheet representation of the Tennessee Eastman Challenge benchmark (from [1]).

Optimal control of large-scale chemical processes consisting of many interconnected units poses a number of challenges, due to the complexity of the process models, the effects of re-cycles, and the presence of uncertain parameters and disturbances. Most control approaches therefore tackle the problem in a top-down layered fashion. At the top level, the process economics are optimized using complex steady-state models, while linear controllers stabilize the process and handle disturbances at the lower level. An alternative to this approach is direct economics optimizing control (DOC), which merges optimal operation and dynamic control. The continuous improvements in numerical algorithms and computing hardware nowadays enable control engineers to realize large-scale dynamic optimizations with nonlinear models in real time.

The Tennessee Eastman Challenge (TEC) process was selected as a test case for this investigation. The TEC, depicted in Figure 1, has been widely employed in many publications as a benchmark for plant-wide control, optimization and monitoring. The control of the process requires manipulating 11 control variables (CVs). Our goal is to maximize the yield of the exothermic reaction in the Reactor (R), while achieving the specified product purity in the Separator (Se). The consumption of raw materials and energy are taken into account, and several safety and operational constraints must be satisfied in all units. The mathematical model of the process consists of 30 nonlinear differential equations and 14 additional algebraic equations. In order to achieve a good performance, the evolution of the process must be predicted for at least 3 hours, which results in a large-scale optimization problem. Solving this control problem in real time requires the use of efficient numerical algorithms. We employ the automatic differentiation algorithms contained in CasADi and the interior point optimization algorithm IPOPT, which are called via the optimal control platform do-mpc. do-mpc was developed at the dyn group in collaboration with Prof. Sergio Lucia. It enables rapid and flexible prototyping of NMPC solutions, with a focus on multi-stage NMPC as a means of dealing with process uncertainties.

Results of applying robust economic NMPC for the TEC benchmark are depicted in Figure 2. The control objective for this study was derived from the original description of the TEC, which outlines the economic aspects, the process constraints and the potential disturbances. We carried out an extensive series of simulations in order to investigate the effects of the disturbances and of the plant-model mismatch on the profitability of the process. The goal of this investigation was to find a good compromise between robustness and optimality while achieving real-time feasibility, as the complexity of a multi-stage NMPC formulation grows rapidly with the number of uncertainties considered and the length of the prediction horizon. It was found that good robust performance for the TEC can be achieved by considering only two sources of uncertainty and their extreme realizations. By designing the economic NMPC appropriately, the controller is able to operate the process safely and profitably, consistently achieving computation times of under 50 seconds, which represents just 25 % of the available sampling time. Furthermore, the robust multi-stage NMPC controller handles randomly varying disturbances well, with a drop in economic profitability of only 7 % compared to the ideal scenario. The results open the door to the industrial application of multi-stage NMPC to complex, large-scale processes similar to the TEC.

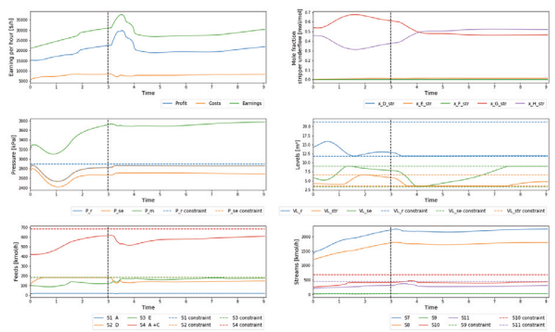

Figure 2: Simulation result of multi-stage NMPC for the TEC benchmark [1]. At t=3 hours the specification of the composition of the product stream is changed.

Contact:
alexandru.tatulea-codrean@bayer.com
sebastian.engell@ tu-dortmund.de

Publications:
[1] A. Tatulea-Codrean, J. Fischer, S. Engell, Multi-stage Economic NMPC for the Tennessee Eastman Challenge Process. Proceedings of the 21st IFAC World Congress, Berlin, 2020 (to appear in IFAC Papers online, Elsevier).

Optimization of the Steelmaking Process in Electric Arc Furnaces

Design, development, and implementation of an optimal operating strategy for an industrial electric arc furnace

Jesús D. Hernández, Sebastian Engell

The steelmaking process via electric arc furnaces (EAFs) is one of the top consumers of electrical energy in the industrial manufacturing sector. The main challenge in modern steelmaking is improving its environmental impact by increasing its energy efficiency and reducing the associated CO_2 emissions. To address this challenge, we developed a dynamic model of an EAF and employed dynamic optimization strategies to compute a set of optimal operative set-points to reduce the energy losses in the process. The optimization framework was tested in one of the ultra-high power EAFs of the largest stainless steel meltshop in Europe, and energy savings of 4.5 %, for one family of stainless-steel products were achieved. These results are equivalent to a net yearly reduction of 12 kton of CO_2 emissions from coal based electrical energy generation.

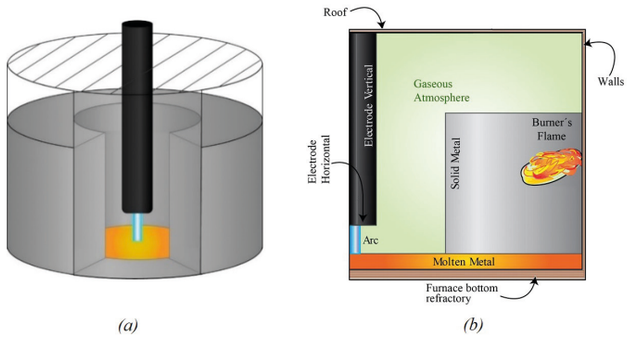

Figure 1: Radial cut of the EAF. (a) 3D model, (b) 2D radial cut with the modeled phases and the participating surfaces.

The EAF was modeled using a system of three phases: the solid scrap, the liquid metal pool, and the gaseous atmosphere. See Figure 1. The dynamic behavior of the process was obtained from the mass and energy balances of each phase. Various energy inputs promote the process: a) electrical current - which is used to create high-power electric arcs –, b) oxyfuel burners, c) oxygen lances, d) the heat provided by exothermic reactions in the liquid and the solid phases, and e) the splashing of liquid metal. The energy contribution of each of these sources to the process was estimated using existing relationships to quantify the heat exchange via radiative, convective, and conductive mechanisms. Shadings and blockages complicate the modeling of the radiative heat exchange in the EAF process. Therefore, Monte Carlo algorithms are used to compute the complicating view factors. Process data was used to adjust the model parameters. After the estimation procedure, the process-model mismatches were less than 5 % in terms of the final melt temperature, the batch time, and the energy demand of the process. The model was used to estimate the energy fluxes in the process, and a dynamic energy efficiency curve of the process was identified for the first time.

A set of optimal operative set-points for the electrical energy input was computed using a control vector parameterization approach with the aim of reducing the electrical energy losses of the process. The full EAF process model was used to compute the predictions of the energy losses during the process. Because the batch´s electrical energy losses are strongly dependent on the length of the electric arc, a novel electric arc model that predicts the geometry of the arc from its electrical set-points was developed and considered in the optimization. It was found that depending on the amount of metal charged to the furnace, the desired processing time, and the required terminal temperature of the liquid metal, different optimal operation policies result. An optimal group of set-points was computed and implemented in one of the EAFs at ThyssenKrupp – Acciai Speciali Terni in Italy. A group of 50 steel batches was processed using the computed set-points. The optimal operation reduced the energy demand and the process batch time by 4.5 % and 4.3 % for one steel type. Figure 2 presents the measured results.

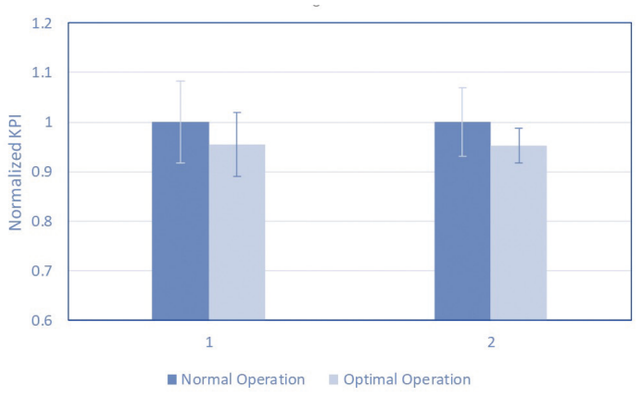

Figure 2: Observed improvements of the batch time (KPI 1) and the energy demand (KPI 2).

Publications:

J. D. Hernández, L. Onofri, S. Engell, Detailed Modeling of Radiative Heat Transfer in Electric Arc Furnaces Using Monte Carlo Techniques, Proc. 8th Int. Conf. on Modeling and Simulation of Metallurgical Processes in Steelmaking (STEELSIM 2019), Toronto, Canada 2019, 295–306.

J.D. Hernández, L. Onofri, S. Engell, Numerical Estimation of the Geometry and Temperature of an Alternating Current Steelmaking Arc, Steel. Res. Int., 202000386, 2020.

J. D. Hernandez, L. Onofri, S. Engell, Optimization of the electric efficiency of the electric steelmaking process, Proc. 21st IFAC World Congress, 2020, to appear in IFAC PapersOnline 2021.

Contact:
jesus.hernandez@tu-dortmund.de
sebastian.engell@tu-dortmund.de

Publications 2020 - 2018

2020

Invited Plenary Talks

- S. Engell
  Real-time optimization and control with inaccurate models
  61st International Conference of the Scandinavian Simulation Society, 22.-24.9.2020

- S. Engell
  Robust Performance Optimizing NMPC by Multistage Optimization
  6th IFAC Symposium on Advances in Control and Optimization of Dynamic Systems, Chennai, 16.-19.2.2020

Journal Papers

- A. Draeger, S. Engell, H. Ranke
  Model Predictive Control Using Neural Networks [25 Years Ago]
  IEEE Control Systems, 40 (5), art. no. 9199326, 11-12 (2020)

- L.S. Maxeiner, S. Engell
  Comparison of dual based optimization methods for distributed trajectory optimization of coupled semi-batch processes
  Optimization and Engineering, 21 (3), 761-802 (2020)

- S. Lucia, S. Subramanian, D. Limon, S. Engell
  Stability properties of multi-stage nonlinear model predictive control
  Systems and Control Letters, 143, art. no. 104743 (2020)

- P.M. Castro, G. Dalle Ave, S. Engell, I.E. Grossmann, I. Harjunkoski
  Industrial Demand Side Management of a Steel Plant Considering Alternative Power Modes and Electrode Replacement
  Industrial and Engineering Chemistry Research, 59 (30), 13642-13656 (2020)

- A.E.F. Bouaswaig, K. Rahimi-Adli, M. Roth, A. Hosseini, H. Vale, S. Engell, J. Birk
  Application of a grey-box modelling approach for the online monitoring of batch production in the chemical industry
  at-Automatisierungstechnik 68 (7), 582-598 (2020)

- S. Thangavel, R. Paulen, S. Engell
  Robust multi-stage nonlinear model predictive control using sigma points
  Processes 8 (7), art. no. 851 (2020)

- S. Klessova, C. Thomas, S. Engell
  Structuring inter-organizational R&D projects: Towards a better understanding of the project architecture as an interplay between activity coordination and knowledge integration
  International Journal of Project Management 38 (5), 291-306 (2020)

- L. Hebing, T. Neymann, S. Engell
  Application of dynamic metabolic flux analysis for process modeling: Robust flux estimation with regularization, confidence bounds, and selection of elementary modes
  Biotechnology and Bioengineering 117 (7), 2058-2073 (2020)

- B. Beisheim, S. Krämer, S. Engell
  Hierarchical aggregation of energy performance indicators in continuous production processes
  Applied Energy 264, art. no. 114709 (2020)

- L.S. Maxeiner, S. Engell
  An accelerated dual method based on analytical extrapolation for distributed quadratic optimization of large-scale production complexes
  Computers and Chemical Engineering 135, art. no. 106728 (2020)

- S. Wenzel, F. Riedl, S. Engell
  An efficient hierarchical market-like coordination algorithm for coupled production systems based on quadratic approximation
  Computers and Chemical Engineering 134, art. no. 106704 (2020)

- L. Hebing, F. Tran, H. Brandt, S. Engell
  Robust Optimizing Control of Fermentation Processes Based on a Set of Structurally Different Process Models
  Industrial and Engineering Chemistry Research 59 (6), 2566-2580 (2020)

- J.D. Hernández, L. Onofri, S. Engell
  Numerical Estimation of the Geometry and Temperature of an Alternating Current Steelmaking Electric Arc
  Steel Research International (2020)

Book Chapters

- S. Engell, A. Kienle
  Process Control
  Preparative Chromatography: Third Edition, 503-524 (2020)

Conference Papers

- Y. Abdelsalam, S. Subramanian, S. Engell
  Asymptotically Stabilizing Multi-Stage Model Predictive Control
  Proceedings of the 59th IEEE Conference on Decision and Control, art. no. 9304357, 710-717 (2020)

- M. Cegla, S. Engell
  Reliable Modelling of Twin-screw Extruders by Integrating the Backflow Cell Methodology into a Mechanistic Model
  Proceedings of the 30th European Symposium on Computer Aided Process Engineering, Computer Aided Chemical Engineering 48, 175-180 (2020)

- P. Azadi, S.A. Minaabad, H. Bartusch, R. Klock, S. Engell
  Nonlinear Prediction Model of Blast Furnace Operation Status
  Proceedings of the 30th European Symposium on Computer Aided Process Engineering, Computer Aided Chemical Engineering 48, 217-222 (2020)

- S. Kaiser, S. Engell
  Integrating Superstructure Optimization under Uncertainty and Optimal Experimental Design in early Stage Process Development
  Proceedings of the 30th European Symposium on Computer Aided Process Engineering, Computer Aided Chemical Engineering 48, 799-804 (2020)

- C. Klanke, V. Yfantis, F. Corominas, S. Engell
  Scheduling of a Large-scale Industrial Make-and-Pack Process with Finite Intermediate Buffer using Discrete-time and Precedence-based Models
  Proceedings of the 30th European Symposium on Computer Aided Process Engineering, Computer Aided Chemical Engineering 48, 1153-1158 (2020)

Publications 2020 - 2018

- S. Gerlich, Y.-N. Misz, S. Engell
  Online Process Monitoring in SMB Processes
  Proceedings of the 30th European Symposium on Computer Aided Process Engineering, Computer Aided Chemical Engineering 48, 1261-1266 (2020)

- E. Leo, S. Engell
  A Novel Multi-stage Stochastic Formulation with Decision-dependent Probabilities for Condition-based Maintenance Optimization
  Proceedings of the 30th European Symposium on Computer Aided Process Engineering, Computer Aided Chemical Engineering 48, 1795-1800 (2020)

- P.D. Schiermoch, B. Beisheim, K. Rahimi-Adli, S. Engell
  A Methodology for Data Based Root-cause Analysis for Process Performance Deviations in Continuous Processes
  Proceedings of the 30th European Symposium on Computer Aided Process Engineering, Computer Aided Chemical Engineering 48, 1873-1878 (2020)

- S. Wenzel, F. Riedl, S. Engell
  Market-like Distributed Coordination of Individually Constrained and Coupled Production Plants with Quadratic Approximation
  Proceedings of the 30th European Symposium on Computer Aided Process Engineering, Computer Aided Chemical Engineering 48, 1927-1932 (2020)

- T. Janus, A. Lübbers, S. Engell
  Neural Networks for Surrogate-assisted Evolutionary optimization of Chemical Processes
  Proceedings of the IEEE Congress on Evolutionary Computation (CEC), Glasgow, United Kingdom, art. no. 9185781, 1-8 (2020)

- A. R. Gottu Mukkula, P. Valiauga, M. Fikar, R. Paulen, S. Engell
  Experimental Real Time Optimization of a Continuous Membrane Separation Plant
  Proceedings of the IFAC World Congress, Berlin, Germany (online) (2020)

- A.R. Gottu Mukkula, S. Kern, M. Salge, M. Holtkamp, S. Guhl, C. Fleicher, K. Meyer, M.P. Remelhe, M. Maiwald, S. Engell
  An Application of Modifier Adaptation with Quadratic Approximation on a Pilot Scale Plant in Industrial Environment
  Proceedings of the IFAC World Congress, Berlin, Germany (online) (2020)

- T. Ebrahim, S. Engell
  A bi-level approach to MPC for switching nonlinear systems
  Proceedings of the IFAC World Congress, Berlin, Germany (online) (2020)

- Y. Abdelsalam, S. Subramanian, S. Engell
  A Simplified Implementation of Tube-Enhanced Multi-Stage NMPC
  Proceedings of the IFAC World Congress, Berlin, Germany (online) (2020)

- J. Hernández, L. Onofri, S. Engell
  Optimization of the electric efficiency of the electric steelmaking process
  Proceedings of the IFAC World Congress, Berlin, Germany (online) (2020)

- V. Yfantis, S. Büscher, C. Klanke, F. Corominas, S. Engell
  A Two-stage Simulated Annealing-based Scheduling Algorithm for a Make-and-Pack Production Plant
  Proceedings of the IFAC World Congress, Berlin, Germany (online) (2020)

- A. Tătulea-Codrean, J. Fischer, S. Engell
  A Multi-stage Economic NMPC for the Tennessee Eastman Challenge Process
  Proceedings of the IFAC World Congress, Berlin, Germany (online) (2020)

- A. Tătulea-Codrean, T. Mariani, S. Engell
  Design and Simulation of a Machine-learning and Model Predictive Control Approach to Autonomous Race Driving for the F1/10 Platform
  Proceedings of the IFAC World Congress, Berlin, Germany (online) (2020)

- S. Thangavel, R. Paulen, S. Engell
  Dual multi-stage NMPC using sigma point principles
  Proceedings of the IFAC World Congress, Berlin, Germany (online) (2020)

- S. Thangavel, S. Engell
  An efficient model-error model update strategy for multi-stage NMPC with model-error model
  Proceedings of the IFAC World Congress, Berlin, Germany (online) (2020)

- S. Thangavel, R. Paulen, S. Engell
  Adaptive multi-stage NMPC using sigma point principles
  Proceedings of the European Control Conference (ECC), art. no. 9143820, 196-201 (2020)

- A.R. Gottu Mukkula, S. Engell
  Guaranteed Model Adequacy for Modifier Adaptation With Quadratic Approximation
  Proceedings of the European Control Conference (ECC), art. no. 9143625, 1037-1042 (2020)

- S. Thangavel, R. Paulen, S. Engell
  Multi-stage NMPC using sigma point principles
  Proceedings IFAC ACODS 2020, Chennai, 16.-19.02.2020, IFAC-PapersOnLine 53 (1), 386-391 (2020)

Conference Presentations

- S. Gerlich, H. Arab, S. Engell
  Online Prozessüberwachung in SMB Prozessen
  Jahrestreffen der ProcessNet-Fachgemeinschaft Prozess-, Apparate- und Anlagentechnik (PAAT), online, 09.–10.11.2020

- B. Pfeiffer, C. Lindscheid
  Advanced Process Control (APC) - Durchführung von APC Projekten
  Jahrestreffen der ProcessNet-Fachgemeinschaft Prozess-, Apparate- und Anlagentechnik (PAAT), online, 09.–10.11.2020

- R. Semrau, F. Tamagnini, A. Tătulea-Codrean, S. Engell
  Dynamische Modellierung und Zustandsschätzung eines kontinuierlichen Coiled Flow Inverter Copolymerisationsreaktors
  Jahrestreffen der ProcessNet-Fachgemeinschaft Prozess-, Apparate- und Anlagentechnik (PAAT), online, 09.–10.11.2020

- T. Janus, A. Lübbers, S. Engell
  Kürzere Optimierungszeiten für Prozessfließbilder in Aspen Plus durch den Einsatz von künstlicher Intelligenz
  Jahrestreffen der ProcessNet-Fachgemeinschaft Prozess-, Apparate- und Anlagentechnik (PAAT), online, 09.–10.11.2020

Publications 2020 - 2018

2019

Invited Plenary Talks

- S. Engell, L.S. Maxeiner, S. Wenzel
  From unit optimization to site-wide optimization and industrial symbiosis
  8th International Symposium PSEASIA, Bangkok, Thailand, January 13-16, 2019

- S. Engell, S. Subramanian
  Robust NMPC by Multistage Optimization – Basic Idea and Further Developments
  22nd International Conference on Process Control, High Tatras, Slovakia, June 12-14, 2019

Journal Papers

- S. Wenzel, Y.-N. Misz, K. Rahimi-Adli, B. Beisheim, R. Gesthuisen, S. Engell
  An optimization model for site-wide scheduling of coupled production plants with an application to the ammonia network of a petrochemical site
  Optimization and Engineering, 20 (4), pp. 969-999 (2019)

- C. Nentwich, J. Winz, S. Engell
  Surrogate Modeling of Fugacity Coefficients Using Adaptive Sampling
  Industrial and Engineering Chemistry Research, 58 (40), pp. 18703-18716 (2019)

- G. Dalle Ave, I. Harjunkoski, S. Engell
  A non-uniform grid approach for scheduling considering electricity load tracking and future load prediction
  Computers and Chemical Engineering, 129, art. no. 106506, in press, (2019

- H. Hadera, J. Ekström, G. Sand, J. Mäntysaari, I. Harjunkoski, S. Engell
  Integration of production scheduling and energy-cost optimization using Mean Value Cross Decomposition
  Computers and Chemical Engineering, 129, art. no. 106436, in press, (2019)

- B. Beisheim, K. Rahimi-Adli, S. Krämer, S. Engell
  Energy performance analysis of continuous processes using surrogate models
  Energy, 183, pp. 776-787 (2019)

- C. Nentwich, S. Engell
  Surrogate modeling of phase equilibrium calculations using adaptive sampling
  Computers and Chemical Engineering, 126, pp. 204-217 (2019)

- I.T. Cameron, S. Engell, C. Georgakis, N. Asprion, D. Bonvin, F. Gao, D.I. Gerogiorgis, I.E. Grossmann, S. Macchietto, H.A. Preisig, B.R. Young
  Education in Process Systems Engineering: Why it matters more than ever and how it can be structured
  Computers and Chemical Engineering, 126, pp. 102-112 (2019)

- A. Ahmad, W. Gao, S. Engell
  A study of model adaptation in iterative real-time optimization of processes with uncertainties
  Computers and Chemical Engineering, 122, pp. 218-227 (2019)

- S. Kern, L. Wander, K. Meyer, S. Guhl, A.R.G. Mukkula, M. Holtkamp, M. Salge, C. Fleischer, N. Weber, R. King, S. Engell, A. Paul, M.P. Remelhe, M. Maiwald
  Flexible automation with compact NMR spectroscopy for continuous production of pharmaceuticals
  Analytical and Bioanalytical Chemistry (2019)

Conference Papers

- M.R. Modeer, S. Engell
  Design and validation of cyber-physical systems through model abstraction
  Proceedings 5th IEEE International Symposium on Systems Engineering (ISSE 2019), art. no. 8984475

- V. Yfantis, F. Corominas, S. Engell
  Scheduling of a consumer goods production plant with intermediate buffer by decomposition and mixed-integer linear programming
  IFAC-PapersOnLine, 52 (13), pp. 1837-1842 (2019)

- C. Nentwich, C. Varela, S. Engell
  Optimization of chemical processes applying surrogate models for phase equilibrium calculations
  Proceedings of the International Joint Conference on Neural Networks, 2019-July, art. no. 8851816 (2019)

- S. Thangavel, S. Engell
  Handling Plant-model Mismatch Using Multi-stage NMPC with Model-error Model
  Proceedings of the 2019 22nd International Conference on Process Control, PC 2019, art. no. 8815032, pp. 1-6 (2019)

- A. Ahmad, A.R. Gottu Mukkula, S. Engell
  Model Adaptation with Quadratic Approximation in Iterative Real-Time Optimization
  Proceedings of the 2019 22nd International Conference on Process Control, PC 2019, art. no. 8815377, pp. 250-255 (2019)

- S. Subramanian, M. Abdelnour, S. Engell
  Robust tube-enhanced multi-stage output feedback MPC for linear systems with additive and parametric uncertainties
  2019 18th European Control Conference, ECC 2019, art. no. 8795680, pp. 331-336 (2019)

- S. Thangavel, S. Subramanian, R. Paulen, S. Engell
  Robust multi-stage NMPC under structural plant-model mismatch without full-state measurements
  2019 *18th European Control Conference, ECC 2019, art. no. 8795794, pp. 781-786 (2019)*

Publications 2020 - 2018

- S. Wenzel, S. Engell
  Coordination of coupled systems of systems with quadratic approximation
  IFAC-PapersOnLine, 52 (3), pp. 132-137 (2019)

- R. Hernández, S. Engell
  Economics optimizing control with model mismatch based on modifier adaptation
  FAC-PapersOnLine, 52 (1), pp. 46-51 (2019)

- M.R. Modeer, S. Vette, S. Engell
  Compensating Signal Loss in RFID-Based Localization Systems
  IFAC-PapersOnLine, 52 (8), pp. 289-294 (2019)

- J.D. Hernandez, L. Onofi, S. Engell
  Model of an Electric Arc Furnace Oxy-Fuel Burner for dynamic simulations and optimisation purposes
  IFAC-PapersOnLine, 52 (14), pp. 30-35 (2019)

- J.D. Hernandez, L. Onofri, S. Engell
  Detailed modeling of radiative heat transfer in electric arc furnaces using Monte Carlo techniques
  Proceedings of the 8th International Conference on Modeling and Simulation of Metallurgical Processes in Steelmaking, STEELSIM 2019, pp. 295-304 (2019)

- S. Thangavel, S. Subramanian, S. Engell
  Robust NMPC using a model-error model with additive bounds to handle structural plant-model mismatch
  (2019) IFAC-PapersOnLine, 52 (1), pp. 592-597

- C. Lindscheid, P. Sakthithasan, S. Engell
  An Ecological Interface Design Based Visualization of the Energy Balance of Chemical Reactors *
  IFAC-PapersOnLine, 51 (34), pp. 308-314 (2019)

- A. Tatulea-Codrean, C. Lindscheid, R. Farrera-Saldana, S. Engell
  Extension of the do-mpc development framework to real-time simulation studies
  IFAC-PapersOnLine, 52 (1), pp. 388-393 (2019)

- T. Janus, M. Cegla, S. Barkmann, S. Engell
  Optimization of a hydroformulation process in a thermomorphic solvent system using a commercial steady-state process simulator and a memetic algorithm
  Proceedings 29th Symposium on Computer-Aided Process Engineering, Computer Aided Chemical Engineering, 46, pp. 469-474 (2019)

- G.D. Ave, M. Alici, I. Harjunkoski, S. Engell
  An Explicit Online Resource-Task Network Scheduling Formulation to Avoid Scheduling Nervousness
  Proceedings 29th Symposium on Computer-Aided Process Engineering, Computer Aided Chemical Engineering, 46, pp. 61-66 (2019)

- K. Rahimi-Adli, P.D. Schiermoch, B. Beisheim, S. Wenzel, S. Engell
  A model identification approach for the evaluation of plant efficiency
  Proceedings 29th Symposium on Computer-Aided Process Engineering, Computer Aided Chemical Engineering, 46, pp. 913-918 (2019)

- V. Yfantis, T. Siwczyk, M. Lampe, N. Kloye, M. Remelhe, S. Engell
  Iterative Medium-Term Production Scheduling of an Industrial Formulation Plant
  Proceedings 29th Symposium on Computer-Aided Process Engineering, Computer Aided Chemical Engineering, 46, pp. 19-24 (2019)

- G. Dalle Ave, J. Hernandez, I. Harjunkoski, L. Onofri, S. Engell
  Demand side management scheduling formulation for a steel plant considering electrode degradation
  IFAC-PapersOnLine, 52 (1), pp. 691-696 (2019)

Conference Presentations

- L. Leo, K. Rahimi-Adli, B. Beisheim, R. Gesthuisen, S. Engell
  Applying Stochastic Optimization to Demand-Side Management of a Combined Heat and Power Plant
  12th European Congress of Chemical Engineering (ECCE 12), Florence, Italy, September 15-19, 2019

- S. Wenzel, Y.-N. Misz, K. Rahimi-Adli, B. Beisheim, S. Engell
  Optimal site-wide planning of a NH3 network – A study on uncertain logistic constraints
  12th European Congress of Chemical Engineering (ECCE 12), Florence, Italy, September 15-19, 2019

- A.R. Gottu Mukkula, S. Engell
  Application of Iterative Real-time Optimization in an Intensified Continuous Plant at Pilot Plant Scale
  12th European Congress of Chemical Engineering (ECCE 12), Florence, Italy, September 15-19, 2019

- C. Klanke, L.S. Maxeiner, S. Engell
  Price-based Coordination of Shared Resources with External Suppliers
  12th European Congress of Chemical Engineering (ECCE 12), Florence, Italy, September 15-19, 2019

- A.P. Elekidis, V. Yfantis, C. Klanke, F. Corominas, M.C. Georgiadis, S., Engell
  Optimal Production Scheduling in the Packaged Consumer Goods Industry
  12th European Congress of Chemical Engineering (ECCE 12), Florence, Italy, September 15-19, 2019

- J.L. Pitarch, C. Jasch, M. Kalliski, Y.-N. Misz, M. Marcos, C. de Prada, G. Seyfriedsberger, S. Engell
  Energy-efficient Operation of a Multi-unit Recovery Cycle in EU's Largest Viscose Fiber Plant
  12th European Congress of Chemical Engineering (ECCE 12), Florence, Italy, September 15-19, 2019

- M. Cegla, T. Janus, S. Tlatlik, P. Krause, T. Bäck, A. Gottschalk, S. Engell
  Flexible and Efficient Process Synthesis and Optimization Based on Aspen Plus Simulations – MTBE Production Case Study
  12th European Congress of Chemical Engineering (ECCE 12), Florence, Italy, September 15.-19.2019

Publications 2020 - 2018

- C. Nentwich, S. Engell
  Optimierung chemischer Prozesse unter Verwendung von Surrogatmodellen
  Jahrestreffen der ProcessNet-Fachgemeinschaft Prozess-, Apparate- und Anlagentechnik (PAAT), Dortmund, 04.-05.11.2019

- S. Wenzel, L.S. Maxeiner, S. Engell
  Gemeinsame Optimierung von Anlagenverbünden ohne Austausch sensitiver Informationen – geht das?
  Jahrestreffen der ProcessNet-Fachgemeinschaft Prozess-, Apparate- und Anlagentechnik (PAAT), Dortmund, 04.-05.11.2019

- L.S. Maxeiner, S. Wenzel, Y.-N. Misz, S. Engell
  Overcoming the modelling bottleneck – Effiziente MILP Modellierung von Verbundstandorten und deren Logistik
  Jahrestreffen der ProcessNet-Fachgemeinschaft Prozess-, Apparate- und Anlagentechnik (PAAT), Dortmund, 04.-05.11.2019

- K. Rahimi-Adli, E. Leo, B. Beisheim, E. Engell
  A framework for the optimization of the operation of an industrial power plant under demand uncertainty
  Jahrestreffen der ProcessNet-Fachgemeinschaft Prozess-, Apparate- und Anlagentechnik (PAAT), Dortmund, 04.-05.11.2019

- R. Lemoine, C. Maul, L.S. Maxeiner, S. Engell
  Preisbasierte Optimierung des Einkaufs technischer Gase
  Jahrestreffen der ProcessNet-Fachgemeinschaft Prozess-, Apparate- und Anlagentechnik (PAAT), Dortmund, 04.-05.11.2019

- S. Gerlich, S. Engell
  Efficient isotherm estimation using neural networks for applications in SMB process design and preparative chromatography
  International PhD Seminar on Chromatographic Separation Science. Quedlinburg, 24.-27.02.2019

2018

Journal Papers

- D. Haßkerl, S. Subramanian, S. Markert, S. Kaiser, S. Engell
  Multi-rate state estimation applied to a pilot-scale reactive distillation process
  Chemical Engineering Science 185, 256-281 (2018)

- S. Thangavel, S. Lucia, R. Paulen, S. Engell
  Dual robust nonlinear model predictive control: A multi-stage approach
  Journal of Process Control 72, 39-51 (2018)

- E. Leo, S. Engell
  Integrated day-ahead energy procurement and production scheduling
  at-Automatisierungstechnik 66(11), 950-963 (2018)

- D. Haßkerl, C. Lindscheid , S. Subramanian, A. Tatulea-Codrean, S. Engell
  Economics optimizing control of a multi-product reactive distillation process under uncertainty
  Computers and Chemical Engineering 118, 25-48 (2018)

- D. Haßkerl, C. Lindscheid, S. Subramanian, A. Górak, S. Engell
  Dynamic Optimization of a Pilot-Scale Distillation Process by Economics Optimizing Control
  Industrial and Engineering Chemistry Research 57(36), 12165–12181 (2018)

- R. Hernandez, J. Dreimann, A. J. Vorholt, A. Behr, S. Engell
  Iterative Real-Time Optimization Scheme for Optimal Operation of Chemical Processes under Uncertainty: Proof of Concept in a Miniplant
  Industrial and Engineering Chemistry Research 57(26), 8750-8770 (2018)

Conference Papers

- T. Ebrahim, S. Subramanian, S. Engell
  Hybrid NMPC for switching Systems Applied to a Supermarket Refrigeration System
  Proceedings of ECC18, European Control Conference, Limassol, Cyprus, 2018, IEEE, 813-818

- E. Leo, S. Engell
  Multi-stage integrated electricity procurement and production scheduling
  Proceedings of PSE18, 13th Symposium on Process System Engineering, Computer Aided Chemical Engineering 44, 1291-1296

- L. S. Maxeiner, S. Wenzel, S. Engell
  Price-based coordination of interconnected systems with access to external markets
  Proceedings of PSE18, 13th Symposium on Process System Engineering, Computer Aided Chemical Engineering 44, 877-882

- Ahmad, W. Gao, S. Engell
  Modifier Adaptation with Model Adaptation in Iterative Real-Time Optimization
  Proceedings of PSE18, 13th Symposium on Process System Engineering, Computer Aided Chemical Engineering 44, 691-696

Publications 2020 - 2018

- G. D. Ave, I. Harjunkoski, S. Engell
  Industrial Demand Side Management Formulation for Simultaneous Electricity Load Commitment and Future Load Prediction
  Proceedings of PSE18, 13th Symposium on Process System Engineering, Computer Aided Chemical Engineering 44, 1237-1242

- E. Leo, S. Engell
  A two-stage stochastic programming approach to integrated day-ahead electricity commitment and production scheduling
  Proceedings of ESCAPE 28, 28th Symposium on Computer Aided Process Engineering, Computer Aided Chemical Engineering 43, 1009-1014

- G. D. Ave, X. Wang, I. Harjunkoski, S. Engell
  A heuristic neighbourhood search-based algorithm for the solution of resource-task network scheduling problems
  Proceedings of ESCAPE 28, 28th European Symposium on Computer Aided Process Engineering, Computer Aided Chemical Engineering 43, 907-912

- S. Wenzel, L. S. Maxeiner, S. Engell
  Virtual splitting of shared resource networks for price-based coordination with portfolio tariffs
  Proceedings of ESCAPE 28, 28th European Symposium on Computer Aided Process Engineering, Computer Aided Chemical Engineering 43, 301-306

- R. Gottu Mukkula, S. Wenzel, S. Engell
  Active Perturbation in Modifier Adaptation for Real Time Optimization to Cope with Measurement Delays
  Proceedings of ACODS2018, 5th IFAC Conference on Advances in Control and Optimization of Dynamical Systems, IFAC-PapersOnLine 51(1), 124-129

- S. Thangavel, S. Subramanian, S. Lucia, S. Engell
  Handling Structural Plant-model Mismatch using a Model-error Model in the Multi-stage NMPC framework
  Proceedings of SYSID2018, 18th IFAC Symposium on System Identification, Stockholm, Sweden, IFAC-PapersOnLine 51(15), 1074-1079

- S. Subramanian, S. Lucia, B. Baradaran, A. Seayed, R. Paulen, S. Engell
  A Combined Multi-stage and Tube-based MPC Scheme for Constrained Linear Systems
  Proceedings of NMPC2018, 6th Conference on Nonlinear Model Predictive Control, Madison, Wisconsin, USA, IFAC-PapersOnLine 51(20), 481-486

- S. Thangavel, M. Aboelnour, S. Lucia, R. Paulen, S. Engell
  Robust Dual Multi-stage NMPC using Guaranteed Parameter Estimation
  Proceedings of NMPC2018, 6th Conference on Nonlinear Model Predictive Control, Madison, Wisconsin, USA, IFAC-PapersOnLine 51(20), 72-77

- R. Hernandez, J. Dreimann, S. Engell
  Reliable Iterative RTO of a Continuously Operated Hydroformylation Process
  Proceedings of ADCHEM 2018, 10th IFAC Symposium of Chemical Processes, Shenyang, China, IFAC-PapersOnLine 51(18), 61-66

- S. Subramanian, S. Lucia, S. Engell
  A Synergistic Approach to Robust Output Feedback Control: Tube-based Multi-stage NMPC
  Proceedings of ADCHEM 2018, 10th IFAC Symposium of Chemical Processes, Shenyang, China, IFAC-PapersOnLine 51(18), 500-505

- R. Gottu Mukkula, S. Wenzel, S. Engelll
  Active Perturbations Around Estimated Future Inputs in Modifier Adaptation to Cope with Measurement Delays
  Proceedings of ADCHEM 2018, 10th IFAC Symposium of Chemical Processes, Shenyang, China, IFAC-PapersOnLine 51(18), 839-844

- A. Ahmad, M. Singhal, W. Gao, D. Bonvin, S. Engell
  Enforcing Model Adequacy in Real-Time Optimization via Dedicated Parameter Adaptation
  Proceedings of ADCHEM 2018, 10th Symposium on Advanced Control of Chemical Processes, Shenyang, China, IFAC-PapersOnLine 51(18), 49-54

- D. Haßkerl, C. Lindscheid, S. Subramanian, S. Markert, A. Gorák, S. Engell
  Application of Economics Optimizing Control to a Two-Step Transesterification Reaction in a Pilot-Scale Reactive Distillation Column
  Proceedings of ADCHEM 2018, 10th Symposium on Advanced Control of Chemical Processes, Shenyang, China, IFAC-PapersOnLine 51(18), 67-72

- C. Lindscheid, P. Shakthihasan, S. Engell
  An Ecological Interface Design Based Visualization of the Energy Balance of Chemical Reactors
  Proceedings of CPHS18, 2nd IFAC Conference on Cyber-Physical & Human Systems, Miami, USA, IFAC-PapersOnLine 51(34), 308-314

- S. Subramanian, S. Nazari, M. A. Alvi, S. Engell
  Robust NMPC Schemes for the Control of Mobile Robots in the Presence of Dynamic Obstacles
  Proceedings of MMAR 2018, Methods and Models in Automation and Robotics, Miedzyzdroje, Poland, IEEE, 768-773

- M. Rantanen Modeer, C. Sonntag, S. Engell
  Towards enabling heterogeneous model inter-operation across abstraction levels
  MATHMOD 2018; Proceedings 9th International Conference on Mathematical Modelling, Vienna, Austria, 105-106 (2018)

Conference Presentations

- S. Wenzel, L. S. Maxeiner, S. Engell
  Steigerung der Energie- und Ressourceneffizienz durch bessere Koordinierung der Produktion in der Prozessindustrie
  Proceedings of ProcessNet 2018, 33. DECHEMA-Jahrestagung der Biotechnologen, Aachen, Germany, Chemie Ingenieur Technik 90(9), 1162-1163 (2018)

- A. R. Gottu Mukkula, S. Engell, S. Kern, S. Guhl, K. Mayer, M. Maiwald
  PAT-basierte iterative Optimierung der Fahrweise eines kontinuierlichen organischen Syntheseprozesses
  Proceedings of ProcessNet 2018, 33. DECHEMA-Jahrestagung der Biotechnologen, Aachen, Germany, Chemie Ingenieur Technik 90(9), 1237-1237 (2018)

- D. Haßkerl, C. Lindscheid, S. Markert, S. Engell
  Dynamische Echtzeitoptimierung einer zweistufigen Umesterungsreaktion in einer Mehrprodukt-Pilotanlage für Reaktivrektifikation
  Proceedings of ProcessNet 2018, 33. Jahrestagung der Biotechnologen, Aachen, Germany, Chemie Ingenieur Technik 90(9), 1236-1236 (2018)

- S. Wenzel, Y.-N. Misz, K. Rahimi-Adli, R. Gesthuisen, S. Engell
  Optimale standortweite Produktionsplanung am Beispiel des NH3-Netzwerkes der INEOS in Köln
  Jahrestreffen der Fachgemeinschaft Prozess-, Apparate- und Anlagentechnik, Köln, Germany (2018)

- C. Nentwich, S. Engell
  Anwendung maschinellen Lernens auf Phasengleichgewichtsberechnungen
  Jahrestreffen 2018 der Fachgemeinschaft Prozess-, Apparate- und Anlagentechnik, Köln

- R. Hernandez, S. Engell
  Achieving Optimal Operation of Chemical Processes with Inaccurate Models – Proof of Concept in a Miniplant
  Jahrestreffen 2018 der Fachgemeinschaft Prozess-, Apparate- und Anlagentechnik, Köln

- B. Beisheim, K. Rahimi-Adli, S. Engell
  Entwicklung und Anwendung von Ressourceneffizienzkennzahlen für das Energiemanagementsystem der INEOS in Köln
  Jahrestreffen 2018 der Fachgemeinschaft Prozess-, Apparate- und Anlagentechnik, Köln

- M. Rantanen Modéer, S. Engell
  Integration of Partial Models of Multi-Agent Systems through Abstraction
  21st Euromicro conference on Digital System Design, Praque, Czech Republic (2018)

Solids Process Engineering (FSV)

Preparation of Solid Dispersions by Electrostatic Precipitation

A process to produce drug formulations with enhanced dissolution behavior

Anna Justen, Adrian Dobrowolski, Gerhard Schaldach, Helmut Wiggers, Markus Thommes

One main challenge in formulation development of pharmaceutical applications is the poor aqueous solubility of many drug substances. Formulations of solid dispersions could be shown to be an appropriate strategy to overcome poor solubility and increase the in vitro dissolution behavior. The challenge within this project is the preparation of submicron drug particles using spray drying, since conventional dispersing methods fail in this particle size range.

The aim of this work is the development of an apparatus, which enables the production of solid dispersions consisting of submicron drug particles embedded in a crystalline carrier matrix.

A spray drying plant, which successfully produces submicron drug particles has been developed. In the custom-made spray drying plant small droplets of active pharmaceutical excipient (API) solutions are produced with ultrasonic atomization technique. After a drying and a condensation step to remove the solvent from the process, submicron API particles result (Figure 1). In future research the spray drying plant will be optimized concerning the yield and be prepared for further processing of the product.

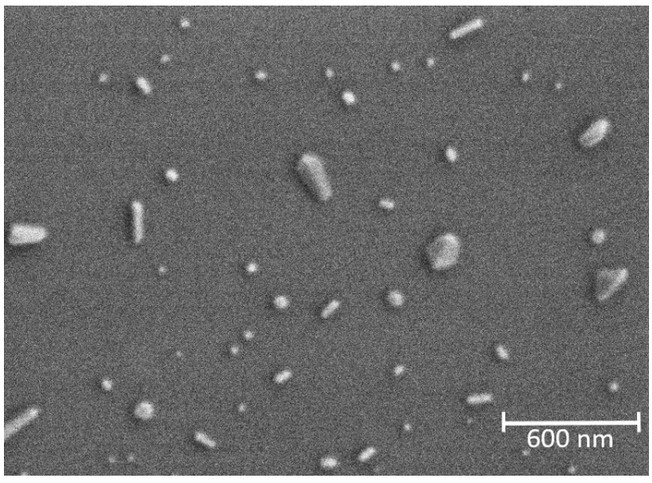

Figure 1: SEM picture of spray dried submicron API particles.

For the embedding of submicron drug particles in a crystalline carrier, electrostatic precipitation technique was found to be an appropriate method. First experiments with a static melt electrostatic precipitator have been conducted [1]. Hereby the concept of the spray drying plant combined with electrostatic precipitation in order to produce solid dispersions could be proven. An experimental set-up has been constructed. Since the drug load was found to be rather small with this plant, a new concept of an electrostatic precipitator will be developed in future research. A main focus will be the dynamic renewing of the melt surface, so that drug particle agglomeration will be avoided and the drug load of the product can be increased.

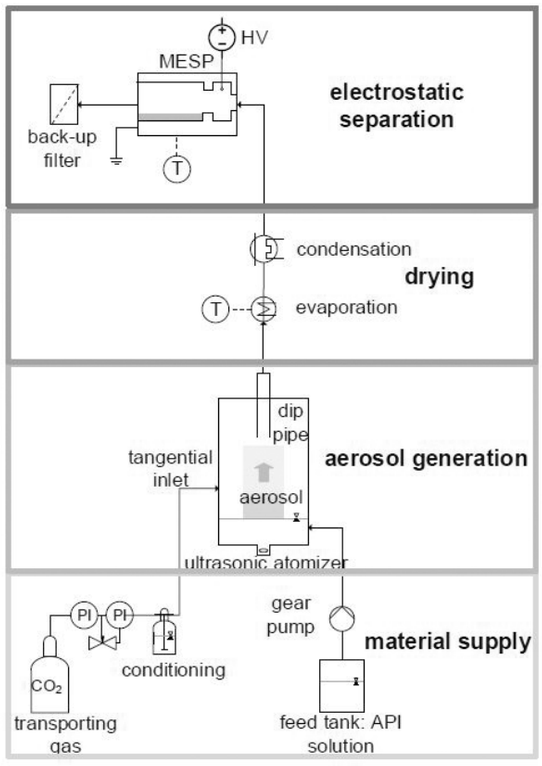

Figure 2: Schematic of a spray drying plant combined with the melt electrostatic precipitation (MESP).

"Funded by the European Union and the state of North Rhine Westphalia"

EFRE.NRW
Investitionen in Wachstum und Beschäftigung

EUROPEAN UNION
Investing in our Future
European Regional Development Fund

Contact:
anna.justen@tu-dortmund.de
gerhard.schaldach@tu-dortmund.de
markus.thommes@tu-dortmund.de

Publications:
M. Thommes, A. Dobrowolski, H. Wiggers, D. Pieloth, G. Schaldach, A. Justen, Electrostatic Precipitator. WO 2020/207680 A1.

Investigations on Powder Residence Time in a Rotary Tablet Press

Maren Zimmermann, Markus Thommes

Recently, pharmaceutical production has been focusing on continuous operational modes to a great extent due to advantages relating to process efficiency, flexibility and cost-effectiveness. In this context, the compression of powder on rotary tablet presses is one essential technology. In most rotary tablet presses a feed frame with rotating paddles is used in order to overcome challenges in powder flow. Residence time distribution (RTD) is an important parameter to derive the mixing capacity of the system as well as the impact of shear forces applied by the feed frame paddles to powder particles. These shear forces can cause overlubrication and changes in particle size, which might have an impact on downstream process steps. The aim of this study was the investigation of the influence of the rotational speed of the feed frame paddles on RTD in a rotary tablet press.

The residence time distribution of powder was measured inline with an UV/Vis probe using a sampling rate of 1.3 Hz on a rotary tablet press. Experiments were performed with three paddle speeds (30, 60 and 90 rpm). A model formulation was used, and theophylline was added as a tracer.
The rotary tablet press showed a broad RTD due to a large hold-up of several powder clusters. It indicates a high degree of backmixing. For quantifying, the measured RTD was fitted to a model based on the combination of plug flow and a continuous stirred tank reactor (CSTR) (Eq. 1), which represented the measured data well (Figure 1).

$$F(t) = \begin{cases} 0, & t < t_{transport} \\ 1 - \exp\{-t_{mixing}^{-1} \cdot (t - t_{transport})\}, & t \geq t_{transport} \end{cases} \quad (1)$$

The width of the RTD was characterized by the inverse mixing time t^{-1}_{mixing} and the displacement of the curve on the time axis was described by the transport time $t_{transport}$. The active time t_{active}, which was specified by the sum of $t_{transport}$ and t_{mixing}, can be used for the identification of dead spaces: for a smaller tactive compared to the hydrodynamic residence time, dead spaces within the feed frame existed. Unexpectedly, the feed frame paddle speed did not influence the inverse mixing time t^{-1}_{mixing} and the transport time $t_{transport}$. Therefore, mixing capacity of the feed frame was not affected by the rotational speed of the feed frame paddles. The active time t_{active} was smaller than the hydrodynamic residence time for all tested feed frame paddle speeds. Consequently, dead spaces existed. The particles, which were trapped in dead spaces, were exchanged more slowly compared to the remaining feed frame volume. This may cause difficulties in tablet manufacturing due to overlubrication and abrasion as these particles experienced shear forces applied by feed frame paddles for a longer time.
In conclusion, powder RTD in a rotary tablet press were broad due to a high degree of backmixing. It showed a negative impact on tablet manufacturing due to overlubrication as well as a positive influence on powder mixing. The positive effect might be important to reduce product quality variations in continuous manufacturing.

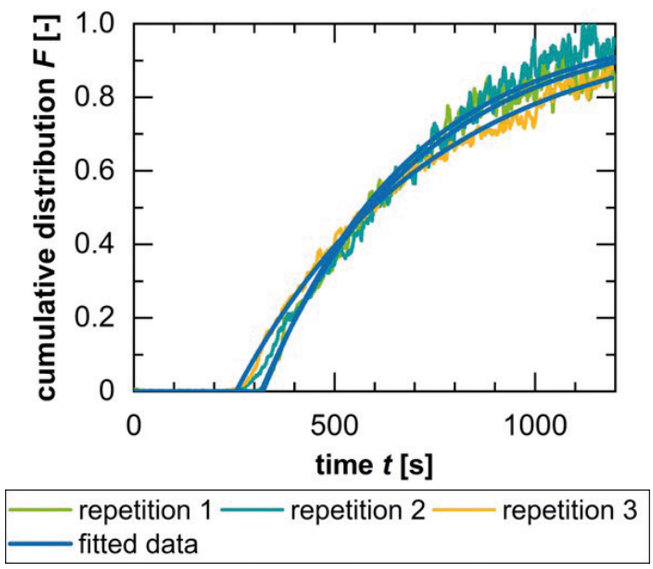

Figure 1: Experimentally-determined (n = 3) and fitted cumulative density function F as function of time t for a rotational speed of the feed frame paddles of 90 rpm.

Publications:
M. Zimmermann, M. Thommes, 2nd APV Continuous Manufacturing Conference, Freiburg, February 2020.

Contact:
jens.bartsch@tu-dortmund.de
markus.thommes@tu-dortmund.de

Development of an Experimental Setup for Determining Characteristic Screw Parameters of Co-Rotating Twin-Screw Extruders

Vanessa Düphans, Vincent Kimmel, Judith Winck, Markus Thommes

Twin-screw extruders have been increasingly applied in pharmaceutical processes as a method to improve the bioavailability of poorly soluble active pharmaceutical ingredients by molecularly dispersing them in polymeric carriers. For the optimal process design the prediction of, for example, the temperature profile, mixing conditions and shear stress is essential. These process parameters can be calculated with the dimensionless screw parameters, which have to be determined experimentally. However, these measurements are rarely carried out in industry and research due to their complexity. Therefore, a novel experimental setup was designed.

The screw parameters are used to characterize a screw element regarding to its throughput, pressure build-up and power input. When plotting the dimensionless pressure build-up and the power input linearly over the dimensionless volume flow, the characteristic screw parameters can be identified as the axis intercepts (Figure 1).

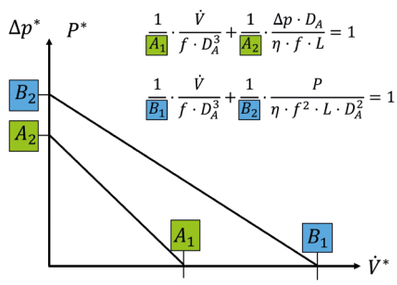

Figure 1: Dimensionless characteristics of twin-screw extruders.

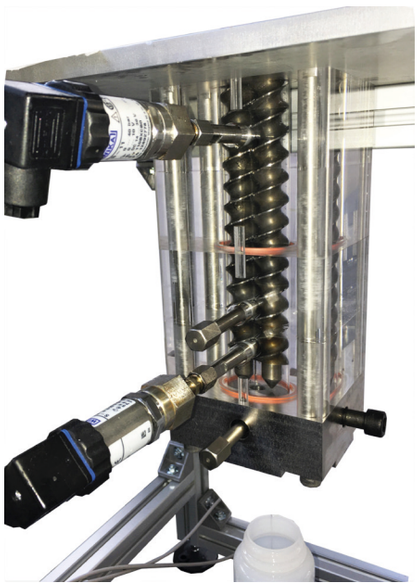

Figure 2: Vertical extruder.

Contact:
vanessa.duephans@tu-dortmund.de
markus.thommes@tu-dortmund.de

For the determination of these screw parameters, an experimental setup was developed that consists of a self-constructed vertical twin-screw extruder, geometrically similar to the commercial Leistritz ZSE 27 extruder. The extruder is powered by a high torque stepper engine, which drives the twin-screws synchronously via toothed belts. In Figure 2, the screw elements are shown, which rotate inside an acrylic barrel. The axial pressure build-up was measured in the intermeshing zone and the torque was determined directly at the screws. The volume flow was calculated with the change of mass over time of the extruded material. In the experiments the die diameter of the extruder, the viscosity, the screw speed and the type of screw elements were varied.

The resulting pressure characteristics are plotted in Figure 3. As expected, the curve is linear and the screw parameters can be identified as the axis intercepts. The dimensionless pressure build-up and the dimensionless volume flow are only influenced by the die diameter. In addition, the dimensionless power input is shown. A small variability of the measured values occurs there. However, the trend is also linear decreasing and depending on the die diameter.

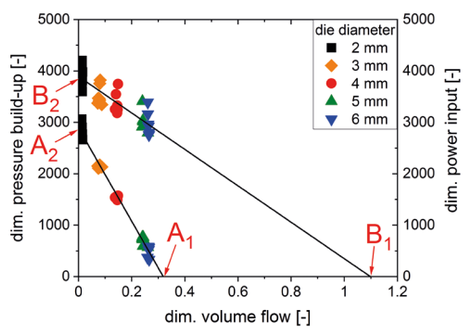

Figure 3: Measured pressure and power characteristics.

In conclusion, the self-constructed twin-screw extruder is a unique setup, which enables a precise determination of dimensionless screw parameters. In the future, these screw parameters can be implemented into simulations in order to predict complex extrusion processes.

Investigation of Particle Separation in Depth Filters

Aerosol Generation and Tomographic Analysis of Particle Depositions

Kevin Hoppe[1,2], Gerhard Schaldach[1], Reiner Zielke[3], Wolfgang Tillmann[3], Markus Thommes[1], Damian Pieloth[1,2]
1: Technische Universität Dortmund, Lehrstuhl für Feststoffverfahrenstechnik
2: Hochschule Anhalt, Fachbereich Angewandte Biowissenschaften und Prozesstechnik
3: Technische Universität Dortmund, Lehrstuhl für Werkstofftechnologie

Not least, the Covid-19 pandemic has brought the study of aerosols and their capture into wide public focus. In many areas, depth filters are used to separate fine particles from gas. Here, the longest possible service life and high separation efficiency are required. An increasing differential pressure limits the separation process. These macroscopic properties are determined by microscopic properties of the filter material (e.g. porosity distribution) and finally responsible for the loading behavior. A deeper understanding of the filtration process, especially the interaction between filter media and operating parameters are a key for the improvement of filtration media. Simulations based on the microstructure of the filter material are often used in this context. In contrast to this, complementary experimental data of deposition specifically at the microscopic level to the simulations are few in the literature. Previous studies on this investigation face the problem of low contrasts between particles and filter materials as well as low spatial resolution. Here, a particle generation process to produce particles with high contrast and defined particle size distribution is presented. Furthermore, the application of an X-ray microscope (XRM) for the analysis of particle depositions is discussed. The developed methods are promising for a further investigation of particle deposition in filters.

Particles were prepared by spray drying of salt solutions having different concentrations using an ultrasonic nebulizer operating at a frequency of about 3 MHz. The finally generated aerosol consists of dry particles having a narrow size distribution and a median particle size ($d_{50,3}$) of 1µm. As the concentration of the feed salt solution decreases, final particle size decreases as expected (Figure 1). Additionally, no difference in particle size was observed for higher salt concentrations for two different salts.

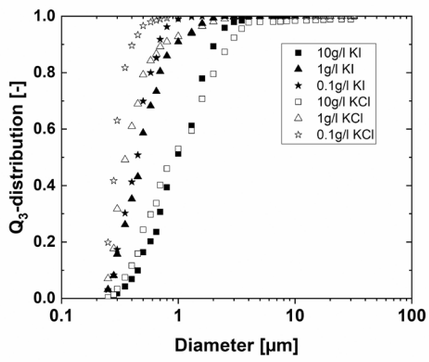

Figure 1: Cumulative size distribution of produced particles at different feed concentrations.

An XRM scan of the filter material was performed before loading. The generated reconstruction of these data (Figure 2, left) allows the investigation of structural properties such as porosity or fiber diameter distribution and direct incorporation into flow simulations.

Particles produced at a salt concentration of 10 g/l ($d_{50,3}$ of 1 µm) were separated in a test filter and the grade separation efficiency of 1 µm Potassium iodide particles was determined, as well as the differential pressure generated by the filter (particle loading of air 1 mg/m³, face velocity of 0.5 m/s). The filter was loaded for approx. 180 min and filtration efficiency and differential pressure were recorded again. As expected, there was an increase in both parameters due to the particle deposition inside the filter material. An XRM-scan (X-ray power: 50 kV) of the loaded sample shows the distribution of particles reflecting the loading behavior of the filter. The potassium iodide particles generate a high contrast, which enables the localization and image analysis of individual deposited particles or deposited particle collectives. The methods presented here overcome previous limitations such as a low contrast between particles and filter material. Furthermore, a high spatial resolution of less than 1µm can be achieved. It opens up further detailed experimental studies of particle separation in filter materials. The experimental data collected can also be used to validate and optimize simulations and calculation models. In this way, the optimization of filter material structure with regard to longer service life can be further optimized.

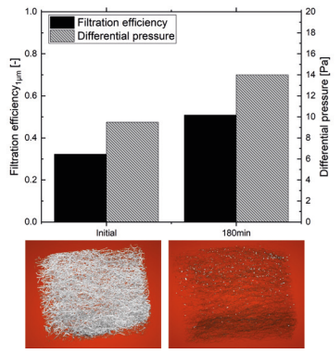

Figure 2: Macroscopic filtration efficiency and differential pressure in the initial state and after 180 min particle loading (above), reconstruction of filter sample structure after XRM-measurement in the initial state (left), and reconstruction of filter sample structure with deposited KI-particles after 180 min particle loading (right).

Contact:
kevin.hoppe@tu-dortmund.de
damian.pieloth@tu-dortmund.de

Publications:
K. Hoppe, M. Maricanov, G. Schaldach, R. Zielke, D. Renschen, W. Tillmann, M. Thommes, D. Pieloth, (2020), Modeling the separation performance of depth filter considering tomographic data. In Environ Prog Sustainable Energy 39 (5). DOI: 10.1002/ep.13423.

K. Hoppe, G. Schaldach, R. Zielke, W. Tillmann, M. Thommes, D. Pieloth, Partikelerzeugung und Untersuchung der Abscheidung in Tiefenfiltern mit röntgentomographischen Verfahren. ProcessNet Gasreinigung, Poster, 18.-19.02.2021, Bamberg.

Publications 2020 - 2018

2020

- R. Schneider, J. Kerkhoff, A. Danzer, A. Mattusch, A. Ohmann, M. Thommes, G. Sadowski
  The interplay of dissolution, solution crystallization and solid-state transformation of amorphous indomethacin in aqueous solution
  International Journal of Pharmaceutics: X 2 (2020) 100063

- R. Strob, T. Babaria, M. Rodeck, G. Schaldach, P. Walzel, M. Thommes
  Evaluation of spray impact on a sphere with a two-fluid nozzle
  (2020) Journal of Aerosol Science 140 (2020) 105483

- T. Feuerbach, S. Kock, M. Thommes
  Slicing parameter optimization for 3D printing of biodegradable drug-eluting tracheal stents
  (2020) Pharmaceutical Development and Technology ISSN 1083-7450 (Print) 1097-9867 (Online), DOI 10.1080/108337450.2020.1727921

- P. Grohn, D. Weis, M. Thommes, S. Heinrich, S. Antonyuk
  Contact Behavior of Microcrystalline Cellulose Pellets Depending on their Water Content
  (2020) Pharmaceutical Development and Technology ISSN 1083-7450 (Print) 1097-9867 (Online), DOI 10.1080/108337450.2020.1727921

- K. Hoppe, M. Maricanov, G. Schaldach, R. Zielke, D. Renschen, W. Tillmann, M. Thommes, D. Pieloth
  Modeling the separation performance of depth filter considering tomographic data
  (2020) Environmental Progress and Sustainable Energy Vol. 39, Issue 5, e13423Accepted 24.02.2020, DOI: 10.1002/ep.13423

- K. Fluegel, R. Hennig, M. Thommes
  Impact of structural relaxation on mechanical properties of amorphous polymers
  Eur J Pharm Biopharm 154 (2020) 214-221

2019

- K. Flügel, R. Hennig, M. Thommes
  Determination of the Structural Relaxation Enthalpy Using a Mathematical Approach
  Journal of Pharmaceutical Sciences 108(11), pp. 3675-3683 (2019)

- J. Wesholowski, K. Hoppe, K. Nickel, C. Muehlenfeld, M. Thommes
  Scale-Up of pharmaceutical Hot-Melt-Extrusion: Process optimization and transfer
  European Journal of Pharmaceutics and Biopharmaceutics, 142, pp. 396-404 (2019)

- A. Dobrowolski, R. Strob, J.F. Dräger-Gillessen, D. Pieloth, G. Schaldach, H. Wiggers, M. Thommes
  Preparation of submicron drug particles via spray drying from organic solvents
  International Journal of Pharmaceutics, 567, Article number 118501 (2019)

- T. Feuerbach, S. Callau-Mendoza, M. Thommes
  Development of filaments for fused deposition modeling 3D printing with medical grade poly(lactic-co-glycolic acid) copolymers
  Pharmaceutical Development and Technology, 24 (4), pp. 487-493 (2019)

- J. Wesholowski, H. Podhaisky, M. Thommes
  Comparison of residence time models for pharmaceutical twin-screw-extrusion processes
  Powder Technology, 341, pp. 85-93 (2019)

- M. Evers, D. Weis, S. Antonyuk, M. Thommes
  Scale-up of the rounding process in pelletization by extrusion-spheronization
  Pharm Dev Technol. 24(8):1014-1020 (2019)

- D. Weis, F. Krull, J. Mathy, M. Evers, M. Thommes, S. Antonyuk
  A contact model for the deformation behaviour of pharmaceutical pellets under cyclic loading
  Advanced Powder Technology, 30(11):2492-2502 (2019)

2018

- D. Weis, M. Evers, M. Thommes, S. Antonyuk
  DEM simulation of the mixing behavior in a spheronization process
  Chemical Engineering Science 192, 803-815 (2018)

- J. Wesholowski, S. Prill, A. Berghaus, M. Thommes
  Inline UV/Vis spectroscopy as PAT tool for hot-melt extrusion
  Drug Delivery and Translational Research 8 (6), 1595-1603 (2018)

- J. Wesholowski, A. Berghaus, M. Thommes
  Investigations concerning the residence time distribution of twin-screw-extrusion processes as indicator for inherent mixing
  Pharmaceutics 10 (4), 207 (2018)

- R. Strob, A. Dobrowolski, D. Pieloth, G. Schaldach, H. Wiggers, P. Walzel, M. Thommes
  Preparation and characterization of spray-dried submicron particles for pharmaceutical application
  Advanced Powder Technology, 29 (12), 2920-2927 (2018)

- T. Feuerbach, S. Kock, M. Thommes
  Characterisation of fused deposition modeling 3D printers for pharmaceutical and medical applications
  Pharmaceutical Development and Technology, 23 (10), 1136-1145 (2018)

- Ł. Pałkowski, M. Karolak, B. Kubiak, J. Błaszczyński, R. Słowiński, M. Thommes, P. Kleinebudde, J. Krysiński
  Optimization of pellets manufacturing process using rough set theory
  European Journal of Pharmaceutical Sciences, 124, 295-303 (2018)

- R. Strob, A. Dobrowolski, G. Schaldach, P. Walzel, M. Thommes
  Preparation of spray dried submicron particles: Part A – Particle generation by aerosol conditioning
  International Journal of Pharmaceutics, 548 (1), 423-430 (2018)

- A. Dobrowolski, R. Strob, J. Nietfeld, D. Pieloth, H. Wiggers, M. Thommes
  Preparation of spray dried submicron particles: Part B – Particle recovery by electrostatic precipitation
  International Journal of Pharmaceutics, 548 (1), 237-243 (2018)

- J. Wesholowski, A. Berghaus, M. Thommes
  Inline determination of residence time distribution in hot-melt-extrusion
  Pharmaceutics, 10 (2), 49 (2018)

- J. Kamplade, I. Hohlfeld, M. Kelz, M. Thommes, P. Walzel
  Effect of Coandă-deflection-openings on the spray behavior of pressure swirl nozzles
  Atomization and Sprays, 28 (3), 281-297 (2018)

Fluid Separations (FVT)

Centrifugally enhanced Gas-Liquid Contacting in Rotating Packed Beds

Performance improvements through anisotropic foam packings and gamma-ray scans

Konrad Gladyszewski, Kai Groß, Mirko Skiborowski, Andrzej Górak, Christoph Held

Separation processes depend largely on mass transport in the apparatus, i.e. on the contact between vapor and liquid. Mass transport directly impacts the operational windows of such apparatus. Conventional gas-liquid contacting equipment, i.e. columns, are limited by the gravitation-driven downward flow of the liquid. Centrifugally enhanced gas-liquid contacting allows for increased capacity and flexibility of the equipment by applying centrifugal accelerations in the range of 10 to 1000 times earth's gravity. Besides, rotational speed can act as an additional operating parameter, which is important to adjust the equipment to varying process requirements. High mass transport requires high specific areas, and thus possibly small diameters of the liquid droplets. Thus, the equipment was provided by fast-spinning structured packing within the rotor to provide high geometric surface areas and to disperse the liquid into fine droplets. This work suggests an adequate packing design that adapts to varying process conditions (liquid loads).

The aim of this work was to improve the liquid distribution within the rotating packing by applying anisotropic foams, which provide different geometric surface areas. Two pilot-scale rotating packed beds (RPBs) have been investigated in this work. Rotor dimensions were in the range of 146 mm and 400-500 mm of the inner and outer diameter, respectively. The axial packing height was 10 mm. Foam rings of four different geometric surface areas have been investigated (cf. Figure 1). The chrome-nickel foams were arranged in a way that the surface area increased from the inner diameter to the outer diameter to compensate the increasing cross-sectional area of the rotor.

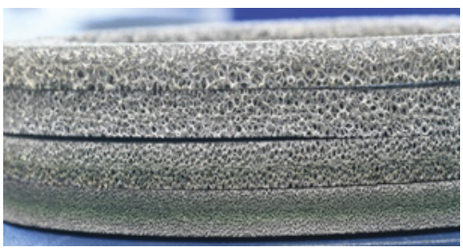

Figure 1: Stacked layers of NCX chrome-nickel foams. From top to bottom: NCX0610 (500 m^{-1}), NCX1116 (1000 m^{-1}), NCX1723 (1600 m^{-1}) and NCX2733 (2800 m^{-1}).

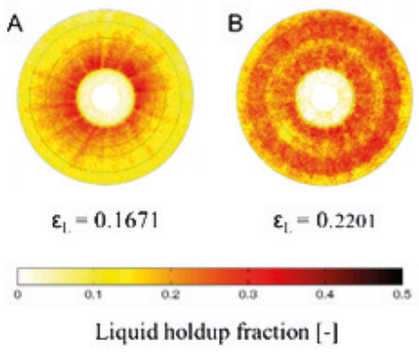

Figure 2: Local liquid holdup obtained with tarCT method at Q_L = 0.36 m^3/h, Q_G = 60 m^3/h and ω = 10 s^{-1} for the isotropic packing NCX1116 (A) and the anisotropic packings (B) from inner to outer radius (NCX0610, NCX1116, NCX1116, NCX1723, NCX1723).

In a collaboration with the Helmholtz Centre Dresden Rossendorf, gamma-ray CT was employed as non-invasive liquid hold-up measurement to avoid the disturbance of the liquid by probes. The gamma-ray CT scanner mainly comprises a ^{137}Cs isotopic source, a radiation detector and a rotary-lift unit. The radiation fan was collimated to 1 mm height and the radiation detector arc contained 320 scintillation detector pixels, also collimated to 1 mm height. By subtraction of a dry reference scan from the wetted packing in operation the volumetric liquid hold-up was evaluated. Figure 2 (right) provides a comparison of the liquid hold-up for an anisotropic foam, consisting of foam rings with different surface areas, compared to an isotropic foam with a fixed surface area (left), highlighting the huge potential of the anisotropic packing for effectively avoiding maldistribution. Moreover, it was observed that the variation of the local morphology for the anisotropic packings equally affects the local liquid hold-up in radially preceding and following parts of the packing. However, the local liquid holdup in the packing has only minor influence on the angular liquid distribution. Therefore, a local decrease in liquid holdup behind the support struts at the center of the packing is propagated through the entire radial length for isotropic and anisotropic foams.

To ensure that the change of the packing morphology is not negatively influencing the mass-transfer performance of the foam, the interfacial area was measured by the Danckwerts method based on chemical absorption of CO_2 with aqueous sodium hydroxide solution. The results indicate a 5 - 15 % higher ratio of the effective interfacial area to the specific geometric surface area for anisotropic packings at Q_L = 0.18 m^3/h (40 $m^3m^{-2}h^{-1}$) and F-factor below 2. However, at higher liquid loads and F-factors both types of morphologies reached similar ratios. The improved distribution can enable a pressure drop reduction of up to 45 % while providing equal interfacial area as the isotropic foam.

Contact:
gladyszewski@rpb-prospin.com
christoph.held@tu-dortmund.de

Publications:
K. Gładyszewski, K. Groβ, A. Bieberle, M. Schubert, M. Hild, A. Górak, M. Skiborowski, Chem. Eng. Sci. 230, 116176, 2021.

Model-Based Evaluation of a Membrane-Assisted Hybrid Extraction-Distillation Process for Energy and Cost-Efficient Purification of Diluted Aqueous Streams

Bettina Scharzec, Kai Fabian Kruber, Mirko Skiborowski

In the face of climate change and an increasing environmental awareness, the processing of renewable resources, as well as the reduction of waste streams and energy requirements are essential needs in the chemical industry. Especially in case of bio-based fermentation processes, a common need is the subsequent concentration of diluted aqueous streams that also have to be treated in wastewater purification. Affinity-based separation processes, such as liquid-liquid extraction, are generally considered favorable to distillation, which however is regularly used for solvent recovery. To reduce the effort for a solvent-based extraction and improve the economic performance, an extended hybrid process concept is considered, which exploits energy-efficient pressure-driven membrane separations, i.e. reverse osmosis or nanofiltration, for preconcentration.

The extended hybrid process considered in this work integrates an additional membrane separation as illustrated in Figure 1. The main purification of the desired organic component (OC) is still performed by solvent extraction and solvent recovery through distillation. But the major advantage of this extension is the increased product concentration in the feed stream of the extraction column, which enables a reduction in terms of solvent demand and energy required for solvent recovery. This presumable energy and cost reduction come at the expense of the required membrane area and energy required for compression. Therefore, an optimal pre-concentration needs to be evaluated considering the respective trade-off. Given the availability and high selectivity of hydrophilic membranes for reverse osmosis and nanofiltration, a selective permeation of water is considered. This option further enables an additional retention of dissolved solvent in the raffinate stream, in case of larger cross solubility in the extraction, by recycling the raffinate to the membrane separation, as indicated by the dashed line in Figure 1.

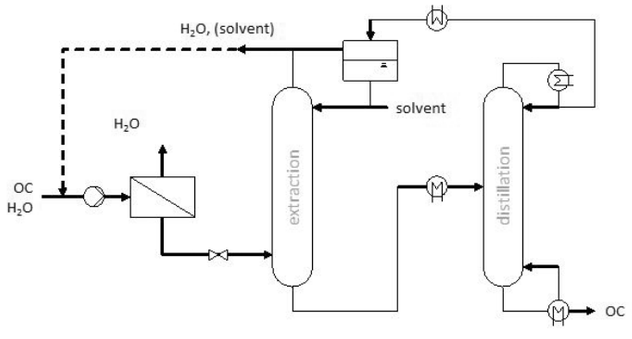

Figure 1: Hybrid process concept for the purification of an organic component (OC) in a diluted aqueous solution including a membrane unit, an extraction and distillation process.

The current work performs a systematic comparative evaluation of such a hybrid process concept for the purification of a diluted γ-valerolactone stream, for which different solvent candidates have been identified in a previous evaluation of the liquid-liquid extraction process. The potential economic savings are first evaluated in a model-based assessment prior to an experimental screening and characterization of a suitable membrane. Finally, a detailed economic evaluation of the processes is conducted by an optimization-based process design, highlighting the potential for a more sustainable and economic purification of the diluted stream. The proposed approach allows to quickly identify a considerable saving potential for the membrane-assisted hybrid process.

In the first step of the approach, the saving potential was identified of a preconcentration disregarding any γ-valerolactone (GVL) losses for two solvent candidates: the benchmark solvent n-butyl-acetate and the alternative solvent toluene. After proving the technical feasibility of the membrane unit, a subsequent membrane screening determined the membrane AMS NanoPro S-3011 as the most promising candidate since the highest flux with a high GVL rejection of 91 % was achieved. This membrane was further characterized and integrated within a final optimization-based process design considering two different initial GVL feed concentrations (2 mol%, 5 mol%). The results indicate a significant potential of the membrane-assisted hybrid process since, for the higher concentrated feed, 35 % (n-butyl acetate) and 27 % (toluene) of the total annual costs could be saved, respectively. For the lower concentrated stream, the saving potential even increases (60 % for n-butyl acetate and 54 % for toluene) as the flux is significantly higher.

Publications:
B. Scharzec, K.F. Kruber, M. Skiborowski, Model-based evaluation of a membrane-assisted hybrid extraction-distillation process for energy and cost-efficient purification of diluted aqueous streams. Chem. Eng. Sci. Submitted (2020).

Contact:
bettina.scharzec@tu-dortmund.de
kai.kruber@tu-dortmund.de
mirko.skiborowski@tu-dortmund.de

Publications 2020 - 2018

2020

Peer Reviewed Journal Papers

- R. Goebel, M. Skiborowski
  Machine-based learning of predictive models in organic solvent nanofiltration: Pure and mixed solvent flux
  Separation and Purification Technology 237 (2020), 116363

- U. Hampel, M. Schubert, A. Döß, J. Sohr, V. Vishwakarma, J.-U. Repke, S. Gerke, H. Leuner, M. Rädle, V. Kapoustina, L. Schmitt, M. Grünewald, J. Brinkmann, D. Plate, E. Kenig, N. Lutters, L. Bolenz, F. Buckmann, D. Toye, W. Arlt, T. Linder, R. Hoffmann, H. Klein, S. Rehfeldt, T. Winkler, H.-J. Bart, D. Wirz, J. Schulz, S. Scholl, W. Augustin, K. Jasch, F. Schlüter, N. Schwerdtfeger, S. Jahnke, A. Jupke, C. Kabatnik, A. Braeuer, M. D'Auria, T. Runowski, M. Casal, K. Becker, A.-L. David, A. Górak, M. Skiborowski, K. Groß, H. Qammar
  Recent Advances in Experimental Techniques for Flow and Mass Transfer Analyses in Thermal Separation Systems
  Chemie Ingenieur Technik 92 (7) (2020), 926–948

- B. Scharzec, J. Holtkötter, J. Bianga, JM. Dreimann, D. Vogt, M. Skiborowski
  Conceptual study of co-product separation from catalyst-rich recycle streams in thermomorphic multiphase systems by OSN
  Chemical Engineering Research and Design 157 (11), (2020), 65-76

- K.F. Kruber, H. Qammar, M. Skiborowski
  Optimization-Based Design of Rotating Packed Beds with Zickzack Packings
  Computer Aided Chemical Engineering 48 (2020), 997-1002

- R. Goebel, T. Glaser, M. Skiborowski
  Machine-based learning of predictive models in organic solvent nanofiltration: Solute rejection in pure and mixed solvents
  Separation and Purification Technology 248 (2020), 117046

- S. Schlüter, K.U. Künnemann, D. Vogt, M. Skiborowski
  Membrangestützte Abtrennung von Koppelprodukten in der Hydroaminomethylierung im thermomorphen Mehrphasensystem
  Chemie Ingenieur Technik 92 (9), (2020), 1311-1312

- T. Waltermann, T. Grueters, D. Muenchrath, M. Skiborowski
  Efficient optimization-based design of energy-integrated azeotropic distillation processes
  Computers & Chemical Engineering 133 (2020), 106676

- M. Skiborowski
  Energy Efficient Distillation by Combination of Thermal Coupling and Heat Integration
  Computer Aided Chemical Engineering 48 (2020), 991-996

- T. Sasi, K. Kruber, M. Ascani, M. Skiborowski
  Automatic Synthesis of Distillation Processes for the Separation of Heterogeneous Azeotropic Multi-component Mixtures
  Computer Aided Chemical Engineering 48 (2020), 1009-1014

- D. Krone, E. Esche, N. Asprion, M. Skiborowski, J.U. Repke
  Conceptual Design Based on Superstructure Optimization in GAMS with Accurate Thermodynamic Models
  Computer Aided Chemical Engineering 48 (2020), 15-20

- T. Waltermann, S. Schlueter, R. Benfer, C. Knoesche, A. Górak, M. Skiborowski
  Model Discrimination for Multicomponent Distillation – A Geometrical Approach for Total Reflux
  Chemie Ingenieur Technik 92 (7) (2020), 890–906

- J. Riese, A. Hoff, J. Stock, A. Górak, M. Grünewald
  Separation Units 4.0 – Trennapparate heute und morgen
  Chemie Ingenieur Technik 92 (7) (2020), 818–830

- M. Jaworska, D. Antos, A. Górak
  Review on the application of chitin and chitosan in chromatography
  Reactive and Functional Polymers 152 (5) (2020), 104606

- I. Lukin, L. Pietzka, K. Groß, A. Górak, G. Schembecker
  Economic evaluation of rotating packed bed use for aroma absorption from bioreactor off-gas
  Chemical Engineering and Processing: Process Intensification 154 (5), (2020), 108011

- K. Groß, M. de Beer, S. Dohrn, M. Skiborowski
  Scale-Up of the Radial Packing Length in Rotating Packed Beds for Deaeration Processes
  Industrial & Engineering Chemisty Research 59 (23) (2020), 11042–11053

- T. Sasi, M. Skiborowski
  Automatic Synthesis of Distillation Processes for the Separation of Homogeneous Azeotropic Multicomponent Systems
  Industrial & Engineering Chemistry Research 59 (47), (2020), 20816–20835

Presentations & Posters

- B. Scharzec, L. Rombach, K. Kruber, M. Skiborowski
  Evaluation eines membrangestützten hybriden Prozesskonzepts
  Presentation at FA FVT 2020 (2020), Berchtesgaden, Germany

- S. Schlueter, K. Kuennemann, T. Roth, D. Vogt, M. Skiborowski
  Membrane-based co-product separation for the hydroaminomethlyation of long-chain alkenes
  Poster at DGMT 2020 Membrane Symposium - Poster Day (2020), Essen, Germany

- S. Schlueter, K. Kuennemann, D. Vogt, M. Skiborowski
  Membrangestützte Abtrennung von Koppelprodukten in der Hydroaminomethylierung im thermomorphen Mehrphasensystem
  Poster at 10. ProcessNet-Jahrestagung und 34. DECHEMA-Jahrestagung der Biotechnologen 2020 (2020), Germany

- T. Sasi, K. Kruber, M. Skiborowski
  Automatic synthesis of distillation processes for azeotropic multicomponent mixtures
  Poster at FA FVT 2020 (2020), Berchtesgaden, Germany

- T. Sasi, K. Kruber, M. Ascani, M. Skiborowski
  Automatic synthesis of distillation processes for the separation of heterogeneous azeotropic multi-component mixtures
  Presentation at ESCAPE 30 (2020), Virtual Symposium

Publications 2020 - 2018

2019

Peer Reviewed Journal Papers

- H. Qammar, K. Gładyszewski, A. Górak, M. Skiborowski
  Towards the Development of Advanced Packing Design for Distillation in Rotating Packed Beds
  Chemie-Ingenieur-Technik 91(11), pp. 1663-1673 (2019)

- E. Brunazzi, T. Cai, T. Kiss, J.U. Repke, M. Skiborowski, E. Sorensen
  Distillation & Absorption 2018
  Chemical Engineering Research & Design 147 (2019), 603-603

- T. Sasi, J. Wesselmann, H. Kuhlmann, M. Skiborowski
  Automatic synthesis of distillation processes for the separation of azeotropic multi-component systems
  Computer Aided Chemical Engineering 46 (2019), 49-54

- K.F. Kruber, T. Grueters, M. Skiborowski
  Efficient design of intensified extractive distillation processes based on a hybrid optimization approach
  Computer Aided Chemical Engineering 46, 859-864

- K.U. Künnemann, S. Schlueter, M. Skiborowski, J.M. Dreimann, D. Vogt
  Process intensification of thermomorphic multiphase systems for the homogeneously catalyzed hydroaminomethylation in a continuously operated miniplant
  International Conference on Circular Economy, DGMK 2019, 2019 (3), 83-86

- K.U. Künnemann, S. Schlueter, M. Skiborowski, J.M. Dreimann, D. Vogt
  Process intensification of thermomorphic multiphase systems for the homogeneously catalyzed hydroaminomethylation in a continuously operated miniplant
  International Conference on Circular Economy, DGMK 2019, 2019 (3), 83-86

- H. Kuhlmann, M. Möller, M. Skiborowski
  Analysis of TBA-Based ETBE Production by Means of an Optimization-Based Process-Synthesis Approach
  Chemie Ingenieur Technik 91 (3), 336-348

- A. Böcking, V. Koleva, J. Wind, Y. Thiermeyer, S. Blumenschein, R. Goebel, M. Skiborowski, M. Wessling
  Can the variance in membrane performance influence the design of organic solvent nanofiltration processes?
  Journal of membrane science 575 (2019), 217-228

- T. Waltermann, M. Skiborowski
  Efficient optimization-based design of energy-integrated distillation processes
  Computers & Chemical Engineering 129 (2019), 106520

- T. Waltermann, S. Sibbing, M. Skiborowski
  Optimization-based design of dividing wall columns with extended and multiple dividing walls for three-and four-product separations
  Chemical Engineering and Processing-Process Intensification 146, 107688

- D. Wenzel, K. Nolte, A. Górak
  Reactive mixing in rotating packed beds: On the packing's role and mixing modeling
  Chemical Engineering and Processing - Process Intensification 143,107596 (2019)

- R. Goebel, M. Schreiber, V. Koleva, M. Horn, A. Górak, M. Skiborowski
  On the reliability of lab-scale experiments for the determination of membrane specific flux measurements in organic solvent nanofiltration
  Chemical Engineering Research and Design 148, pp. 271-279 (2019)

- K. Groß, A. Bieberle, K. Gladyszewski, M. Schubert, U. Hampel, M. Skiborowski, A. Górak
  Analysis of Flow Patterns in High-Gravity Equipment Using Gamma-Ray Computed Tomography
  Chemie-Ingenieur-Technik 91(7), pp. 1032-1040 (2019)

- D. Wenzel, N. Gerdes, M. Steinbrink, L.S. Ojeda, A. Górak
  Liquid Distribution and Mixing in Rotating Packed Beds
  Industrial and Engineering Chemistry Research 58(15), pp. 5919-5928 (2019)

- J. Wojtasik, K. Gładyszewski, M. Skiborowski, A. Górak, M. Piątkowski
  Enzyme-enhanced CO_2 absorption process in rotating packed bed
  Chemical Papers 73(4), pp. 861-869 (2019)

Publications 2020 - 2018

2018

Peer Reviewed Journal Papers

- M. Blatkiewicz, A. Antecka, A. Górak, S. Ledakowicz
  Continuous laccase concentration in an aqueous two-phase system
  Chemical Papers 72, 3, 555-566 (2018)

- M. Skiborowski
  Process synthesis and design methods for process intensification
  Current Opinion in Chemical Engineering 22, 216-225 (2018)

- Y. Thiermeyer, S. Blumenschein, M. Skiborowski
  Solvent dependent membrane-solute sensitivity of OSN membranes
  Journal of Membrane Science 567, 7-17 (2018)

- T. Goetsch, P. Zimmermann, B. Scharzec, S. Enders, T. Zeiner
  Adsorption Isotherms of Liquid Isomeric Mixtures
  Industrial & Engineering Chemistry Research 57, 11210–11218

- B. Bertleff, R. Goebel, J. Claußnitzer, W. Korth, M. Skiborowski, P. Wasserscheid, A. Jess, J. Albert
  Investigations on Catalyst Stability and Product Isolation in the Extractive Oxidative Desulfurization of Fuels Using Polyoxometalates and Molecular Oxygen
  Chem. Cat. Chem. 10, 20, 4602–4609 (2018)

- M. Jaworska, I. Stępniak, M. Galiński, D. Kasprzak, D. Biniaś, A. Górak
  Modification of chitin structure with tailored ionic liquids
  Carbohydrate Polymers 202, 397–403 (2018)

- D. Haßkerl, C.Lindscheid, S. Subramanian, S. Markert, A. Górak, S. Engell
  Dynamic Performance Optimization of a Pilot-Scale Reactive Distillation Process by Economics Optimizing Control
  Industrial & Engineering Chemistry Research 57, 12165-12181 (2018)

- D. Wenzel, M. Assirelli, H. Rossen, M. Lopattschenko, A. Górak
  On the reactant concentration and the reaction kinetics in the Villermaux-Dushman protocol
  Chemical Engineering and Processing - Process Intensification 130, 332–341 (2018)

- *K.* Neumann, K. Gladyszewski, K. Groß, H. Qammar, D. Wenzel, A. Górak, M. Skiborowski
  A guide on the industrial application of rotating packed beds
  Chemical Engineering Research and Design 134, 443–462 (2018)

- H. Kuhlmann, H. Veith, M. Möller, K.-P. Nguyen, A. Górak, M. Skiborowski
  Optimization-Based Approach to Process Synthesis for Process Intensification
  Industrial & Engineering Chemistry Research 57, 10, 3639–3655 (2018)

- K. Gładyszewski, M. Skiborowski
  Additive manufacturing of packings for rotating packed beds
  Chemical Engineering and Processing - Process Intensification 127, 1–9 (2018)

- M. Blatkiewicz, A. Antecka, T. Boruta, A. Górak, S. Ledakowicz
  Partitioning of laccases derived from Cerrena unicolor and Pleurotus sapidus in polyethylene glycol – phosphate aqueous two–phase systems
  Process Biochemistry 67, 165–174 (2018)

- D. Wenzel, A. Górak
  Review and analysis of micromixing in rotating packed beds
  Chemical Engineering Journal 345, 492–506 (2018)

- M. Jaworska, A. Górak
  New ionic liquids for modification of chitin particles
  Research on Chemical Intermediates 164, 341–341 (2018)

- M. Skiborowski, S. Recker, W. Marquardt
  Shortcut-based optimization of distillation-based processes by a novel reformulation of the feed angle method
  Chemical Engineering Research and Design 132, 135–148 (2018)

- K. Neumann, S. Hunold, M. de Beer, M. Skiborowski, A. Górak
  Mass Transfer Studies in a Pilot Scale RPB with Different Packing Diameters
  Ind. Eng. Chem. Res. 57, 6 , 2258–2266 (2018)

- A. Kiss, R. Geertman, M. Wierschem, M. Skiborowski, B. Gielen, J. Jordens, J. John, T. van Gerven
  Ultrasound-assisted emerging technologies for chemical processes
  Journal of Chemical Technology & Biotechnology 93, 1219-1227 (2018)

- M. Wierschem, A. Langen, J. Lins, R. Spitzer, M. Skiborowski
  Model validation for enzymatic reactive distillation to produce chiral compounds
  Journal of Chemical Technology & Biotechnology 93, pp. 498–507 (2018)

- M. Leimbrink, K. Nikoleit, R. Spitzer, S. Salmon, T. Bucholz, A. Górak, M.Skiborowski
  Enzymatic reactive absorption of CO_2 in MDEA by means of an innovative biocatalyst delivery system
  Chemical Engineering Journal 334, 1195–1205 (2018)

Peer Reviewed Conference Papers

- M. Skiborowski
  Fast screening of energy and cost efficient intensified distillation processes
  Chemical Engineering Transactions 69, 199-204 (2018)

- M. Skiborowski, P. Temmann, C. Brandenbusch
  Analyzing the link between GE-model parameter regression and optimal process design
  Computer Aided Chemical Engineering 43, 103-108 (2018)

- D. Haßkerl, C. Lindscheid, S. Subramanian, S. Markert, A. Górak, S. Engell
  Application of Economics Optimizing Control to a Two-step Transesterification Reaction in a Pilot-Scale Reactive Distillation Column
  IFAC-PapersOnLine 51, 18, 67-72 (2018)

- J.F. Mackowiak, K. Syring, A. Thomas, M. Leimbrink, M. Skiborowski, A. Górak, J. Mackowiak
  Absorption of carbon dioxide using enzyme activated amine solution in columns with random packings
  Chemical Engineering Transactions 69, 115-120 (2018)

- T. Waltermann, R. Benfer, S. Schlueter, A. Reinhardt, C. Knoesche, A. Górak, M. Skiborowski
  Choosing the right model for distillation processes in packed columns: theory and experiments
  Chemical Engineering Transactions 69, 367–372 (2018)

Publications 2020 - 2018

- T. Waltermann, T. Grueters, M. Skiborowski
  Optimization of extractive distillation - integrated solvent selection and energy integration
  Computer Aided Chemical Engineering 44, 187–192 (2018)

- K. Kruber, J. Scheffczyk, K. Leonhard, A. Bardow, M. Skiborowski
  A hierarchical approach for solvent selection based on successive model refinement
  Computer Aided Chemical Engineering 43, 325–330 (2018)

- R. Goebel, T. Glaser, I. Niederkleine, M. Skiborowski
  Towards predictive models for organic solvent nanofiltration
  Computer Aided Chemical Engineering 43, 115–120 (2018)

- H. Qammar, F. Hecht, M. Skiborowski, A. Górak
  Experimental Investigation and Design of Rotating Packed Beds for Distillation
  Chemical Engineering Transactions 69, 655–660 (2018)

- K. Groß, K. Neumann, M. Skiborowski, A. Górak
  Analyzing the Operating Limits in High Gravity Equipment
  Chemical Engineering Transactions 69, 661–666 (2018)

- K. Groß, A. Bieberle, K. Gladyszweski, M. Schubert, M. Skiborowski, U. Hampel, A. Górak
  Evaluation of Liquid Hold-up in a Rotating Packed Bed for High Gravity Fluid Separation using Process-Synchronized Gamma-Ray Computed Tomography
  Proceedings of the 9th World Congress on Industrial Process Tomography 831–838 (2018)

Book Chapters

- A. Mitsos, U. Lee, S. Recker, M. Skiborowski
  Conceptual Process Design and Process Optimization
  In: Green Chemical Engineering, Volume 12 (Eds. Anastas P. T., Lapkin A.) Wiley, 2018

- K. Werth, M. Skiborowski
  Organic Solvent Nanofiltration for an Intensified Processing of Renewable Raw Materials
  In: Intensification of Bio-Based Processes (Eds. Górak, A.; Stankiewicz, A.) Royal Society of Chemistry, 2018

- M. Wierschem, M. Leimbrink, M. Skiborowski, R. Heils, I. Smirnova, I., A. Górak
  Enzymatic Reactive Absorption and Distillation
  In: Intensification of Bio-Based Processes (Eds. Górak, A.; Stankiewicz, A.) Royal Society of Chemistry, 2018

- A. Górak, A. Stankiewicz
  Preface
  In: Intensification of Bio-Based Processes (Eds. Górak, A.; Stankiewicz, A.) Royal Society of Chemistry, 2018

- M. Barecka, M. Skiborowski, A. Górak
  Process Intensification in practice: ethylene glycol case study
  In: Practical aspects of Chemical Engineering (Eds.: M. Ochowiak, S. Woziwodzki, M. Doligalski, P. Mitkowski) Springer, 2018

- M. Wierschem, A. Górak
  Reactive Distillation
  In: Reference Module in Chemistry, Molecular Sciences and Chemical Engineering (Ed. Reedijk, J.) Elsevier, 2018

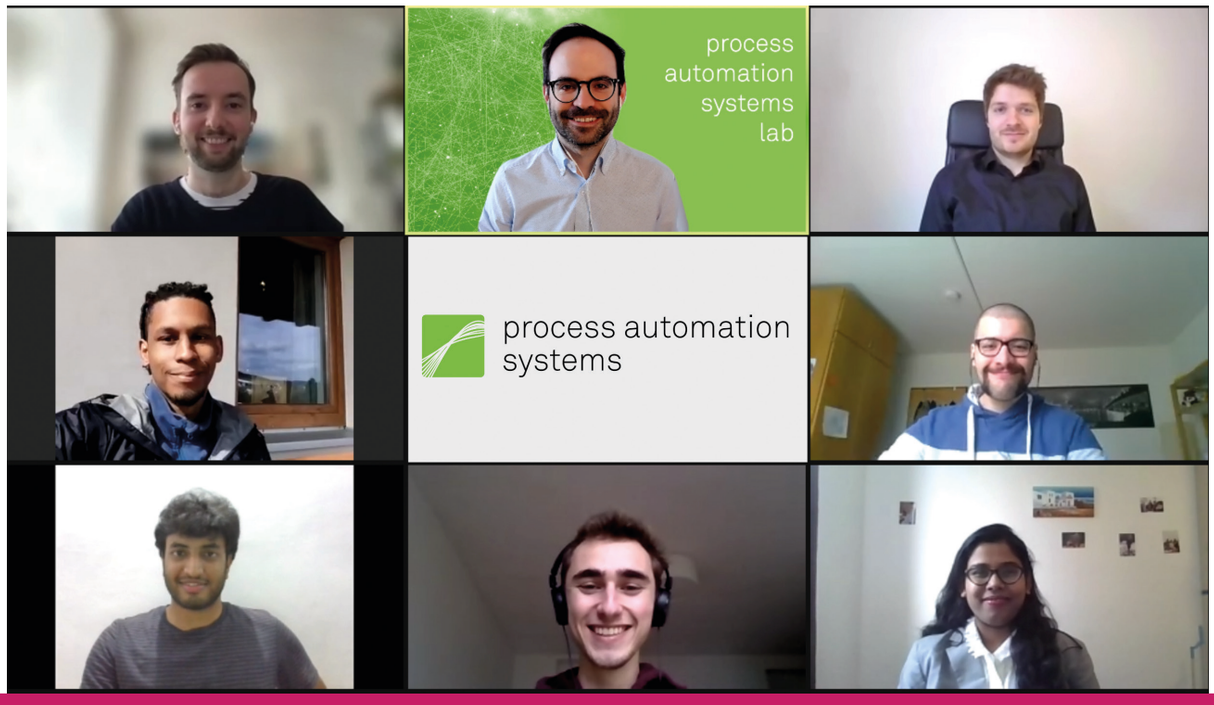

Process Automation Systems (PAS)

Energy-Efficient Operation of Water Distribution Networks

Combining deep learning, clustering and optimal control

Felix Fiedler, Andrea Cominola, Sergio Lucia

The advanced control of large-scale water distribution networks (WDNs) is key to enhance the energy efficiency and resilience of these critical infrastructure systems while reliably meeting water consumers' demands. Energy-related costs can constitute up to 65 % of a utility's operating budget. Thus, improved operation of WDNs can lead to significant energy and cost savings. An optimization and model-based control approach can in theory achieve a high-performance control of such systems. However, the large size of the systems and the absence of control-oriented models are important obstacles for the development of optimization-based control of WDNs. To avoid these difficulties, we propose the use of a clustering technique that automatically groups nodes in the distribution network that behave similarly, leading to a reduced problem size. Available simulators of large networks are then used to generate data based on which a surrogate model of the reduced problem can be learnt. The surrogate model is then employed within a model predictive control approach to achieve advanced control. Simulation results show that this methodology can lead to energy savings of more than 5 % while still being robust to uncertainty in water demand prediction.

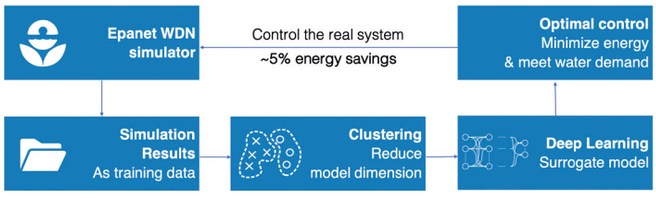

Figure 1: Flowchart of the ANN- and clustering-based optimal control method proposed in Fiedler et al., 2020.

Several optimal control schemes for WDNs have been proposed in the literature. The main obstacle to develop an optimal control method is that a mathematical model that can be used within numerical optimization frameworks is necessary. Finding such a model, which should also accurately capture the nonlinear behavior of the system and should be computationally efficient, is an important challenge. The computational complexity of hydraulic models for WDNs (e.g., EPANET models) limits their usability in optimization frameworks. Considerable savings in computational costs can be obtained by using substitute, simplified models, called surrogate models. Artificial neural networks (ANNs) and in particular deep neural networks are a promising candidate to approximate complex hydraulic models of water distribution networks especially if large amounts of data can be generated for learning. This is however not enough to avoid the large dimension of the system because models of WDNs usually consist of hundreds of nodes for which water demand should be met. A surrogate model that still needs to consider a large number of nodes might be intractable. To reduce the size of the problem, we propose a hierarchical clustering method that significantly reduces the number of nodes that need to be considered in the final surrogate model. The clustering method explicitly considers the topology of the network and it groups demand nodes in which the water pressure behaves similarly. The water demand for each cluster is aggregated by adding the water demands of the individual nodes that form a cluster.

The proposed approach, which combines a clustering method and surrogate models is depicted in Figure 1. A deep learning surrogate model is trained on the clustered data to obtain a control-oriented model which is used as a prediction model in a model predictive control scheme. Numerical results have been obtained for the benchmark WDN of C-Town depicted in Figure 2 a). Figure 2 b) shows the result of the clustering method, which reduces the size of the network from 378 nodes to 25 clusters. The implementation of model predictive control on the surrogate model shows that, compared to a traditional rule-based control scheme, the proposed method could lead to energy savings larger than 5 %. In addition, the proposed method also demonstrated to be robust to uncertain water demand predictions.

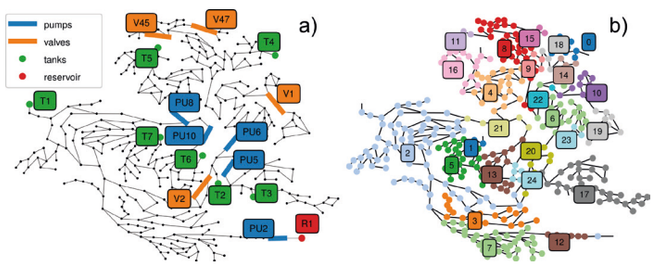

Figure 2: a) Water distribution network with pumps and valves to control the system. b) Clustered nodes (hierarchical clustering) to reduce problem size.

Contact:
felix.fiedler@tu-dortmund.de
andrea.cominola@tu-berlin.de
sergio.lucia@tu-dortmund.de

Publications:
F. Fiedler, A. Cominola, S. Lucia, (2020), Economic nonlinear predictive control of water distribution networks based on surrogate modeling and automatic clustering. In Proc. of the IFAC World Congress, Berlin, 2020 (in Press).

Making Advanced Control Algorithms Real-Time Capable via Machine Learning

Benjamin Karg, Sergio Lucia

Model predictive control (MPC) has established itself as one of the most prominent advanced process control schemes. The main advantages of MPC include the possibility of dealing with nonlinear systems with many inputs and outputs and considering process constraints explicitly. The main drawbacks are that it needs a model of reasonable accuracy and it requires the solution of a numerical optimization problem in real-time. Recent advances in algorithms and computing hardware have enabled the fast solution of optimization problems in many different applications. However, the consideration of nonlinear models and uncertainties can still make the solution of the resulting optimization problems in real-time impossible. The proposed approach leverages recent advances in machine learning and proposes deep neural networks to closely approximate the behavior of optimization-based algorithms while only requiring a fraction of the computational power. Simulation studies show that it is possible to closely approximate the behavior of MPC controllers even for a highly nonlinear polymerization reactor, enabling the deployment of advanced control in real-time virtually everywhere.

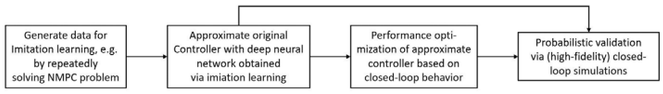

Figure 1: Design process of explicit controllers in the form of deep neural networks.

Model predictive control algorithms enable the operation of nonlinear systems subject to uncertainties while satisfying constraints. The main drawback of this approach is that solving the resulting optimization problem in real-time can be challenging. This is especially relevant when the models that are used to predict the behavior of a system are nonlinear and uncertain, leading to problems of significant computational complexity. An alternative approach for the online solution of the required optimization problems is presented in Figure 1. Instead of solving the optimal control problem online in each control interval, the problem is solved offline for many combinations of possible initial conditions of the system and realizations of the uncertain parameters. The generated data set can then be used for imitation learning, where the weights of a deep neural network are adapted such that the deep neural network closely approximates the solution of the original optimization problem. Figure 2 compares the performance of robust NMPC, which exactly solves an optimization problem at each control interval, and a deep neural network controller for a semi-batch polymerization reactor. It can be seen that the evolution of the reactor temperature is very similar for the exact and the approximate controller. The main advantage of the proposed approach is that evaluating the deep neural network controller is extremely easy and it takes a few milliseconds, enabling its deployment on simple industrial controllers or even on cheap microcontrollers. In contrast, the typical solution of the NMPC problem requires several seconds on a powerful laptop.

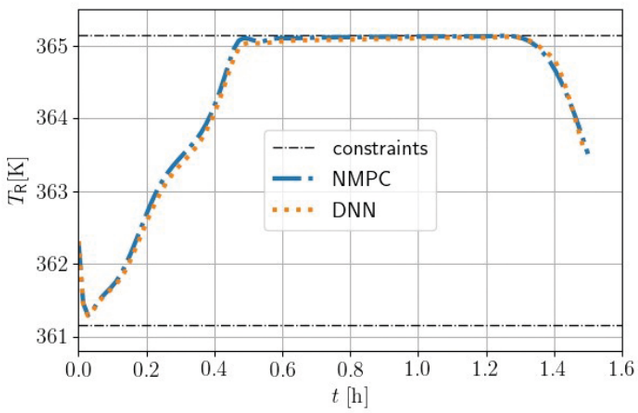

Figure 2: Comparison of NMPC and a deep neural network controller for controlling the reactor temperature of a (semi-) batch polymerization reactor with uncertain parameters.

If the original optimization-based controller was designed such that it guarantees satisfaction of process constraints (and stability of the closed-loop system), the learning-based controller does not automatically inherit these properties due to approximation errors. However, it is possible to validate the obtained controllers based on closed-loop simulations. Since a new control input is obtained by evaluating a simple arithmetic function (a deep neural network) instead of solving a potentially complex optimization problem, it is possible to easily generate large amounts of data and take advantage of probabilistic validation techniques to systematically check the safety of the controllers.

Publications:

B. Karg, S. Lucia, Efficient representation and approximation of model predictive control laws via deep learning. IEEE Transactions on Cybernetics 50.9, 3866-3878 (2020).

B. Karg, S. Lucia, Stability and feasibility of neural network-based controllers via output range analysis. In Proc. of the 59th IEEE Conference on Decision and Control (CDC), 4947-4954 (2020).

B. Karg, S. Lucia, Approximate moving horizon estimation and robust nonlinear model predictive control via deep learning. Computers and Chemical Engineering, 2020 (in Press).

Contact:
benjamin.karg@tu-dortmund.de
sergio.lucia@tu-dortmund.de

Publications 2020

2020

Journal Papers

- S. Lucia, S. Subramanian, D. Limon, S. Engell
  Stability properties of multi-stage nonlinear model predictive control
  Systems & Control Letters 143, 104743 (2020)

- B. Karg, S. Lucia
  Efficient representation and approximation of model predictive control laws via deep learning
  IEEE Transactions on Cybernetics 50 (9), 3866-3878 (2020)

- M.H. Ghasemi, O. Lucía, S. Lucia
  Computing in the blink of an eye: Current possibilities for edge computing and hardware-agnostic programming
  IEEE Access 8, 41626-41636 (2020)

- S. Lucia, D. Navarro, B. Karg, H. Sarnago, O. Lucia
  Deep learning-based model predictive control for resonant power converters
  IEEE Transactions on Industrial Informatics 17 (1), 409-420 (2020)

Peer reviewed Conference Papers

- N. Krausch, S. Hans, F. Fiedler, S. Lucia, P. Neubauer, M.N.C. Bournazou
  From Screening to Production: a Holistic Approach of High-throughput Model-based Screening for Recombinant Protein Production
  Computer Aided Chemical Engineering 48, 1723-1728 (2020)

- S. Braun, S. Albrecht, S. Lucia
  Hierarchical Attack Identification for Distributed Robust Nonlinear Control
  Proc. of the 21st IFAC World Congress, in Press (2020)

- F. Fiedler, A. Cominola, S Lucia
  Economic nonlinear predictive control of water distribution networks based on surrogate modeling and automatic clustering
  Proc. of the 21st IFAC World Congress, In Press (2020)

- K. Eckhoff, M. Kok, S. Lucia, T. Seel
  Sparse Magnetometer-free Inertial Motion Tracking -- A Condition for Observability in Double Hinge Joint Systems
  Proc. of the 21st IFAC World Congress. In Press (2020)

- M. Mammarella, T. Alamo, S. Lucia, F. Dabbene
  A probabilistic validation approach for penalty function design in Stochastic Model Predictive Control
  Proc. of the 21st IFAC World Congress. In Press (2020)

- F. Fiedler, D. Baumbach, A. Börner, S. Lucia
  A Probabilistic Moving Horizon Estimation Framework Applied to the Visual-Inertial Sensor Fusion Problem
  Proc. of the European Control Conference (ECC), 1009-1016 (2020)

- S. Braun, S. Albrecht, S. Lucia
  Identifying Attacks on Nonlinear Cyber-Physical Systems in a Robust Model Predictive Control Setup
  Proc. of the European Control Conference (ECC), 513-520 (2020)

- F. Fiedler, C. Döpmann, F. Tschorsch, S. Lucia
  PredicTor: Predictive Congestion Control for the Tor Network
  Proc. of the IEEE Conference on Control Technology and Applications (CCTA), 863-870 (2020)

- B. Karg, S. Lucia
  Stability and feasibility of neural network-based controllers via output range analysis
  Proc. of the 59th IEEE Conference on Decision and Control (CDC), 4947-4954 (2020)

- S. Braun, S. Albrecht, S. Lucia
  A Hierarchical Attack Identification Method for Nonlinear Systems
  Proc. of the 59th IEEE Conference on Decision and Control (CDC), 5035-5042 (2020)

Fluid Mechanics (SM)

Publications 2020 - 2018

2020

Peer reviewed Journals

- J. Chaudhuri, K. Boettcher, P. Ehrhard
  Numerical investigation of coalescence filtration: Multiphase flow through fibrous structures
  Separation and Purification Technology (2020), in press

- K. Boettcher, A. Behr
  Usage of a virtual environment to improve the teaching of fluid mechanics
  International Journal of Online and Biomedical Engineering (2020), in press

- K. Boettcher, A. Behr
  Teaching Fluid Mechanics in a Virtual-Reality Based Environment
  IEEE Global Engineering Education Conference, Porto, Portugal 1563-1567 (2020) DOI: 10.1109/EDUCON45650.2020.9125348

- S. Grünendahl, D.M. Brandner, P. Ehrhard
  Experimental investigations on rising bubbles in vertical capillaries
  Proceedings Applied Mathematics and Mechanics 20 (2020) DOI: 10.1002/pamm.202000184

- L. Gödeke, W. Oswald, N. Willenbacher, P. Ehrhard
  Dimensional analysis of droplet size and ligament length during high-speed rotary bell atomization
  Journal of Coatings Technology and Research (2020), in press

Books & Books Articles

- P. Ehrhard
  Kapitel Mikroströmungen
  Prandtl-Führer durch die Strömungslehre (ed. Oertel jun., H.H.), 15. Auflage, Springer Vieweg, Wiesbaden (2020), in press

- K. Boettcher, D. Boettcher, A. Behr
  Virtuelle Realität des Unsichtbaren: Verständnisfördernde Visualisierung und Interaktivierung strömungsmechanischer Phänomene
  Sammelband Labore in der Hochschullehre: Labordidaktik, Digitalisierung, Organisation, WBV Verlag (2020), in press

2019

- J. Chaudhuri, A. Baukelmann, K. Boettcher, P. Ehrhard
  Pressure drop in fibrous filters
  European Journal of Mechanics B/Fluids, Vol. 76, pp. 115-121, 2019

- K. Boettcher, T. Neumann, P. Ehrhard
  Permeability and flow through a packed bed of beads in a rectangular cross-section affected by overlapping wall effects
  Proc. Angewandte Mathematik und Mechanik, Vol. 19, DOI: 10.1002/pamm.201900302, 2019, in press

- J. Chaudhuri, K. Boettcher, P. Ehrhard
  Pressure drop in fibrous filter – representative domain size and effect of fibre orientation
  Separation and Purification Technology, 2019, in press

- A.K. Höffmann, J. Schmidt, P. Ehrhard
  Numerical investigations of the hydrodynamics and the oxygen mass-transfer in aerated tanks
  Proc. Angewandte Mathematik und Mechanik, Vol. 19, DOI: 10.1002/pamm.201900279, 2019, in press

- S. Mohan, J. Chaudhuri, L. Gödeke, P. Ehrhard
  Numerical investigation of aerosol deposition on a single 2D fiber
  Proc. Angewandte Mathematik und Mechanik, Vol. 19, DOI: 10.1002/pamm.201900350, 2019, in press

- W. Oswald, J. Lauk, L. Gödeke, P. Ehrhard, N. Willenbacher
  Analysis of paint flow Pulsations during high-speed rotary bell atomization
  Coatings, Vol. 9, pp. 674-682, 2019

- W. Oswald, L. Gödeke, P. Ehrhard, N. Willenbacher
  Influence of the elongational flow resistance and pigmentation of coating fluids on high-speed rotary bell atomization
  Atomization and Sprays, Vol. 29, pp. 913-935, 2019

- L. Gödeke, W. Oswald, N. Willenbacher, P. Ehrhard
  Dimensional analysis of droplet size and ligament length during high-speed rotary bell atomization
  Journal of Coatings Technology and Research, 2019, in press

2018

- A.K. Höffmann, P. Lakshmanan, C. Hollmann, T. Ostermann
  An experimental study on oil-dispersion baths generated by the Jungebad apparatus
  Complementary Therapies in Medicine, Vol. 41, pp. 147-153, 2018

- S.F. Reinecke, A.K. Höffmann, M. Stachowske, U. Hampel, P. Ehrhard
  Effizienzsteigerung von Kläranlagen
  GIT Labor-Fachzeitschrift 4/2018, pp. 53-56, 2018

- J. Chaudhuri, A. Baukelmann, K. Boettcher, P. Ehrhard
  Pressure drop in fibrous filters
  European Journal of Mechanics B/Fluids, Vol. 76, pp. 115-121, 2019

- J. Chaudhuri, P. Ehrhard
  Numerical investigation of coalescing filtration process
  Proc. Angewandte Mathematik und Mechanik, Vol. 18, in press, 2018

- L. Gödeke, S. Grünendahl, F. Burzinski, P. Ehrhard
  Experimentelle Untersuchung des Blaseneinschlusses beim Tropfenaufprall auf festen Wänden
  Proc. Fachtagung Experimentelle Strömungsmechanik (GALA), Nr. 10, Rostock, 4.-6. September 2018

Technical Biochemistry (TB)

Evaluation of Callus Cultures to Elucidate the Metabolism of Tebuconazole, Flurtamone, Fenhexamid and Metalaxyl-M in *Brassica napus* L., *Glycine max* (L.) Merr., *Zea mays* L. and *Triticum aestivum* L.

Leonie Hillebrands, Marc Lamshoeft, Andreas Lagojda, Andreas Stork, Oliver Kayser

Development and registration of the most promising and safest pesticides needs the determination of its metabolic behavior in plants to elucidate their nature of residues by using 14C-labeled pesticides. During the development of a research candidate these studies were guided by the OECD and EPA guidelines. This data is even in early research and development phase very helpful and an in vitro screening test would be an option. Based on these results a first risk assessment for human and environment can be implemented as soon as possible. Therefore, it was checked if a short-term in vitro *tool with plant callus cultures and usage of non-radioactive labeled pesticides can be utilized. It is known that callus cultures can be used for different biotechnological approaches. One is, to apply pesticides to predict their metabolic behavior. The here tested protocol utilizes non-labeled pesticides and a new approach to apply them* in vitro.

Plant cell cultures of *Brassica napus* L. (oilseed rape), *Glycine max* (L.) Merr. (soybean), *Zea mays* L. (maize) and *Triticum aestivum* L. (wheat) were established and incubated with 10 µM tebuconazole, flurtamone, fenhexamid and metalaxyl-M for 14 days. The pesticide entered the plant cells by passive diffusion out of the nutrition agar. To compare the metabolic capability of these callus cultures, young plants were hydroponically exposed to the same pesticides. Results out of the *in vitro* and *in planta* experiments were compared against each other and data obtained out of regulatory guideline studies.

All samples were extracted by the identical protocol and in the following steps analyzed by high-resolution mass spectrometry. The comparison of both experiments showed that the metabolic degradation is well described by *in vitro* callus cultures. Figure 1 gave the qualitative overview about 160 plants and callus cultures. The uptake of all pesticides was detectable. Monitoring the uptake in the intracellular compartment of the plant cells was served as basis for a new application protocol by passive diffusion out of the nutrition agar.

The results exhibited all phases of plant specific metabolism beginning with the most important phase I reactions. Hydroxy-tebuconazole, metalaxyl-M, -fenhexamid and -flurtamone indicated the enzymatic activity of P450 monooxygenases (CYP) in the used plant callus cultures. Demethylation, desaturation and hydrolysis of the pesticides were detected as well. Glycosylation and the conjugation with malonic acids are important metabolic reactions in phase II. Moreover, they indicated the compartmentalization of xenobiotic compounds in callus cultures of *Brassica napus* L., *Glycine max* (L.) Merr., *Zea mays* L. and *Triticum aestivum* L. during phase III.

Callus cultures are an efficient and reliable system to generate plant specific metabolites and to distinguish between crop plants and its ability of xenobiotic metabolism. Overall, the comparability of the nature of residues out of both experiments with the regulatory guideline metabolism studies could be demonstrated.

The results confirm that this assay is capable to conduct a metabolic profile and a preliminary pathway in callus cultures after 14 days with small quantities of the applied pesticides. The metabolic degradation of fenhexamid, metalaxyl-M, tebuconazole and flurtamone in *in vitro* callus cultures and *in planta* experiments resulted in qualitative comparable metabolites. In addition, the comparability of pathways of degradation out of *in vitro* and *in planta* experiments with the regulatory guideline metabolism studies was demonstrated.

Contact:
oliver.kayser@tu-dortmund.de

Our results support the idea, that callus culture is a good approach for miniaturization from whole *in planta* experiments to *in vitro* applications. The new application protocol is easy to conduct and offers a perfect standardization. Considering the full capability of callus cultures to metabolize the exposed pesticides within a few days, an application in the daily lab routine is possible. We recommend this *in vitro* assay as a screening tool to characterize the metabolism of pesticides in crop plants.

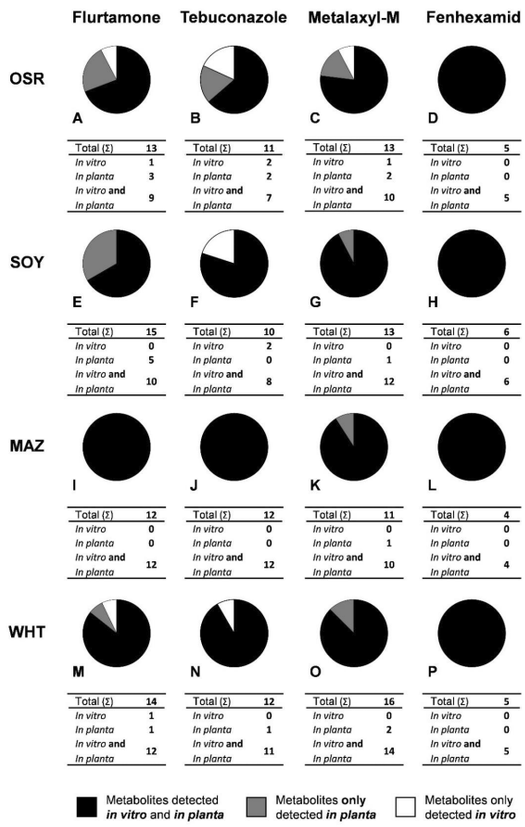

Figure 1: Qualitative overview of the *in vitro* and *in planta* metabolites of flurtamone, tebuconazole, metalaxyl-M and fenhexamid in *Brassica napus* L., *Glycine max* (L.) Merr., *Zea mays* L., *Triticum aestivum* L. after 14 days of incubation.

Publications:
L. Hillebrands, M. Lamshoeft, A. Lagojda, A. Stork, O. Kayser, Evaluation of Callus Cultures to Elucidate the Metabolism of Tebuconazole, Flurtamone, Fenhexamid and Metalaxyl-M in *Brassica napus* L., *Glycine max* (L.) Merr., *Zea mays* L. and *Triticum aestivum* L. J Agric Food Chem, 68: 14123-14134 (2020)

Publications 2020 - 2018

2020

Peer reviewed Papers and Reviews

- F. Thomas, C. Schmidt, O. Kayser
  Bioengineering studies and pathway modeling of the heterologous biosynthesis of tetrahydrocannabinolic acid in yeast
  Appl *Microbiol Biotechnol 2020, DOI: 10.1007/s00253-020-10798-3*

- G.-N. Nguyen, O. Kayser
  Biosynthesis and chemical modifications of minor cannabinoids
  In: *eLS. John Wiley & Sons, LTD: Chichester. May 2020. DOI: 10.1002/9780470015902.a0028875*

- A. Hensel, R. Bauer, M. Heinrich, V. Spiegler, O. Kayser, G. Hempel, K. Kraft
  Challenges at the time of Covid-19: Opportunities and innovations in antivirals from nature
  Planta Med 2020, 86: 659-664

- N.J.H. Averesch, O. Kayser
  Editorial: Biotechnological Production and Conversion of Aromatic Compounds and Natural Products
  Front. Bioeng. Biotechnol. doi: 10.3389/fbioe.2020.00646

- P. Rodziewicz, O. Kayser
  Cultivation and breeding of *Cannabis sativa* L. for medicinal use
  In: Handbook of Plant Breeding - Medicinal, aromatic and stiumlant plants.Vol. 12. Eds.: J. Novak, J.-W. Blüthner, Springer International Publishing, Springer Nature Switzerland AG, ISBN 987-3-030-38791-4, 2020

2019

Peer reviewed Papers and Reviews

- F. Thomas, O. Kayser
  Minor cannabinoids of *Cannabis sativa* L.
  Journal of Medicinal Sciences 88, 141-149 (2019)

- W. Vautz, C. Hariharan, O. Kayser
  Fast Detection of recent *Cannabis sativa* L. consumption in exhaled breath using a mobile ion mobility spectrometer
  Journal of Forensic Research Crime Studies 3, 1-11 (2019)

- R. Riga, N. Happyana, A. Quentmeier, C. Zammarelli, O. Kayser, E.H. Hakim
  Secondary metabolites from *Diaporthe lithocarpus* isolated from *Artocarpus heterophyllus*
  Natural Product Research https://doi.org/10.1080/14786419.2019.1672685 (2019)

- M. Heinrich, G. Appendino, T. Effert, R. Fürst, A.A. Izzo, O. Kayser, J.M. Pezzuto, A. Viljoen
  Best practice in research - overcoming common challenges in phytopharmacological research
  J. Ethnopharm 2019, https://doi.org/10.1016/j.jep.2019.112230 (2019)

- P. Rodziewicz, S. Loroch, L. Marczak, A. Sickmann, O. Kayser
  Cannabinoid synthases and osmoprotective metabolites accumulate in the exudates of *Cannabis sativa* L. glandular trichomes
  Plant Science 284, 108-116 (2019)

- T. Hussain, R.V. Espley, J. Gertsch, T. Whare, F. Stehle, O. Kayser
  Demystifying the liverwort *Radula marginata*, a critical review on its taxonomy, genetics, cannabinoid phytochemistry and pharmacology
  Phytochemical Reviews 18, 953-965 (2019)

- K.L. Kohnen-Johannsen, O. Kayser
  Tropane alkaloids: chemistry, pharmacology, biosynthesis and production
  Molecules 2019, 24: 796

- H. Aati, A. El-Gamal, O. Kayser
  Chemical composition and biological activity of the essential oil from the root of *Jatropha pelargoniifolia* Courb. native to Saudi Arabia
  Saudi Pharmaceutical Journal, 27, 88-95 (2019)

- H. Aati, A. El-Gamal, H. Shaheen, O. Kayser
  Traditional use of ethnomedicinal native plants in the Kingdom of Saudi Arabia
  Journal of Ethnobiology and Ethnomedicine 2019, 15: 1-9 (2019)

Proceedings & Book Chapters

- P. Rodziewicz, O. Kayser
  Cultivation and Breeding of *Cannabis sativa* L. for medicinal use, Handbook of Plant Breeding – Medicinal, aromatic and stimulant plants
  Novak, J. Blüthner J.-W., eds (2019)

Publications 2020 - 2018

Presentations

- O. Kayser
  Trends and prospects in biotechnology
  Trends and Prospects in Medical and Pharma Biotechnologies in Europe 2019, 15.11.2019, Poznan, Poland

- O. Kayser
  Ethnobotany and medicinal plant biotechnology: From tradition to modern aspects of drug development
  Trends and Prospects in Medical and Pharma Biotechnologies in Europe 2019, 03.06.-04.06.2019, Bratislava, Slovakia

2018

Proceedings & Book Chapters

- J. Schachtsiek, H. Warzecha, O. Kayser, F. Stehle
  Current Perspectives on Biotechnological Cannabinoid Production in Plants
  Planta Med. 84, 214-220 (2018)

- B. Zirpel, O. Kayser, F. Stehle
  Elucidation of structure-function relationship of THCA and CBDA synthase from *Cannabis sativa* L.
  Journal of Biotechnology 284, 17–26 (2018)

- P. Ebersbach, F. Stehle, O. Kayser, E. Freier
  Chemical fingerprinting of single glandular trichomes of *Cannabis sativa* by Coherent anti-Stokes Raman scattering (CARS) microscopy
  BMC Plant Biology, 18:275 (2018)

- B. Zirpel, F. Degenhardt, C. Zammarelli, D. Wibberg, J. Kalinowski, F. Stehle, O. Kayser
  Optimization of Δ^9-tetrahydrocannabinolic acid synthase production in *Komagataella phaffii* via post-translational bottleneck identification
  Journal of Biotechnology 272–273, 40–47 (2018)

- M. Geissler, J.Volk, F. Stehle, O. Kayser, H. Warzecha
  Subcellular localization defines modification and production of Δ^9-tetrahydrocannabinolic acid synthase in transiently transformed *Nicotiana benthamiana*
  Biotechnology Letters https://doi.org/10.1007/s10529-018-2545-0 (2018)

- H. Aati, A. El-Gamal, O. Kayser, A. Ahmed
  The Phytochemical and Biological Investigation of *Jatropha pelargoniifolia* Root Native to the Kingdom of Saudi Arabia
  Molecules. 23 pii: E1892. doi: 10.3390/molecules23081892 (2018)

- O. Kayser
  Ethnobotany and Medicinal Plant Biotechnology: From Tradition to Modern Aspects of Drug Development
  Planta Med. 84, 834-838 (2018)

- L. Kohnen, S. Sezgin, M. Spiteller, H. Hagels, O. Kayser
  Localization and Organization of Scopolamine Biosynthesis in *Duboisia myoporoides* R. Br.
  Plant Cell Physiol. 59, 107-118 (2018)

- T. Hussain, B. Plunkett, M. Ejaz, R. Espley, O. Kayser
  Identification of Putative Precursor Genes for the Biosynthesis of Cannabinoid-Like Compound in *Radula marginata*
  Front Plant Sci. 9, 537. doi: 10.3389/fpls.2018.00537 (2018)

Presentations & Poster

- T. Hussain O. Kayser
  Transcriptomic analysis of Radula marginata revealed identification of genes for cannabinoid-like compounds
  Emerging Trends in Natural Product Biotechnology, Dortmund, Germany

- T. Pitaktbut, S. Kusari, M. Spiteller, O. Kayser
  Regeneration of Maytenus heterophylla by a stem cutting technique and genome mining for cross-species maytansine biosynthesis
  Emerging Trends in Natural Product Biotechnology, Dortmund, Germany

- J. Schachtsiek, O. Kayser, F. Stehle
  CRISPR-Cas9 mediated reduction of the nicotine content of tetraploid smoking tobacco (*Nicotiana tabacum*)
  Emerging Trends in Natural Product Biotechnology, Dortmund, Germany

- P. Rodziewicz, S. Loroch, L. Marczak, A. Sickmann, O. Kayser
  Catalytic activity of cannabinoid synthases in organic phase
  Emerging Trends in Natural Product Biotechnology, Dortmund, Germany

- T. Hussain, O. Kayser
  ***Radula marginata*: a prospective liverwort an alternate source of cannabinoid-like compounds**
  EMBO Workshop, New shores in land plant evolution, Lisboa, Portugal

Patents

- F. Stehle, O. Kayser
  Biotechnologische Herstellung von Cannabinoiden
  2018071713343200DE (2018)

Technical Biology (TBL)

Charting the Layout of a Bacterial Factory for Anticancer Drugs

Genome sequencing of *Nostoc* sp. ATCC 53789

Anna Tippelt, Markus Nett

The cryptophycins are a family of macrocyclic depsipeptides that are produced by the lichen symbiont Nostoc *sp. ATCC 53789. Previous studies revealed that these compounds induce apoptosis in tumor cells by halting the polymerization of tubulin. Unlike other chemotherapeutics that interfere with microtubule dynamics, the cryptophycins are no substrates of the efflux system, which is responsible for resistance development in cancer cells. Hopes are therefore great to turn these bioactive molecules into new anticancer drugs. Up to now, however, no economically feasible process exists for their biotechnological production. Here, we explore the production of cryptophycins in microbial hosts that are more amenable to industrial processes than the native producer.*

Although the genes involved in cryptophycin biosynthesis were identified some years ago, information on their integration into the metabolic network of the producing strain *Nostoc* sp. ATCC 53789 was scarce. To complement the available data, we decided to sequence the genome of this phototrophic bacterium. For this purpose, the strain was cultivated in a mineral salt medium under diurnal illumination for one month. We confirmed the production of cryptophycins by liquid chromatography-coupled mass spectrometry (Figure 1) and continued with the isolation of genomic DNA.

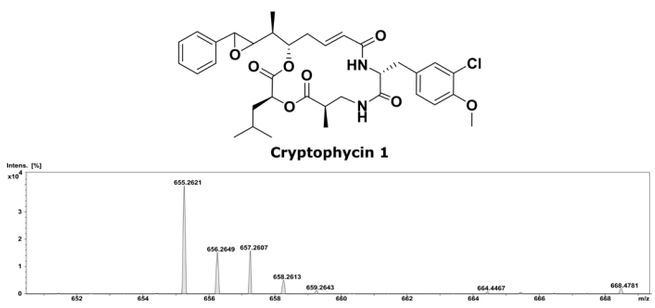

Figure 1: ESI-MS spectrum of cryptophycin 1 recorded in positive ion mode.

High quality DNA for sequencing purposes was obtained by phenol-chloroform extraction of the biomass and subsequent isopropanol precipitation. The genome of *Nostoc* sp. ATCC 53789 was reconstructed from short- and long-read DNA data sets obtained by Illumina and Nanopore sequencing. This approach revealed 13 discrete replicons with a total size of 8.7 Mbp and a medium G+C content of 40 - 42 %. In addition to one circular chromosome of 7.34 Mbp (Figure 2), the replicons comprise 2 linear and 10 circular plasmids ranging in size from 34.75 kbp to 337.07 kbp. Genome annotation resulted in the assignment of 7408 genes, 7300 protein-coding sequences, 88 tRNAs, 12 rRNAs and 8 ncRNAs.

Overall, the genomic features of *Nostoc* sp. ATCC 53789 were found to be consistent with other members of this genus, even though the number of extrachromosomal replicons is comparatively large. Unlike other *Nostoc* spp., the cryptophycin producer exhibits a very distinctive secondary metabolome. An inspection of the genome with antiSMASH 6.0 revealed a unique combination of 24 biosynthetic gene clusters (BGCs) that are involved in the assembly of bacteriocins, lantipeptides, lasso peptides, linear azol(in)e-containing peptides, nonribosomal peptides, polyketides and terpenes. The majority of these loci reside on the chromosome, while 4 BGCs are located on plasmids. Intriguingly, the cryptophycin biosynthesis genes turned out to be plasmid-borne. The corresponding locus was found on the circular plasmid c, where it is flanked by transposase genes. It is possible that the plasmid-driven biosynthesis and the associated metabolic burden contribute to the instable production of cryptophycin during the fermentation of *Nostoc* sp. ATCC 53789.

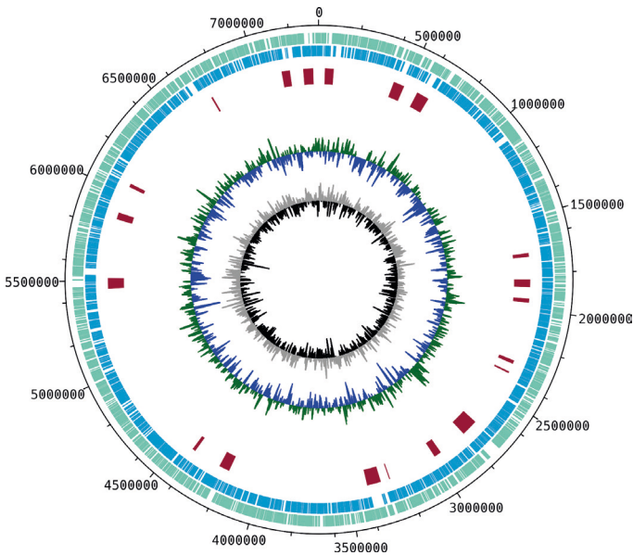

Figure 2: Chromosome map of *Nostoc* sp. ATCC 53789. The outer size-scale is given in 0.5 Mbp intervals. Circle 1 (mint): forward strand ORFs. Circle 2 (blue): reverse strand ORFs. Circle 3 (red): biosynthetic gene clusters. Circle 4: G + C content (dark green = above average, dark blue = below average). Circle 5: G + C skew (grey = above average, black = below average). The genome map was designed using DNAPlotter.

Contact:
anna.tippelt@tu-dortmund.de
markus.nett@tu-dortmund.de

Publications:
A. Tippelt, T. Busche, C. Rückert, M. Nett, Microbiol Resour Announc, 9, e00040-20 (2020).

Biotechnological Production of Customized Quinolone Antibiotics

Precursor-directed biosynthesis in a myxobacterium

S. Kruth, A. Sester, K. Stüer-Patowsky, M. Nett

Whole-cell biotransformation is a well-established method for the production of fine chemicals, especially for the pharmaceutical industry. In some cases, synthetic analogues of metabolic intermediates can be processed through entire pathways to give compounds that are not readily accessible by chemical means. In this study, we investigated the plasticity of a myxobacterial pathway, which directs the production of a family of highly potent quinolone antibiotics. We could show that halogen moieties can be regiospecifically introduced into these bioactive molecules by applying simple feeding strategies.

The aurachins constitute a large family of prenylated quinolone antibiotics, which were first discovered in cultures of the myxobacterium *Stigmatella aurantiaca* and later also found in other *Stigmatella* spp. as well as members of the actinomycete genera *Rhodococcus* and *Streptomyces*. Despite potent antimicrobial bioactivities, the understanding of structure-activity relationships (SAR) of this compound class was rather limited. While the importance of the prenyl side chain had been thoroughly explored, the effect of different substituents on the quinolone core was unclear. This was surprising in consideration of the structural similarity of aurachins to synthetic quinolone antibiotics, such as ciprofloxacin.

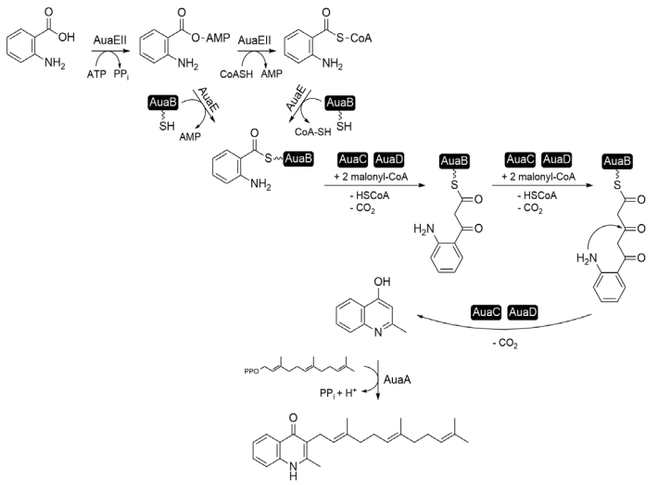

Figure 1: Early steps in aurachin biosynthesis.

Isotopic labeling studies as well as biochemical experiments had previously shown that the aurachins originate from anthranilic acid, which is condensed with two malonyl units upon enzymatic activation (Figure 1). Since anthranilic acid derivatives can be easily prepared by chemical synthesis (unlike the aurachins), we tested the biosynthetic incorporation of such precursor analogues in a series of batch fermentation experiments of the native producer *Stigmatella erecta*. It turned out that the aurachin pathway is particularly permissive for halogenated anthranilic acids. The incorporation rates of these molecules revealed a regiopreference for halogen substitution as well as steric limitations of enzymatic substrate tolerance (Figure 2). In general, fluorine substituents were more readily accepted than analogues featuring the more bulky chlorine atom. Among the fluorinated precursors, 5-fluoroanthranilic acid showed the highest conversion, followed by the aromatic acids bearing the halogen substituent in positions 3 and 4, respectively. In comparison, the 6-fluoroanthranilic acid-derived aurachins were produced in lower quantities. Since no accumulation of any intermediate was observed in the feeding studies, we assume that substrate discrimination already occurs in the early steps of aurachin biosynthesis.

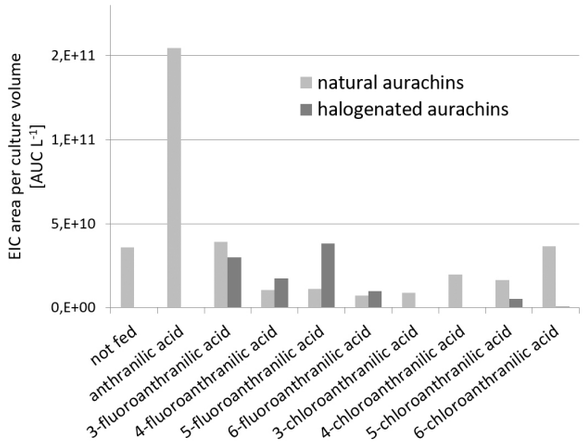

Figure 2: Normalized quantification of aurachins in *S. erecta* cultures after feeding with halogenated anthranilic acids. EIC = extracted ion chromatogram.

Upscaling of the fermentation and improvement of the downstream processing allowed the production of selected aurachin derivatives in preparative amounts. Bioactivity testing of these compounds showed that they are equipotent to the naturally occurring aurachins. Yet, they might exhibit more favorable pharmacokinetic properties, which is currently under evaluation.

Publications:
A. Sester, K. Stüer-Patowsky, W. Hiller, F. Kloss, S. Lütz, M. Nett, ChemBioChem, 21, 2268-2273 (2020).

Contact:
sebastian.kruth@tu-dortmund.de
markus.nett@tu-dortmund.de

Publications 2020 - 2018

2020

Publications

- A. Sester, J. Korp, M. Nett
  Secondary metabolism of predatory bacteria
  The Ecology of Predation at the Microscale, edited by E. Jurkevitch, R. J. Mitchell, pp. 127-154, Springer Nature Switzerland (2020)

- A. Sester, K. Stüer-Patowsky, W. Hiller, F. Kloss, S. Lütz, M. Nett
  Biosynthetic plasticity enables production of fluorinated aurachins
  ChemBioChem 21, 2268-2273 (2020)

- A. Tippelt, T. Busche, C. Rückert, M. Nett
  Complete genome sequence of the cryptophycin-producing cyanobacterium *Nostoc* sp. strain ATCC 53789
  Microbiology Resource Announcements 9, e00040-20 (2020)

- A. Tippelt, M. Nett, M. S. Vela Gurovic
  Complete genome sequence of the lignocellulose-degrading actinomycete *Streptomyces albus* CAS922
  Microbiology Resource Announcements 9, e00227-20 (2020)

- K. Rosenthal, M. Becker, J. Rolf, R. Siedentop, M. Hillen, M. Nett, S. Lütz
  Genomics-inspired discovery of massiliachelin, an agrochelin epimer from *Massilia* sp. NR 4-1
  ChemBioChem 21, 3225-3228 (2020)

- L. Winand, A. Sester, M. Nett
  Bioengineering of anti-inflammatory natural products
  ChemMedChem 15, doi: 10.1002/cmdc.202000771 (2020)

Presentations & Poster

- A. Tippelt, M. Nett
  Towards the reconstitution of cryptophycin biosynthesis
  VAAM Annual Conference, Leipzig, March 2020

- L. Winand, M. Nett
  Heterologous production of the cholinomimetic drug physostigmine in *Myxococcus xanthus*
  VAAM Annual Conference, Leipzig, March 2020

- M. Hofmann, L. Malik, J.H. Diettrich, M. Nett, D. Tischler, T. Heine
  A new metallophore from *Variovorax paradoxus* EPS
  VAAM Annual Conference, Leipzig, March 2020

2019

Publications

- A. Sester, L. Winand, S. Pace, W. Hiller, O. Werz, M. Nett
  Myxochelin- and pseudochelin-derived lipoxygenase inhibitors from a genetically engineered *Myxococcus xanthus* strain
  Journal of Natural Products 82, 2544-2549 (2019)

- J. Diettrich, H. Kage, M. Nett
  Genomics-inspired discovery of massiliachelin, an agrochelin epimer from *Massilia* sp. NR 4-1
  Beilstein Journal of Organic Chemistry 15, 1298-1303 (2019)

- C. Kurth, I. Wasmuth, T. Wichard, G. Pohnert, M. Nett
  Algae induce siderophore biosynthesis in the freshwater bacterium *Cupriavidus necator* H16
  Biometals 32, 77-88 (2019)

- F. Baldeweg, D. Hoffmeister, M. Nett
  A genomics perspective on natural product biosynthesis in plant pathogenic bacteria
  Natural Product Reports 36, 307-325 (2019)

- E. Geib, F. Baldeweg, M. Doerfer, M. Nett, M. Brock
  Cross-chemistry leads to product diversity from atromentin synthetases in Aspergilli from section Nigri
  Cell Chemical Biology 26, 223-234 (2019)

- N. Kallscheuer, H. Kage, L. Milke, M. Nett, J. Marienhagen
  Microbial synthesis of the type I polyketide 6-methylsalicylate with *Corynebacterium glutamicum*
  Applied Microbiology and Biotechnology 103, 9619-9631 (2019)

Presentations & Poster

- M. Nett
  Myxobacterial secondary metabolites – from compound identification to pathway engineering
  Microbial substrate conversion (MiCon) seminar series, Ruhr University Bochum, February 2019

- A. Sester, J. Korp, L. Winand, M. Nett
  Engineering pseudochelin production in *Myxococcus xanthus*
  Dechema – 31. Irseer Naturstofftage. Kloster Irsee, February 2019

- A. Sester
  Heterologous production of pseudochelin in *Myxococcus xanthus*
  VAAM Annual Conference, Mainz, March 2019

- L. Winand, J. Korp, A. Sester, M. Nett
  Unraveling the enzymatic basis of pseudochelin biosynthesis
  VAAM Annual Conference, Mainz, March 2019

- H. Kage
  A novel bacterial chassis system for the production of secondary metabolites
  VAAM Annual Conference, Mainz, March 2019

- M. Nett
  Towards the engineering of natural product biosynthesis in myxobacteria
  FZ Jülich colloquium series, Jülich, April 2019

Publications 2020 - 2018

- M. Nett
  Genetic tools for directing natural product biosynthesis in myxobacteria
  Synthetic Biology for Natural Products Conference, Puerto Vallarta, Mexico, June 2019

- A. Sester
  Generation of myxochelin-derived lipoxygenase inhibitors in a genetically modified *Myxococcus xanthus* strain
  Annual Meeting of the American Society of Pharmacognosy, Madison, WI, USA, July 2019

- S. Kruth, L. Winand, J. Korp, M. Nett
  Design of a modular vector-based expression system in *Myxococcus xanthus*
  German Conference on Synthetic Biology, Aachen, September 2019

- A. Tippelt, M. Nett
  Towards the reconstitution of cryptophycin biosynthesis
  German Conference on Synthetic Biology, Aachen, September 2019

- A. Sester, K. Stüer-Patowsky, S. Lütz, M. Nett
  Precursor-directed biosynthesis towards aurachin derivatives
  VAAM Workshop Biology of bacteria producing natural products, Jena, September 2019

- A. Tippelt, M. Nett
  Towards the reconstitution of cryptophycin biosynthesis
  VAAM Workshop Biology of bacteria producing natural products, Jena, September 2019

- L. Winand, P. Schneider, S. Kruth, J. Pietruszka, M. Nett
  Plasmid-based expression of natural product gene clusters in *Myxococcus xanthus*
  VAAM Workshop Biology of bacteria producing natural products, Jena, September 2019

- S. Kruth, L. Winand, J. Korp, M. Nett
  Design of a modular vector-based expression system in *Myxococcus xanthus*
  CKB symposium, Düsseldorf, October 2019

- L. Winand, B. David, A. Loeschcke, P. Schneider, H. Gohlke, J. Pietruszka, M. Nett
  Target-directed mutasynthesis of the cholinesterase inhibitor physostigmine
  CKB symposium, Düsseldorf, October 2019

2018

Publications

- J. Korp, L. Winand, A. Sester, M. Nett
  Engineering pseudochelin production in *Myxococcus xanthus*
  Applied and Environmental Microbiology 84, e01789-18 (2018)

- C. Kurth, I. Wasmuth, T. Wichard, G. Pohnert, M. Nett
  Algae induce siderophore biosynthesis in the freshwater bacterium *Cupriavidus necator* H16
  Biometals, doi: 10.1007/s10534-018-0159-6 (2018)

- F. Baldeweg, D. Hoffmeister, M. Nett
  A genomics perspective on natural product biosynthesis in plant pathogenic bacteria
  Natural Product Reports, doi: 10.1039/c8np00025e (2018)

- E. Geib, F. Baldeweg, M. Doerfer, M. Nett, M. Brock
  Cross-chemistry leads to product diversity from atromentin synthetases in Aspergilli from section Nigri
  Cell Chemical Biology, doi: 10.1016/j.chembiol.2018.10.021 (2018)

Presentations & Poster

- J. Diettrich, M. Nett
  Massithiazole, a natural product from *Massilia* sp.
  VAAM Workshop Biology of bacteria producing natural products 33 (2018)

- H. Kage
  A genome streamlining-based bacterial chassis generation
  VAAM Workshop Biology of bacteria producing natural products 46 (2018)

- S. Kruth, M. Nett
  Design of vector-based expression systems for myxobacteria
  VAAM Workshop Biology of bacteria producing natural products 38 (2018)

- A. Sester, J. Korp, L. Winand, M. Nett
  Engineering pseudochelin production in *Myxococcus xanthus*
  Emerging Trends in Natural Product Biotechnology 41 (2018)

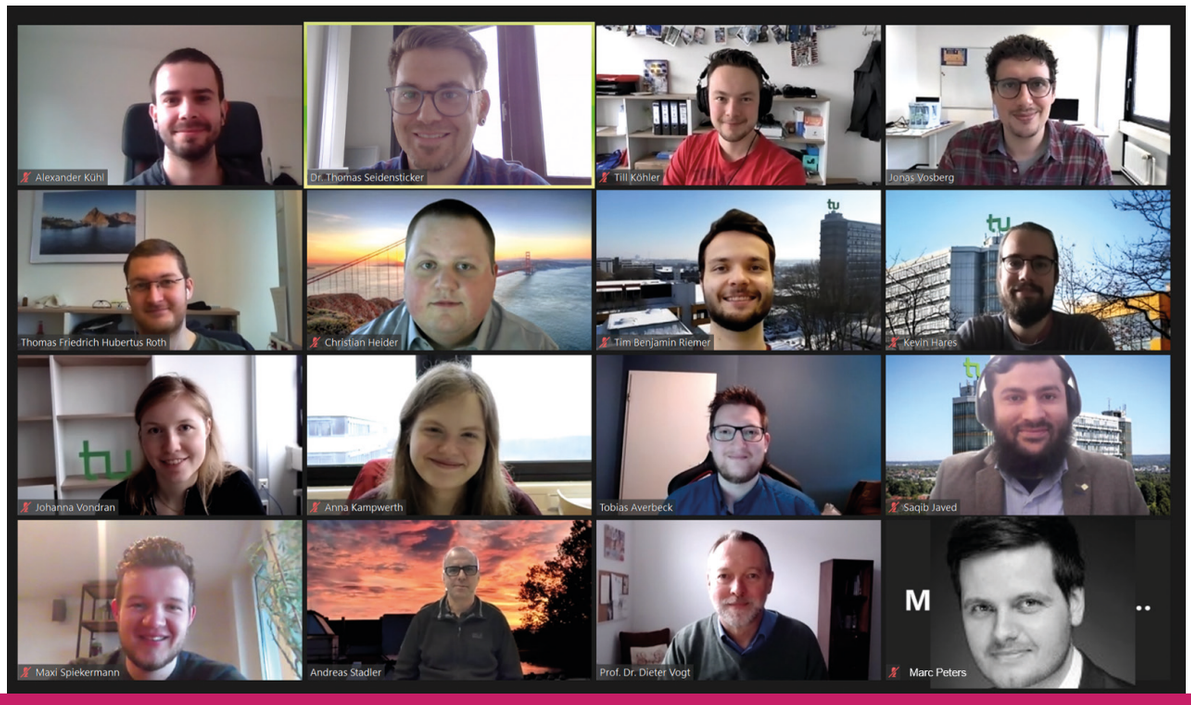

Industrial Chemistry (TC)

One-Pot Synthesis of Aldoximes from Alkenes via Rh-Catalysed Hydroformylation in an Aqueous Solvent System

M. Terhorst, C. Plass, A. Hinzmann, A. Guntermann, T. Jolmes, J. Rösler, D. Panke, H. Gröger, D. Vogt, A. J. Vorholt, T. Seidensticker

The direct formation of C-N bonds starting from non-functionalised base chemicals is still a challenging task. The involved reactions are often lacking selectivity or by- as well as side products are formed whereby unnecessary waste is generated. In this regard, homogeneous catalysis can help to reduce energy costs and waste formation, yet it remains challenging to produce primary aliphatic amines as value products. In this sense, the selective formation of aldoximes by combination of homogeneously catalysed hydroformylation of 1-alkenes with consecutive condensation represents a viable alternative. Through implementation of an aldoxime, a great share of value chemicals is accessible, such as primary amines, amides or nitriles. To be in accordance with the current standards of sustainability, this reaction has been developed using aqueous hydroxylamine, instead of the hydrochloric salt, as reagent for condensation and water as environmentally benign solvent for the reaction.

For the first time, the effective combination of hydroformylation and aldoxime formation in a one-pot reaction was achieved, yielding aldoximes directly from alkenes in a single preparative step. An excessive salt formation has been bypassed by application of aqueous hydroxylamine. The utilisation of sulfoxantphos as ligand was found to be purposeful, as it allows the selective synthesis of linear products and immobilises the catalyst in an aqueous phase. A solvent system, composed of the green solvents water and 1-butanol, was key to success, as it enables sufficient contact of the aqueous catalyst phase and organic substrate phase. Using 1-octene as the model substrate, conditions were successfully optimised via Design of Experiments (DoE), yielding > 85 % of the desired, linear oxime. The reaction conditions were successfully transferred to eight different substrates, while high linear selectivities of above 90 % were maintained at yields above 85 %. Varying reaction rates of the substrates and turnover frequencies of over 2000 h^{-1} were observed by the application of constant pressure and monitoring the gas consumption. Even functionalised renewable substrates were effectively converted to multifunctional compounds, although the consecutive reactions of the aldoxime group dominated and yields of the nitrile over 40 % were observed. The additional implementation of a further reaction step and selectivity control towards aldoximes, nitriles or amides seems promising and will be part of ongoing research. In a concluding investigation, the terminal oximes have been transformed to the corresponding linear nitriles using oxime-dehydratases in a sustainable, highly selective and energy-efficient reaction. The overall reaction sequence thus formally represents an anti-Markovnikov hydrocyanation of readily available 1-alkenes. Concerning 1-octene, nonanitrile was synthesised over three reaction steps (two of them in a one-pot process) in 85 % overall yield and 95 % regioselectivity in only 2 h, with water as the only by-product.

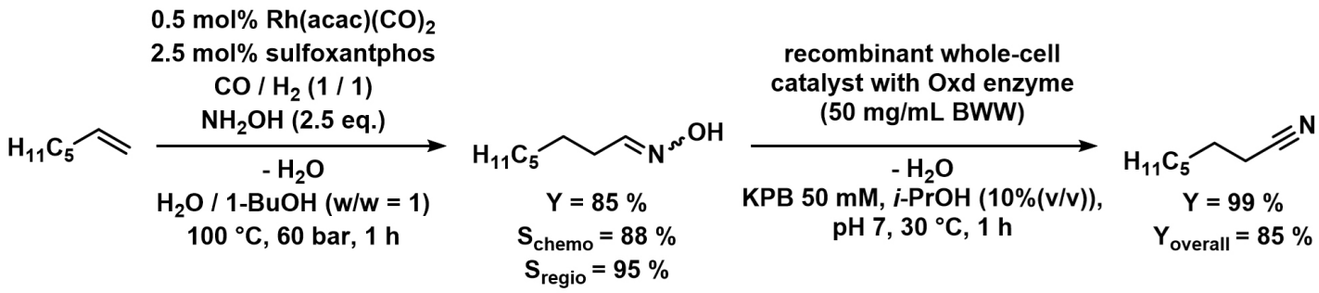

Figure 1: One-pot hydroformylation / aldoxime formation with consecutive biocatalytic dehydration, yielding linear nonanenitrile from 1-octene.

Contact:
thomas.seidensticker@tu-dortmund.de
dieter.vogt@tu-dortmund.de

Publications:
M. Terhorst, C. Plass, A. Hinzmann, A. Guntermann, T. Jolmes, J. Rösler, D. Panke, H. Gröger, D. Vogt, A. J. Vorholt, T. Seidensticker, Green Chem., 2020, 22, 7974-7982. DOI: 10.1039/D0GC03141K.

Solvent Selection in Homogeneous Catalysis

Optimization of Kinetics and Reaction Performances

J. Bianga, F. Huxoll, F. Jameel, T. Seidensticker, M. Stein, G. Sadowski, D. Vogt

Solvents have an enormous impact on yield and turnover of chemical reactions in complex media. There is, however, a lack of consistent model-based tools to a priori identify the appropriate solvent for homogeneously catalyzed reactions. Here, a thermodynamically consistent approach for a reductive amination reaction is presented. It combines solvent screening using a thermodynamic-activity model and quantum chemical calculations. The optimization of activity coefficient-based predicted kinetics gives a suitable list of candidate solvents. The results were confirmed by batch experiments in selected solvents. This approach allows reducing time and lab resources for solvent selection to a minimum.

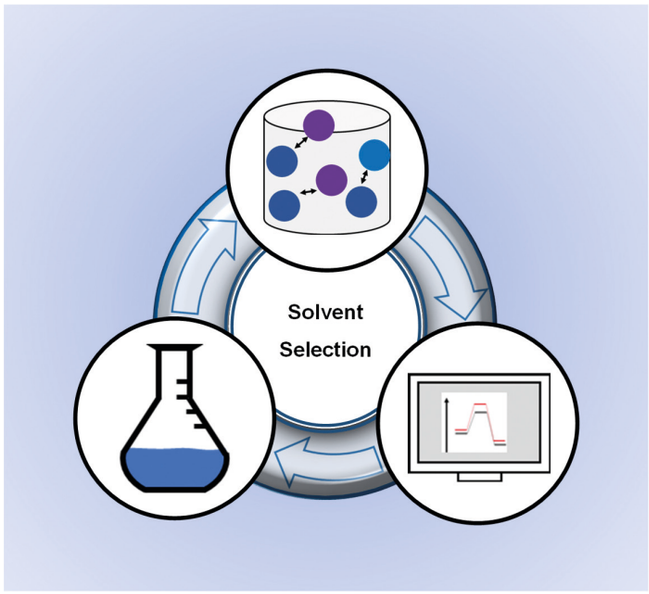

Figure 1: Solvent selection for homogeneous catalysis comprised of a thermodynamic activity model and quantum chemical calculations.

The newly developed workflow combines a thermodynamic activity model with quantum chemical calculations (Figure 1). The thermodynamic consistent workflow consists of four distinct steps:

- Calculation of reactant activity coefficients
- Minimization of transition state activation energy
- Avoidance of catalyst inhibition
- Experimental validation

This workflow was applied on the homogeneously catalyzed reductive amination of the aldehyde undecanal with diethylamine as model reaction (Figure 2). Starting from a short list of commercial solvents, the first two steps of the workflow roughly rank each solvent's potential. The third step is significantly more computationally demanding. Thus, the workflow includes only the investigation of the most promising candidates within this step. Although *N,N*-dimethylformamide (DMF) was identified within the first two steps as the most promising solvent candidate, the third step showed that DMF strongly suppresses the coordination of hydrogen to the catalyst complex due to its higher binding energy to the catalyst. Instead, methanol is weaker binding and proved to be a more suitable solvent for the homogeneously catalyzed reductive amination. Performed batch experiments validated the whole workflow, including experiments with promising solvents such as DMF, methanol and 1-butanol as well as less favorable solvents such as toluene and *n*-heptane. As expected from the predictive calculations, the highest yields were achieved by using methanol as solvent.

In conclusion, this workflow identified short-chain alcohols, especially methanol, as auspicious solvents leading to high performances in the reductive amination of undecanal with diethylamine. The alcohols provide easy proton transfer in the amination step and accelerate it considerably. This comprehensive solvent selection workflow offers the potential to reduce the laboratory work effort drastically.

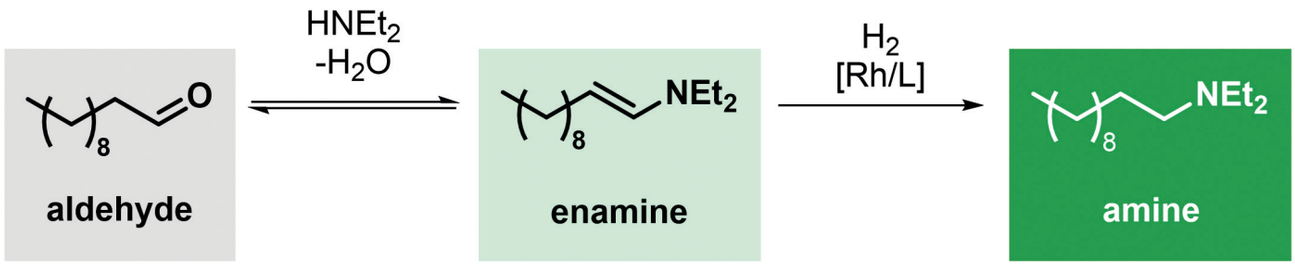

Figure 2: Reductive amination of undecanal with diethylamine to *N,N*-diethylundecylamine.

Publications:
F. Huxoll, F. Jameel, J. Bianga, T. Seidensticker, M. Stein, G. Sadowski, D. Vogt, ACS Catal. 11, 2, 590–594 (2021).

Contact:
dieter.vogt@tu-dortmund.de
gabriele.sadowski@tu-dortmund.de
thomas.seidensticker@tu-dortmund.de

Continuous Hydroformylation of 1-Decene in an Aqueous Biphasic System Enabled by Methylated Cyclodextrins

K. U. Künnemann, L. Schurm, D. Lange, T. Seidensticker, S. Tilloy, E. Monflier, J. M. Dreimann, D. Vogt

Hydroformylation is a widely used chemical reaction in industry to manufacture high-value-added intermediate products such as aldehydes and alcohols. It is considered to be one of the largest homogenously catalyzed reactions in industry. A major issue persisting with the use of homogenous catalysts is their recovery and separation from the product mixture, however, this is important due to the cost of the employed transition metals. Therefore, the challenge involved in formulating techniques to convert higher olefins in hydroformylation persist, particularly in a manner that can address the separation problem and minimize environmental impact, while not compromising on catalyst selectivity and activity. The use of water as a solvent in combination with mass transfer agents is in these cases particularly beneficial from economic and environmental impact viewpoints since water is fairly accessible, nontoxic, nonflammable, odorless, and has a high heat capacity and heat of vaporization.

For the first time, randomly methylated β-cyclodextrins (β-CD) were applied as mass transfer agents in a continuously operated, homogeneously catalyzed process. On the example of the Rh-catalyzed hydroformylation of 1-decene, process development was shown, where cyclodextrins were used together with a catalyst system that was continuously recovered and recycled using an aqueous biphasic system. In initial experiments, water-soluble and commercially available Rh/TPPTS and Rh/sulfoxantphos catalyst systems were scaled up from 50 ml into 1000 ml high-pressure autoclave systems to demonstrate their scalability. Both catalyst systems were compared, and they afforded excellent chemoselectivity (> 99 %) towards the desired linear aldehyde product. In particular, higher regioselectivity (up to 31) was achieved for the Rh/sulfoxantphos system. Investigations regarding the long-term stability of the mass transfer agent and both catalys systems were carried out in a continuously operated miniplant process. It was shown that the process can be successfully operated in steady state for over 200 h with chemoselectivity of > 97% toward the desired aldehyde product. Simultaneously, extremely low Rh-leaching (total: 0.59 %) was observed over the entire period of 200 h. Process optimization was successfully described by the continuous distillation of the product mixture (undecanal, 1-decene, and iso-decene) and recovering non-converted 1-decene substrate with 94 % purity. With the possibility of continuous distillation of the non-converted substrate, a new process concept (Figure 1) was proposed by implementing a second recycling loop into the process. Therefore, combining an aqueous biphasic hydroformylation process using methylated β-CDs for higher olefins with extremely low catalyst leaching and high chemo- and regio-selectivities toward the corresponding aldehyde product can be achieved

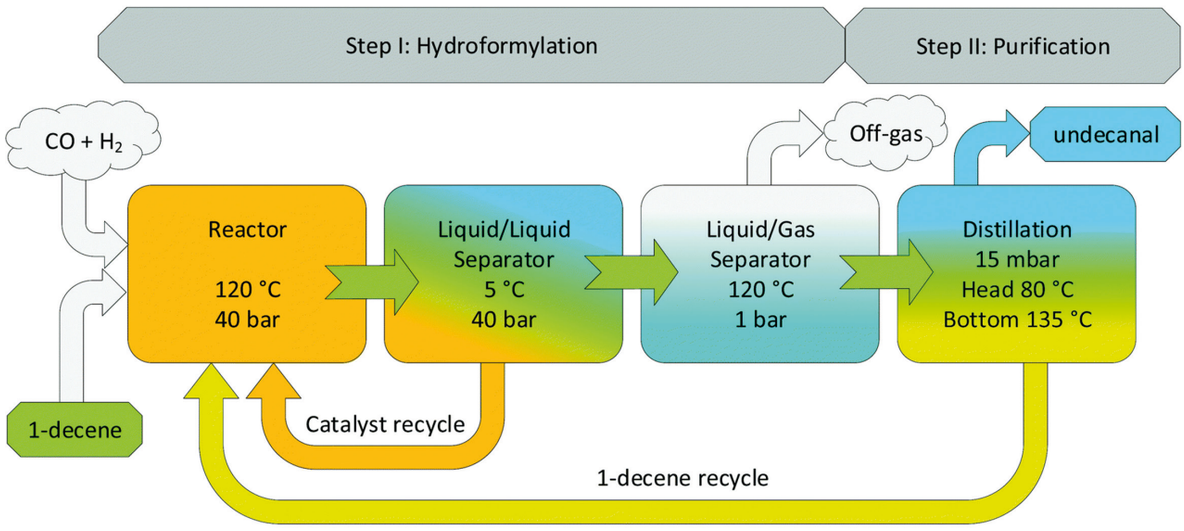

Figure 1: Developed process concept for an intensified process for the cyclodextrin based aqueous biphasic hydroformylation of 1-decene.

Contact:
dieter.vogt@tu-dortmund.de
thomas.seidensticker@tu-dortmund.de

Publications:
K.U. Künnemann, L. Schurm, D. Lange, T. Seidensticker, S. Tilloy, E. Monflier, D. Vogt, J.M. Dreimann, Green Chem., 2020,22, 3809-3819. DOI: 10.1039/D0GC00820F.

Publications 2020 - 2018

2020

- K. U. Künnemann, D. Weber, C. Becquet, S. Tilloy, E. Monflier, T. Seidensticker, D. Vogt
  Aqueous Biphasic Hydroaminomethylation enabled by Methylated Cyclodextrins: Sensitivity analysis for transfer into a Continuous Process
  ACS Sust. Chem. Eng. 2021, 409. SFB
  https://doi.org/10.1021/acssuschemeng.0c07125, first published on the web 18 December 2020

- F. Huxoll, F. Jameel, J. Bianga, T. Seidensticker, M. Stein, G. Sadowski, D. Vogt
  Solvent Selection in Homogeneous Catalysis – Optimization of Kinetics and Reaction Performance
  ACS Catal. 2021, 11, 590-594. SFB
  https://doi.org/10.1021/acscatal.0c04431, first published on the web 29 December 2020

- S. Schlüter, K. U: Künnemann, M. Freis, T. Roth, D. Vogt, J. M. Dreimann, M. Skiborowski
  Continuous co-product separation by organic solvent nanofiltration for the hydroaminomethylation in a thermomorphic multiphase system
  Chem. Eng. J. 2020, submitted SFB
  https://doi.org/10.1016/j.cej.2020.128219, first published on the web 5 January 2020

- M. Terhorst, C. Plass, A. Hinzmann, A. Guntermann, T. Jolmes, J. Rösler, D. Panke, H. Gröger, D. Vogt, A. J. Vorholt, T. Seidensticker
  One-Pot Synthesis of Aldoximes from Alkenes via Rh-catalyzed Hydroformylation in an Aqueous Solvent System
  Green Chem. 2020, 22, 7974-7982
  https://doi.org/10.1039/D0GC03141K, first published on the web 28 October 2020

- J. Bianga, N. Kopplin, J. Hülsmann, D. Vogt, T. Seidensticker
  Rhodium-Catalyzed Reductive Amination for the Synthesis of Tertiary Amines
  Adv. Synth. Catal. 2020, 362, 4415-4424. SFB
  https://doi.org/10.1002/adsc.202000746, first published on the web 9 August 2020

- M. Terhorst, C. Heider, A. J. Vorholt, D. Vogt, T. Seidensticker
  Productivity leap in the homogeneous ruthenium-catalysed alcohol amination through catalyst recycling avoiding volatile organic solvents
  ACS Sust. Chem.Eng. 2020, 8, 9962-9967. SFB
  https://doi.org/10.1021/acssuschemeng.0c03413, first published on the web 10 June 2020

- R. Savela, D. Vogt, R. Leino
  Ruthenium Catalyzed N-Alkylation of Cyclic Amines with Primary Alcohols
  Eur JOC 2020, 3030-3040
  https://doi.org/10.1002/ejoc.20200016, first published on the web 16 April 2020

- J. Bianga, K. U. Künnemann, L. Goclik, L. Schurm, D. Vogt, T. Seidensticker
  Tandem Catalytic Amine Synthesis from Alkenes in Continuous Flow Enabled by Integrated Catalyst Recycling
  ACS Catal. 2020, 10, 6463-6472. SFB
  https://doi.org/10.1021/acscatal.0c01465, first published on the web 11 May 2020

- K. U. Künnemann, N. Gumbiowski, P. Müller, Y. Jirmann, J. M. Dreimann, D. Vogt
  Chemometrics in the Homogeneously Catalyzed Reductive Amination: Combing in-situ FT-IR & Band-Target Entropy Minimization
  Ind. Eng. Chem. Res. 2020, 59, 9055-9065. SFB
  http://dx.doi.org/10.1021/acs.iecr.0c01527, first published on the web 21 April 2020

- K. U. Künnemann, L. Schurm, D. Lange, S. Seidensticker, S. Tilloy, E. Monflier, D. Vogt, J. M. Dreimann
  Continuous Hydroformylation of 1-Decene in an Aqueous Biphasic System using Methylated Cyclodextrins
  Green Chem. 2020, 22, 3809-3819. SFB
  https://doi.org/10.1039/d0gc00820f, first published on the web 14 April 2020

- B. Scharzec, J. Holtkötter, J. Bianga, J. Dreimann, D. Vogt, M. Skiborowski
  Membrane-based separation of co-products from catalyst-rich recycle streams in thermomorphic multiphase systems
  Chem. Eng. Res. Design 2020, 157, 65-76. SFB
  https://doi.org/10.1016/j.cherd.2020.02.028, first published on the web 4 March 2020

- M. Terhorst, A. Kampwerth, A. Marschand, D. Vogt, A. J. Vorholt, T. Seidensticker
  Facile Catalyst Recycling by Thermomorphic Behavior Avoiding Organic Solvents: A Reactive Ionic Liquid in the Homogeneous Pd-Catalysed Telomerization of the Renewable β-Myrcene
  Catal. Sci. Technol. 2020, 10, 1827-1834. SFB
  https://doi.org/10.1039/C9CY02569C, first published on the web 3 February 2020

- K. U. Künnemann, J. Bianga, R. Scheel, T. Seidensticker, J. M. Dreimann, D. Vogt
  Process Development for the Rhodium-Catalyzed Reductive Amination in a Thermomorphic Multiphase System
  Org. Proc. Res. Dev. 2020, 24, 41-49. SFB
  https://doi.org/10.1021/acs.oprd.9b00409, first published on the web 14 December 2019

- N. Herrmann, J. Bianga, M. Palten, T. Riemer, D. Vogt, J. M. Dreimann, T. Seidensticker
  Improving Aqueous Biphasic Hydroformylation of Unsaturated Oleochemicals Using a Jet-Loop-Reactor
  Eur. J. Lipid Sci. Technol. 2020, 122, 1900166. SFB
  https://doi.org/10.1002/ejlt.201900166, first published on the web 10 October 2019

- J. Bianga, N. Herrmann, L. Schurm, T. Gaide, J. Dreimann, D. Vogt, T. Seidensticker
  Improvement of Productivity for Aqueous Biphasic Hydroformylation of Methyl 10-Undecenoate – A Detailed Phase Investigation
  Eur. J. Lipid Sci. Technol. 2020, 122, 1900317. SFB
  https://doi.org/10.1002/ejlt.201900317, first published on the web 26 September 2019

- N. Herrmann, K. Köhnke, T. Seidensticker
  Selective Product Crystallization for Concurrent Product Separation and Catalyst Recycling in the Isomerizing Methoxycarbonylation of Methyl Oleate
  ACS Sust. Chem. Eng. 2020, 8, 29, 10633–10638
  https://doi.org/10.1021/acssuschemeng.0c03432, first published on the web 19 November 2019

Publications 2020 - 2018

- D. Vogelsang, J. Vondran, K. Hares, K. Schäfer, T. Seidensticker, A. J. Vorholt
  Palladium Catalysed Acid-Free Carboxytelomerisation of 1,3-Butadiene with Alcohols Accessing Pelargonic Acid Derivatives Including Triglycerides under Selectivity Control
  Adv. Synth. Catal, 2020, 362, 679-687
  https://doi.org/10.1002/adsc.201901383, first published on the web 19 November 2019

2019

- N. Herrmann, J. Bianga, T. Gaide, M. Drewing, D. Vogt, T. Seidensticker
  Aqueous biphasic hydroformylation of methyl oleate: A green solvent-only strategy for homogeneous catalyst recycling
  GreenChem 2019, 21, 6738-6745

- J. Bianga, K. U. Künnemann, T. Gaide, A. J. Vorholt, T. Seidensticker, J. M. Dreimann, D. Vogt
  Thermomorphic Multiphase Systems - Switchable Solvent Mixtures for the Recovery of Homogeneous Catalysts in Batch and Flow Processes
  Chem. Eur. J. 2019, 25, 11586-11608

- M. Jokiel, K. H. G. Rätze, N. M. Kaiser, K. U. Künnemann, J.-P. Hollenbeck, J. M. Dreimann, D. Vogt, K. Sundmacher
  Miniplant-Scale Evaluation of a Semibatch-Continuous Tandem Reactor System for the Hydroformylation of Long-Chain Olefins
  Ind. Eng. Chem. Res. 2019, 58, 2471-2480

- R. Kuhlmann, K. U. Künnemann, L. Hinderink, A. Behr, A. J. Vorholt
  CO_2 Based Synthesis of Various Formamides in Miniplant Scale: A Two-Step Process Design
  ACS Sustainable Chem. Eng. 2019, 7, 5, 4924-4931

- J. Esteban, H. Warmeling, A. J. Vorholt
  An Approach to Chemical Reaction Engineering and Process Intensification for the Lean Aqueous Hydroformylation Using a Jet Loop Reactor
  Chem. Ing. Tech. 2019, 91, 560-566

- J. M. Dreimann, E. Kohls, H. F. W. Warmeling, M. Stein, L. F. Guo, M. Garland, T. N. Dinh, A. J. Vorholt
  In Situ Infrared Spectroscopy as a Tool for Monitoring Molecular Catalyst for Hydroformylation in Continuous Processes
  ACS Catal. 2019, 9, 5, 4308-4319

- C. Plass, A. Hinzmann, M. Terhorst, W. Brauer, K. Oike, H. Yavuzer, Y. Asano, A. J. Vorholt, T. Betke, H. Gröger
  Approaching Bulk Chemical Nitriles from Alkenes: A Hydrogen Cyanide-Free Approach through a Combination of Hydroformylation and Biocatalysis
  ACS Catal. 2019, 9, 6, 5198-5203

- D. Vogelsang. J. Vondran, K. Hares, K. Schäfer, T. Seidensticker, A. J. Vorholt
  Palladium Catalysed Acid-Free Carboxytelomerisation of 1,3-Butadiene with Alcohols Accessing Pelargonic Acid Derivatives Including Triglycerides under Selectivity Control
  Adv. Synth. Catal. 2019, 362, 679-687

Publications 2020 - 2018

2018

- A. Behr, R. Kuhlmann
  Chemical Conversion of Carbon Dioxide
  Chem. Ing. Tech. 90 (5), 593–601 (2018)

- B. Bibouche, D. Peral, D. Stehl, V. Söderholm, R. Schomäcker, R. von Klitzing, D. Vogt
  Multiphasic Aqueous Hydroformylation of 1-Alkenes with Micelle-like Polymer Particles as Phase Transfer Agents
  RSC Adv. 8 (41), 23332–23338 (2018)

- A. Falk, J. M. Dreimann, D. Vogt
  Polyhedral Oligomeric Silsesquioxane Modification of Metathesis Catalysts: Improved Recycling and Lifetime in Membrane Separation
  ACS Sustain. Chem. Eng. 6 (6), 7221–7226 (2018)

- T. A. Faßbach, S. Püschel, A. Behr, S. Romanski, D. Leinweber, A. J. Vorholt
  Towards a Process for the Telomerization of Butadiene with N-Methylglucamine
  Chem. Eng. Sci. 181, 122–131 (2018)

- T. A. Faßbach, F. O. Sommer, A. J. Vorholt
  Hydroaminomethylation in Aqueous Solvent Systems - An Efficient Pathway to Highly Functionalized Amines
  Adv. Synth. Catal. 360 (7), 1473–1482 (2018)

- S. Fuchs, D. Lichte, T. Jolmes, T. Rösler, G. Meier, H. Strutz, A. Behr, A. J. Vorholt
  Synthesis of Industrial Primary Diamines via Intermediate Diols - Combining Hydroformylation, Hydrogenation and Amination
  ChemCatChem. 10 (18), 4126–4133 (2018)

- S. Fuchs, T. Rösler, B. Grabe, A. Kampwerth, G. Meier, H. Strutz, A. Behr, A. J. Vorholt
  Synthesis of Primary Amines via Linkage of Hydroaminomethylation of Olefins and Splitting of Secondary Amines
  Appl. Catal., A. 550, 198–205 (2018)

- R. Hernandez, J. Dreimann, A. Vorholt, A. Behr, S. Engell
  Iterative Real-Time Optimization Scheme for Optimal Operation of Chemical Processes under Uncertainty: Proof of Concept in a Miniplant
  Ind. Eng. Chem. Res. 57 (26), 8750–8770 (2018)

- R. Hernández, J. Dreimann, S. Engell
  Reliable Iterative RTO of a Continuously Operated Hydroformylation Process
  IFAC-PapersOnLine. 51 (18), 61–66 (2018)

- N. Herrmann, D. Vogelsang, A. Behr, T. Seidensticker
  Homogeneously Catalyzed 1,3-Diene Functionalization – A Success Story from Laboratory to Miniplant Scale
  ChemCatChem. 10 (23), 5342–5365 (2018)

- R. Kuhlmann, M. Nowotny, K. U. Künnemann, A. Behr, A. J. Vorholt
  Identification of key mechanics in the ruthenium catalyzed synthesis of N,N-dimethylformamide from carbon dioxide in biphasic solvent systems
  J. Catal. 361, 45–50 (2018)

- D. Peral, D. Stehl, B. Bibouche, H. Yu, J. Mardoukh, R. Schomäcker, R. von Klitzing, D. Vogt
  Colloidal Polymer Particles as Catalyst Carriers and Phase Transfer Agents in Multiphasic Hydroformylation Reactions
  J. Colloid Interface Sci. 513, 638–646 (2018)

- M. Peters, D. Vogelsang, T. Seidensticker, D. Vogt, J. M. Dreimann
  Prozessintensivierung via organophiler Nanofiltration - Entwicklungen in der Rückgewinnung homogener Übergangsmetallkatalysatoren
  Chem. Ing. Tech. 90 (9), 1177 (2018)

- D. Pingen, J.-H. Choi, H. Allen, G. Murray, P. Ganji, P. W. N. M. van Leeuwen, M. H. G. Prechtl, D. Vogt
  Amide Versus Amine Ligand Paradigm in the Direct Amination of Alcohols with Ru-PNP Complexes
  Catal. Sci. Technol. 8 (15), 3969–3976 (2018)

- D. Pingen, J. B. Schwaderer, J. Walter, J. Wen, G. Murray, D. Vogt, S. Mecking
  Diamines for Polymer Materials via Direct Amination of Lipid- and Lignocellulose-based Alcohols with NH 3
  ChemCatChem. 10 (14), 3027–3033 (2018)

- D. Vogelsang, M. Dittmar, T. Seidensticker, A. J. Vorholt
  Palladium-Catalysed Carboxytelomerisation of B-Myrcene to Highly Branched C 21 -Esters
  Catal. Sci. Technol. 8 (17), 4332–4337 (2018)

- D. Vogelsang, T. A. Faßbach, P. P. Kossmann, A. J. Vorholt
  Terpene-Derived Highly Branched C 30 -Amines via Palladium-Catalysed Telomerisation of β -Farnesene
  Adv. Synth. Catal. 360 (10), 1984–1991 (2018)

- D. Vogelsang, B. A. Raumann, K. Hares, A. J. Vorholt
  From Carboxytelomerization of 1,3-Butadiene to Linear α,ω-C10 -Diester Combinatoric Approaches for an Efficient Synthetic Route
  Chem. Eur. J. 24 (9), 2264–2269 (2018)

- D. Vogelsang, J. Vondran, A. J. Vorholt
  One-Step Palladium Catalysed Synthetic Route to Unsaturated Pelargonic C9-Amides Directly From 1,3-Butadiene
  J. Catal. 365, 24–28 (2018)

Books & Bookarticles

- A. Behr, T. Seidensticker
  Einführung in die Chemie nachwachsender Rohstoffe
  Springer Spektrum

Thermodynamics (TH)

Optimization of an Extraction System for Purification of Biomolecules

Applying (additional) Excipients as Tool for improving Biomolecule Stability

Maximilian Wessner, Christoph Brandenbusch

The production of high-value biomolecules such as biopharmaceuticals has seen a dramatic increase in (industrial) attention within the last decades. One promising initial purification step is the aqueous two-phase extraction (ATPE) using an aqueous two-phase system (ATPS). However, phase-formers that are used to generate the ATPS often reduce the conformational and colloidal stability of the biomolecule. Within this work, we overcome this drawback by using excipient, selected based on methods derived from (bio)pharmaceutical formulation development. It is shown, that selecting L-arginine as excipient for the ATPE of Immunoglobulin G (IgG), the IgG precipitation is significantly reduced (25 wt% to 1.2 wt% [wt/wt]), whilst simultaneously increasing the extraction yield to 90 wt%.

Process development for high-value biomolecules has mainly focused on the upstream rather than the downstream processing. This leads to the fact that the specific costs for the downstream processing can account for up to 80 % of the total production costs. With up to 90 % of the costs for the downstream processing, chromatographic steps are the main cost drivers. An alternative, cost-efficient purification technology, offering different operation modes (batch or continuous) is the ATPE using an ATPS.

To rapidly select a suitable ATPS for a target biomolecule, a physical sound approach based on investigations on the ATPS phase behavior and the conformational (unfolding temperature) and colloidal stability (second osmotic virial coefficient B_{22}) of the biomolecule has been developed within this work [1]. The approach identified an optimized ATPS for the ATPE of IgG using the phase formers sodium glutamate (NaGlu) and polyethylene glycol 2000 (PEG2000). However, as shown in Figure 1a, the colloidal stability is still decreased (negative B_{22}-values), resulting in an IgG precipitation of 25.2 wt% within ATPS 1 (Figure 1b) for high phase former concentrations. Under knowledge of the phase equilibria, optimization of the process window by decreasing phase former concentration enables a decrease in IgG precipitation by 22.1 wt% (to 3.1 wt% [ATPS 2]). To further increase the ATPS extraction performance, excipients such as amino acids or sugars were investigated applying concepts from (bio)pharmaceutical formulation development recently [2]. As presented in Figure 1a, the addition of L-arginine (L-Arg) as excipient can drastically increase the colloidal stability of IgG (increasing B_{22}-values), and compensate the negative effect of the phase formers applied. Due to the improved stability of IgG, the yield was further increased to 90 wt%, simultaneously decreasing the precipitation to 1.2 wt%. Prospectively, the optimization of ATPS using suitable excipients will support the integration of ATPE in downstream processing of biomolecules.

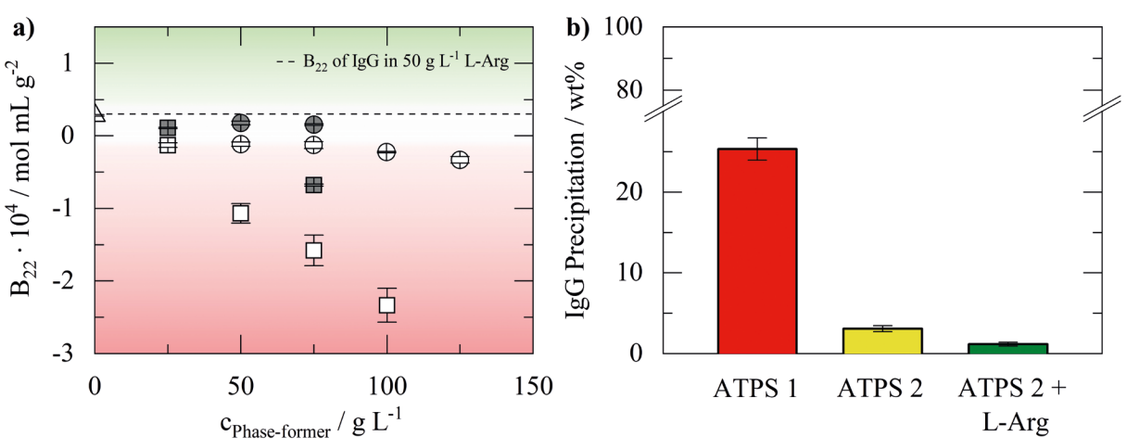

Figure 1: a) B_{22}-values of IgG in presence of: (1) L-Arg in 50 mM PBS (white triangle at 0 g L^{-1} and dashed line). (2) An increasing concentration of one phase former in 50 mM PBS (open symbols: squares = PEG2000, circles = NaGlu). (3) 50 g L^{-1} L-Arg and one phase-former in 50 mM PBS (filled, gray symbols). b) Precipitation of IgG (Feed = 0.02 wt%) after ATPE using different ATPS (ATPS 1: 16.5 wt% NaGlu, 16.5 wt% PEG2000 and 8 wt% NaCl; ATPS 2: 15 wt% NaGlu, 15 wt% PEG2000 and 8 wt% NaCl; ATPS 2 + L-Arg: 15 wt% NaGlu, 15 wt% PEG2000, 8 wt% NaCl and 5 wt% L-Arg). All measurements were performed at 298.15 K, 1 bar and pH 7. Error bars show the standard deviation resulting from a duplicate measurement.

Contact:
maximilian.wessner@tu-dortmund.de
christoph.brandenbusch@tu-dortmund.de

Publications:
[1] M. Wessner, M. Nowaczyk, C. Brandenbusch, J. Mol. Liq. 314, 113655 (2020).
[2] M. Schleinitz, L. Nolte, C. Brandenbusch, J. Mol. Liq. 298, 112011 (2020).

Viscosity of Amorphous Solid Dispersions at Humid Conditions

Friederike Wolbert[1, 2], Christian Luebbert[2], Gabriele Sadowski[2]
[1]INVITE GmbH, Drug Delivery Innovation Center (DDiC)
[2]TU Dortmund University, Laboratory of Thermodynamics

Amorphous solid dispersions (ASDs) are mixtures of active pharmaceutical ingredients (APIs) and polymers. They are e.g. used as medical tablets. If the concentration of the API exceeds its equilibrium solubility in the polymer, it tends to crystallize. This should be avoided during the shelf life of the ASD as it decreases the bioavailability of the API in the human body. One factor influencing the ASD shelf life is the molecular mobility of the API in the polymer. Since these molecular motions are physically related to viscosity, the molecular mobility can be evaluated based on viscosity. We proposed an approach to predict the viscosity of ASDs only based on the temperature dependence of the viscosity of the neat polymer as well as the predicted water content in the ASD at certain relative humidity (RH) using the Perturbed-Chain Statistical Associating Fluid Theory (PC-SAFT). This approach helps to remarkably reduce the experimental effort for identifying suitable polymers to be used in ASDs.

Rheological investigations of ASDs are often performed to design hot-melt-extrusion processes and thus only data at high temperatures (above the melting temperature) and high shear rates are available in literature. The focus of this work was to investigate the viscosity at storage-relevant temperatures (far below the HME-process window) and no-shear conditions (zero-shear viscosity, ZSV η_0). The ZSV of the pure polymers poly(vinyl acetate) (PVAc) and poly(vinyl pyrrolidone-co-vinyl acetate) (PVPVA) as well as of ASDs containing the API ibuprofen and either PVAc or PVPVA were measured at dry and humid conditions.

It was found that temperature, API content, as well as RH, have a significant influence on the ZSV. E.g., the addition of 20 % ibuprofen to PVAc led to a ZSV reduction by 97 %. The absorption of only 4.4 wt.% water at 75 % RH and 70 °C led to a ZSV reduction by even 99 %. Water has a much stronger plasticizing effect than ibuprofen, which can be explained by the much lower glass-transition temperature (Tg) of water (-135.15 °C) compared to the one of ibuprofen (- 42.30 °C).

The Williams-Landel-Ferry (WLF) equation was used to model the temperature dependence of the ZSV of the pure polymers. To account for the influence of ibuprofen and water on the ZSV the system temperature used in the WLF equation was replaced by an apparent temperature. This apparent temperature accounts for the fact that due to the presence of API and water, the Tg of the ASD is reduced compared to the Tg of the pure polymer. Thus, different systems are considered at the same distance to their own Tg. Using the apparent temperature, the influence of ibuprofen on the ZSV of ASDs composed of ibuprofen/PVAc and ibuprofen/PVPVA could be described very well with the same WLF parameters as for the pure polymer. Also, the plasticizing effect of absorbed water on the ZSV could be fully explained by the reduced Tg of the wet polymer or wet ASD compared to the one of the pure polymer (Figure 1).

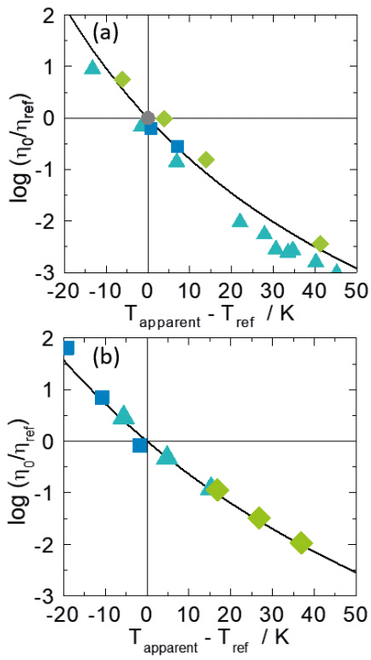

Figure 1: log(η_0/η_{ref}) as function of the temperature difference $T_{apparent}$ - T_{ref} for (a) PVAc at different RHs (squares) and ibuprofen/PVAc ASDs at 0 % RH (diamonds) and ibuprofen/PVAc ASDs at different RHs (triangles).The circle denotes the reference point (70 °C, 0 % RH, 0% API) and the solid line is the WLF modeling using c_1 = 8.86, c_2 = 101.60 K. (b) PVPVA at 60 % RH and different temperatures (squares) and ibuprofen/PVPVA ADS with 10.5 wt.% ibuprofen at 0 % RH at different temperatures (diamonds) and an ibuprofen/PVPVA ASD with 20 wt.% ibuprofen (triangles).The solid line is the WLF modeling using c_1 = 10.04, c_2 = 147.4 K and T_{ref} = 150 °C.

This means that ASDs stored at the same temperature distance from their Tg have the same viscosity regardless of whether the Tg distance is generated by temperature, API loading, RH increase, or a combination thereof. Thus, the ZSV of an ASD can be predicted without any additional viscosity measurements once the temperature dependence of the ZSV of the pure polymer and the Tg of the ASD is known. Together with the crystallization driving force in a metastable ASD, this approach allows estimating the API crystallization kinetics and thus the shelf life of ASDs.

Contact:
friederike.wolbert@tu-dortmund.de
christian.luebbert@tu-dortmund.de
gabriele.sadowski@tu-dortmund.de

Publications:
F. Wolbert, J. Stecker, C. Luebbert, G. Sadowski, Eur. J. Pharm. Biopharm. 154, 387-396 (2020).

Modeling the CO_2 Solubility in Electrolyte Solutions with ePC-SAFT

CO_2 solubility is predicted as function of pressure, temperature and salt concentration

Daniel Pabsch, Christoph Held, Gabriele Sadowski

Carbon dioxide (CO_2) solubility in aqueous electrolyte solutions is of special interest for carbon capture and storage or utilization, particularly as function of temperature, pressure, and electrolyte concentration. Unfortunately, experimental determination at such multivariable conditions is laborious. Therefore, the ion-based model ePC-SAFT was used to model the CO_2 solubility in such systems in a broad range of conditions. The CO_2 solubility was successfully modeled in water and in aqueous electrolyte solutions containing alkali and earth alkali chlorides and nitrates or mixtures thereof.

Knowledge on the CO_2 solubility in water and in various electrolyte solutions is important in many different applications in the chemical industry. Many data sets exist in the literature, some of them being very old or unreliable, or without knowledge of the experimental uncertainty. Still, thermodynamic models that have been applied do not cover all of the studied experimental conditions in terms of temperature, pressure, and type and concentration of electrolyte. Thus, in this work ePC-SAFT was applied to fill this research gap. First, the basic system CO_2 + water was characterized as shown in Figure 1. For temperatures up to 423 K and pressures up to 150 bar the pH was found to be in a range between 2.5 – 4.0 depending on the amount of dissolved CO_2. In these pH ranges, CO_2 dissociation reactions were found to be negligible. Thus, only the molecular species water and CO_2 were considered and dissociation species were neglected. Accounting for cross hydrogen bonds between water and CO_2 allowed modeling the system quantitatively correct.

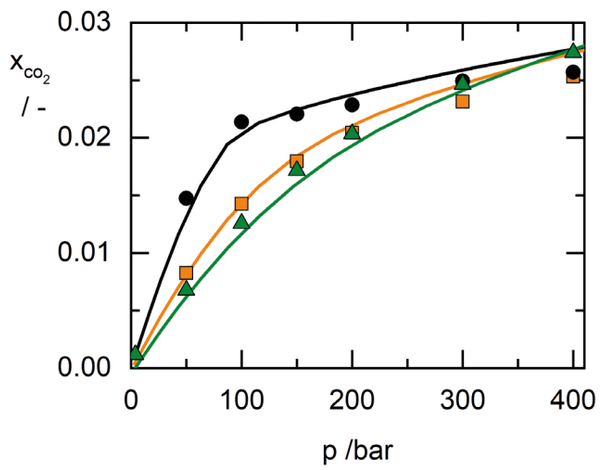

Figure 1: CO_2 mole fraction solubility as function of pressure at three different temperatures varying from 323 K to 413 K (circles T = 323 K, squares T = 373 K, triangles T = 413 K). Lines are ePC SAFT modeling results.

Further, the influence of different concentrations and types of electrolytes (i.e. the salts containing chloride and nitrate alkali and alkaline-earth metals) was investigated. The salting-out effect of NaCl for different concentrations varying from 1 to 5 mol salt per kg water is shown in Figure 2. Compared to the solubility in pure water, adding salt successively increases the salting-out effect, i.e. reduces the CO_2 solubility. This behavior was observed for all investigated systems. ePC-SAFT was found to be able to accurately model the CO_2 solubility in in aqueous systems containing electrolytes over a broad range of temperatures, pressures, and salt concentrations.

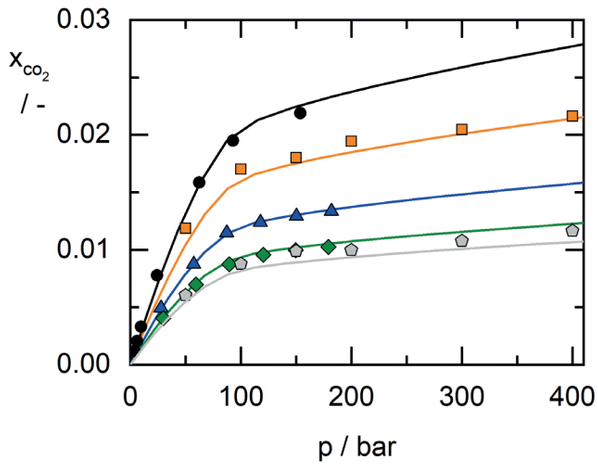

Figure 2: CO_2 mole fraction solubility as function of pressure at T = 323 K for different NaCl molalities (circles salt free), squares $\tilde{m}$ = 1 mol kg^{-1}, up-triangles $\tilde{m}$ = 2.5 mol kg^{-1} , diamonds $\tilde{m}$ = 4 mol kg^{-1} , and pentagons $\tilde{m}$ = 5 mol kg^{-1}. Lines are ePC SAFT modeling results.

To conclude, ePC-SAFT is now available to predict successfully the influence of pressure, temperature and kind and concentration of salt and salt mixtures on the CO_2 solubility.

Contact:
daniel.pabsch@tu-dortmund.de
christoph.held@tu-dortmund.de
gabriele.sadowski@tu.dortmund.de

Publications:
D. Pabsch, C. Held, G. Sadowski, J. Chem. Eng. Data 65, 5768–5777 (2020).

Melting Properties of Amino Acids as an Access to the Solubility Modeling

New values for melting properties allows consistently modeling of solubility in water

Hoang Tam Do, Yeong Zen Chua, Dzmitry Zaitsau, Christoph Schick, Christoph Held

Knowledge about the melting properties of biomolecules is extremely important for process design, as such data influence the solubility behavior in solvents, and such data are required for solubility modeling. However, melting properties for amino acids were not accessible before this work because the amino acids decompose upon slow heating. By means of 'fast scanning calorimetry', a method that applies very high heating rates, the melting properties of 20 proteinogenic amino acids were measured in this work. The new data were further used as an input data for thermodynamic modeling, which is used to predict amino-acid solubilities in water. This is the maximum equilibrium amount of amino acid in the liquid phase at defined temperature and pressure. The model prediction results were in very good agreement to the experimental solubility data. The successful modeling results were accompanied by new experimental solubility data, pH measurements of the liquid phase, and X-ray diffraction of the solid phase, which are important data to validate the model predictions.

The separation and purification of amino acids is usually realized through crystallization, for which the knowledge of solubility is essential. Due to cost-intensive and time-consuming determination of experimental solubility, the solubility modeling based on physical data such as melting properties is highly desired.

Modeling solubility requires a solid-liquid equilibrium between the amino acid in the saturated phase and in the solid phase. In this work, the temperature dependency of the melting enthalpy was taken into account by considering the difference in the heat capacities of the solid and liquid state Δc_{p0i}^{SL}. Assuming a pure compound in solid state the solubility x_i^L can be calculated with Eq. (1) with the assumption of a linear temperature dependency of Δc_{p0i}^{SL} in Eq. (2)

$$\ln\left(x_i^L \cdot \gamma_i^L\right) = \frac{\Delta h_{0i}^{SL}}{R \cdot T_{0i}^{SL}}\left(1 - \frac{T_{0i}^{SL}}{T}\right) - \frac{1}{R \cdot T}\int_{T_{0i}^{SL}}^{T} \Delta c_{p0i}^{SL}(T)\,dT + \frac{1}{R}\int_{T_{0i}^{SL}}^{T} \frac{\Delta c_{p0i}^{SL}(T)}{T}\,dT \quad (1)$$

$$\Delta c_{p0i}^{SL}(T) = \left(a_{c_{p0i}^L} - a_{c_{p0i}^S}\right) \cdot T + \left(b_{c_{p0i}^L} - b_{c_{p0i}^S}\right) \quad (2)$$

with γ_i^L as the activity coefficient of component *i*, *R* the universal gas constant, Δh_{0i}^{SL} the melting enthalpy, and T_{0i}^{SL} the melting temperature. The function $\Delta c_{p0i}^{SL}(T)$ was described by the parameters $a_{c_{p0i}^L}$, $a_{c_{p0i}^S}$, $b_{c_{p0i}^L}$, and $b_{c_{p0i}^S}$.

Access to γ_i^L was provided by PC-SAFT. All pure-component parameters were taken from the literature. Figure 1(a) shows that the solubility of glycine, L-alanine, L-valine and L-leucine can be modeled with high accuracy in a broad temperature range. It can be seen that the amino acid with highest melting temperature does not necessarily has the lowest solubility.

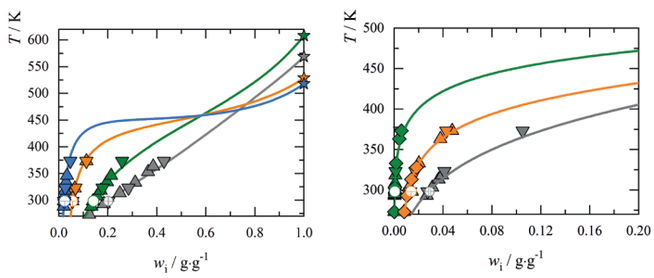

Figure 1: Temperature-dependent solubility of amino acids in water at p = 1 atm in weight fraction at pH = pI. Triangles represent literature data sets; empty circles represent the solubility measurements from this work; lines represent PC-SAFT modeling; stars represents the melting temperatures measured with the FSC. **LEFT:** Amino acids with non-polar substituents: glycine (grey), L-alanine (green), L-valine (orange), L-leucine (blue). **RIGHT:** Amino acids with aromatic substituents: L phenyl alanine (grey) L-tyrosine (green), L-tryptophan (orange).

Figure 1(b) shows that PC-SAFT allowed modeling also for very low-soluble amino acids (Phe, Tyr and Trp). The values for $\Delta c_{p0i}^{SL}(T)$ considerably contributed to the success of the modeling results. The influence of the activity coefficients is also pronounced on the result of Eq. (1), they were found to vary between three orders of magnitude for the conditions under study. Moreover, X-ray diffraction detected crystal changes in solubility experiments for several amino acids, which excluded application of Eq. (1).

To conclude, the melting properties of 20 proteinogenic amino acids determined by means of FSC were used to model solubility successfully. The modeling results and the data were in good agreement in a broad temperature range. The synergy between new FSC data, pH and X-ray diffraction measurements and PC SAFT allowed an accurate and reliable solubility modeling. This opens the door for the future for modeling solubility of any biomolecules that decompose before melting upon slow heating.

Publications:
H. T. Do et al., RSC Adv., 10, 44205–44215 (2020).

Contact:
hoangtam.do@tu-dortmund.de
christoph.held@tu-dortmund.de

Self-Induced Odd-Even Effect in Enzyme-Catalyzed Reactions

Finding explanations through thermodynamic modeling of molecular interactions

Mark Bülow, Christoph Held

Enzyme-catalyzed reactions often take place in water. In this work, ionic liquids (ILs) were added to water to shift the reaction equilibrium of enzyme-catalyzed reactions with the goal to increase the reaction yield of the product methylated 1-phenylethanol (Me-PE). Tetrahydrothiophene-based ILs (THT-ILs) were used with varying IL-cation chain length and constant IL-anion. An odd–even effect of the IL-cation chain length on the yield was discovered. Beneficially, the addition of small amounts of THT-ILs with odd numbered chain length allowed very high yields, while adding THT-ILs with even numbered chain length caused lower yields. Reasoning behind this odd-even effect was found in molecular interactions of the IL cation and the reaction product Me-PE and, further, critical micellar concentration measurements validated the observations.

Tetrahydrothiophene-based ionic liquids (THT-ILs) are introduced in this work as a new IL class based on cyclic sulfonium (Scheme 1). Common ILs drastically decrease the activity of enzymes even at small concentration in the reaction medium. Additionally, the utilized enzyme alcohol dehydrogenase (ADH) needs dry storage at 18 °C. Remarkably, pure THT-ILs were found to stabilize the enzyme for over one month at ambient condition in liquid phase; a large benefit boosting the activity about 500 times. THT-ILs were thus found suitable to additives in bio reactions.

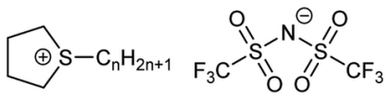

$[C_nTHT][NTf_2]$ (n = 4-8)

Scheme 1: Chemical structures of the tetrahydrothiophenium cation ($[C_nTHT]+$; 3 < n < 9) and bis(trifluoromethanesulfonyl)imide anion ($[NTf_2]-$).

The investigated ADH-catalyzed reaction is visualized in Scheme 2. 4-methylacetophenone (Me-ACP) reacts to methylated 1-phenylethanol (Me-PE) using the co factor nicotinamide adenine dinucleotide (NADH).

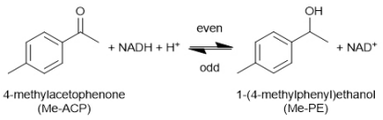

Scheme 2: Reaction scheme of the alcohol dehydrogenase reaction from Me-ACP to Me-PE with the mandatory co-factor NADH.

The influence of THT-ILs on the percent conversion of the ADH reaction was monitored using UV/Vis spectroscopy. The resulting difference in experimental equilibrium conversions at 298 K are depicted in Figure 1 with the baseline showing the conversion in the neat buffer (X = 87 %).

While even numbered THT-ILs already at very small concentrations of 10 mmol/L largely decrease the conversion (-7 %), the odd numbered THT-IL additives highly benefit the reaction (+9 %) to reach almost quantitative conversion. This odd even effect was never before reported for any (bio)reaction. One possible approach to find reasons for the odd even effect is thermodynamic modeling applying electrolyte models, which are required as the reacting agents are charged.

Contact:
mark.buelow@tu-dortmund.de
christoph.held@tu-dortmund.de

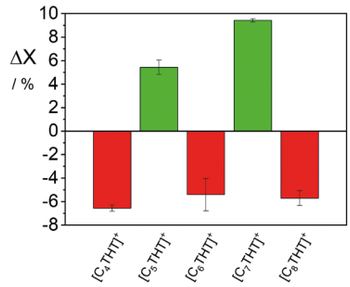

Figure 1: Difference in experimental conversion of the ADH reaction between buffer + 10 mmol/kg IL and neat buffer (base line) for THT-ILs at 298 K and 1 bar.

The thermodynamic model ePC-SAFT is suitable for this as it accounts for charges and hydrogen bonding. ePC-SAFT was used in this work to screen intermolecular forces that might explain the odd even effect. Therefore, the activity coefficients of reactants and products were modeled. Figure 2 shows the activity coefficients γ_i^{eq} for Me-ACP (blue bars) and Me-PE (orange bars). As expected, $\gamma_{Me\text{-}ACP}^{eq}$ monotonically rises with increasing IL cation chain length. In contrast, $\gamma_{Me\text{-}PE}^{eq}$ underlies an odd-even effect. That is, Me-PE beneficially interacts with the THT-IL with odd-number IL cation chain length, explaining the increased conversion from a theoretical point of view.

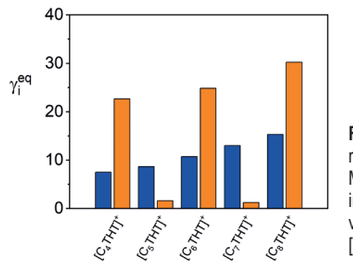

Figure 2: Activity coefficients γ_i^{eq} of the reactant Me-ACP (blue) and the product Me-PE (orange) in the reaction medium in presence of 10 mmol/L THT-IL with varied alkyl chain length n within the [CnTHT] cation.

The findings with ePC-SAFT were afterwards backed by measurements of the critical micellar concentration showing the same characteristic behavior favoring the odd numbered THT-ILs. That said, a high performance thermodynamic model like ePC-SAFT describing the reaction conditions is essential for deriving and screening of new co solvents and process variables.

Publications:
M. Bülow, A. Schmitz, T. Mahmoudi, D. Schmidt, F. Junglas, C. Janiak, C. Held, RSC Adv. 10, 28351-28354 (2020).

Predicting Protein-Protein Interactions using the ePC-SAFT Equation Of State

An efficient formulation design based on thermodynamic modeling

Miko Schleinitz, Lea Nolte, Christoph Brandenbusch

Thermodynamic models are increasingly recognized as essential part in pharmaceutical formulation development of "small-molecule" drugs. However, modeling of highly complex (bio-)pharmaceuticals (e.g., monoclonal antibodies) remains a challenging task. Within this work, we developed a modeling approach to access protein-protein and protein-excipient interactions for pharmaceutical proteins in the presence of different excipients using the ePC-SAFT equation of state. This approach gives access to protein phase behavior in these complex solutions and allows to gain a mechanistic understanding on the complex interactions involved enabling an optimized formulation development.

Thermodynamic models are rarely applied in the biopharmaceutical space, due to several challenges of protein formulations compared to small-molecule drugs as e.g., their size/complexity, complex interactions in solution, and the lack of experimental data for fitting pure-component parameters and binary interaction parameters. Heuristic approaches still mark the state-of-the-art for formulation design, including the selection of excipients stabilizing the protein in solution. The insight into molecular interactions gained through this approach is quite unclear. Being able to predict determinants such as B_{22}-(protein-protein interactions) and B_{23}-values (protein-excipient interactions), allows to characterize the nature of intermolecular interactions, and thus the behavior of the protein in solution in the presence of e.g., excipients.

Within this work, we developed an approach to fit ePC-SAFT pure-component parameters of IgG and binary interaction parameters of IgG with excipients to the amino acid sequence of the protein (pure component parameters) as well as static light scattering (SLS) data of varying protein-excipient combinations (binary interaction parameters). Using these parameters, modeling of B_{22}- and B_{23}-values and thus, protein-protein and protein-excipient interactions in the presence of excipients is possible.

Figure 1 shows the modeling results of SLS data (Figure 1A) as well as B_{22}-coefficients of IgG-sucrose systems (Figure 1B) in comparison to experimental data. Even though the absolute values are not matched by the predictions, the increasing trend of B_{22} can be confirmed. Aside B_{22}, the SLS data used to retrieve the cross-virial coefficient B_{23} can also be determined with high accuracy leading to a qualitative as well as quantitative determination of B_{23} between IgG and sucrose (data not shown).

This novel approach proves, that thermodynamic models such as the ePC-SAFT equation of state can be applied successfully to calculate and even predict the complex interactions in aqueous protein solutions. In addition, this method reduces the experimental effort in determining protein-protein and protein-excipient interactions and thus aids to identify optimal formulation conditions for specific proteins.

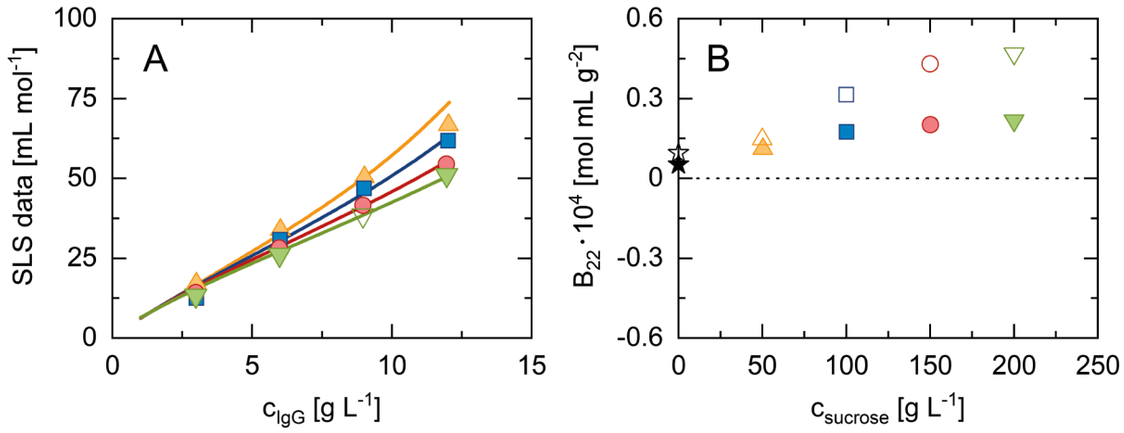

Figure 1: A *SLS data* at pH 7.0, 298.15 K in 50 mM K_2HPO_4-NaH_2PO_4 phosphate buffer and constant sucrose concentration (50 g L^{-1} [triangles], 100 g L^{-1} [squares], 150 g L^{-1} [circles], 200 g L^{-1} [reversed triangles]) as a function of immunoglobulin G concentration. Solid lines correspond to predicted *SLS data* using ePC-SAFT equation of state. B Comparison of experimental B_{22}-values of immunoglobulin G (filled symbols) with predicted B_{22}-values (empty symbols) at pH 7.0 and 298.15 K in 50 mM K_2HPO_4-NaH_2PO_4 phosphate buffer as a function of sucrose concentration.

Publications:
M. Schleinitz, L. Nolte, C. Brandenbusch, J. Mol. Liq. 298, 112011 (2020).

Contact:
lea.nolte@tu-dortmund.de
christoph.brandenbusch@tu-dortmund.de

Publications 2020 - 2018

2020

- T. Weinbender, M. Knierbein, L. Bittorf, C. Held, R. Siewert, S. P. Verevkin, S. Sadowski, O. Reiser
  High-pressure-mediated thiourea-organocatalyzed Michael addition to (hetero) aromatic nitroolefins: Prediction of reaction parameters by PCP-SAFT modelling
  ChemPlusChem, 85, 6, 1292-1296 (2020)

- T. Greinert, K. Vogel, J. K. Mühlenweg, G. Sadowski, T. Maskow, C. Held
  Standard Gibbs energy of metabolic reactions: VI. Glyceraldehyde 3-phosphate dehydrogenase reaction
  Fluid Phase Equilibria, 517,112597 (2020)

- T. Greinert, K. Vogel, A. I. Seifert, R. Siewert, I. V. Andreeva, S. P. Verevkin, T. Maskow, G. Sadowski, C. Held
  Standard Gibbs energy of metabolic reactions: V. Enolase reaction
  Biochimica et Biophysica Acta (BBA)-Proteins and Proteomics, 1868 (2020)

- T. Greinert, K. Baumhove, G. Sadowski, C. Held
  Standard Gibbs energy of metabolic reactions: IV. Triosephosphate isomerase reaction
  Biophysical Chemistry, 258, 106330 (2020)

- R. Schneider, J. Kerkhoff, A. Danzer, A. Mattusch, A. Ohmann, M. Thommes, G. Sadowski
  The interplay of dissolution, solution crystallization and solid-state transformation of amorphous indomethacin in aqueous solution
  International Journal of Pharmaceutics: X, 100063 (2020)

- S. Dohrn, P. Reimer, C. Lübbert, K. Lehmkemper, S. O. Kyeremateng, M. Degenhardt, S. Sadowski
  Thermodynamic modeling the solvent-impact on phase separation of amorphous solid dispersions during drying
  Molecular Pharmaceutics, In Press, 17, 7, 2721-2733 (2020)

- S. Dohrn, C. Lübbert, K. Lehmkemper, S. O. Kyeremateng, M. Degenhardt, G. Sadowski
  Phase behavior of pharmaceutically relevant polymer/solvent mixtures
  International Journal of Pharmaceutics, 577, 119065 (2020)

- S. Capecci, Y. Wang, V. Casson Moreno, C. Held, S. Leveneur
  Solvent effect on the kinetics of the hydrogenation of n-butyl levulinate to g-valerolactone
  Chemical Engineering Science, 116315 (2020)

- R. Schneider, L. Taspinar, Y. Ji, G. Sadowski
  The influence of polymeric excipients on desupersaturation profiles of active pharmaceutical ingredients. 1: Polyethylene glycol
  International Journal of Pharmaceutics, 582, 119317 (2020)

- N. Haarmann, A. Reinhardt, A. Danzer, G. Sadowski, S. Enders
  Modeling of Interfacial Tensions of Long-Chain Molecules and Related Mixtures using PC-SAFT and the Density Gradient Theory
  J. Chem. Eng. Data, 65, 1005-1018 (2020)

- M. Wessner, M. Nowaczyk, C. Brandenbusch
  Rapid identification of tailor-made aqueous two-phase systems for the extractive purification of high-value biomolecules
  Journal of Molecular Liquids, 314, 113655 (2020)

- M. Wessner, K. Diederich, C. Brandenbusch
  Influence of Sodium Chloride and Lithium Bromide on the Phase Behavior of a Citrate–Polyethylene Glycol 2000 Aqueous Two-Phase System
  Journal of Chemical & Engineering Data, In Press, 65, 8, 4009-4017 (2020)

- M. Schleinitz, L. Nolte, C. Brandenbusch
  Predicting protein-protein interactions using the ePC-SAFT equation-of-state
  Journal of Molecular Liquids, 298 (2020)

- M. Knierbein, M. Voges, C. Held
  5-Hydroxymethylfurfural Synthesis in Nonaqueous Two-Phase Systems (NTPS)–PC-SAFT Predictions and Validation
  Organic Process Research & Development, In Press, 24, 6, 1052-1062 (2020)

- M. Knierbein, C. Held, G. Sadowski
  The Role of Molecular Interactions on Michaelis Constants of α-Chymotrypsin Catalyzed Peptide Hydrolyses
  The Journal of Chemical Thermodynamics, 148, 106142 (2020)

- M. Bülow, A. Schmitz, T. Mahmoudi, D. Schmidt, F. Junglas, C. Janiak, C. Held
  Odd–even effect for efficient bioreactions of chiral alcohols and boosted stability of the enzyme
  RSC Advances, 10, 28351-28354 (2020)

- K. Wysoczanska, H. T. Do, G. Sadowski, E. A. Macedo, C. Held
  Partitioning of water-soluble vitamins in biodegradable aqueous two-phase systems: Electrolyte Perturbed-Chain Statistical Associating Fluid Theory predictions and experimental validation
  AIChE Journal, 66, e16984 (2020)

- K. Vogel, T. Greinert, M. Reichard, C. Held, H. Harms, T. Maskow
  Thermodynamics and Kinetics of Glycolytic Reactions. Part I: Kinetic Modeling Based on Irreversible Thermodynamics and Validation by Calorimetry
  International Journal of Molecular Sciences, 21, 8341 (2020)

- K. Vogel, T. Greinert, M. Reichard, C. Held, H. Harms, T. Maskow
  Thermodynamics and Kinetics of Glycolytic Reactions. Part II: Influence of Cytosolic Conditions on Thermodynamic State Variables and Kinetic Parameters
  International Journal of Molecular Sciences, 21, 7921 (2020)

- K. Vogel, T. Greinert, H. Harms, G. Sadowski, C. Held, T. Maskow
  Influence of cytosolic conditions on the reaction equilibrium and the reaction enthalpy of the enolase reaction accessed by calorimetry and van't Hoff
  Biochimica et Biophysica Acta (BBA) - General Subjects, 1864, 129675 (2020)

- K. Vogel, T. Greinert, C. Held, H. Harms, T. Maskow
  Application of Irreversible Thermodynamics to Determine the Influence of Cell Mimicking Conditions on the Kinetics of Equilibrium Reactions of the Glycolysis
  Biophysical Journal, 118, 346a-347a (2020)

Publications 2020 - 2018

- J. Sauer, H.-D. Kühl
  Theoretically and experimentally founded simulation of the appendix gap in regenerative machines
  Applied Thermal Engineering, 166, 114530 (2020)

- M. J. Lubben, R. I. Canales, Y. Lyu, C. Held, M. Gonzalez-Miquel, M. A. Stadtherr, J. F. Brennecke
  Promising Thiolanium Ionic Liquid for Extraction of Aromatics from Aliphatics: Experiments and Modeling
  Industrial & Engineering Chemistry Research, 59, 15707-15717 (2020)

- J. Brinkmann, L. Exner, C. Lübbert, G. Sadowski
  In-Silico Screening of Lipid-Based Drug Delivery Systems
  Pharmaceutical Research, 37, 249 (2020)

- J. Brinkmann, F. Rest, C. Lübbert, G. Sadowski
  Solubility of Pharmaceutical Ingredients in Natural Edible Oils
  Molecular Pharmaceutics, In Press, 17, 7, 2499–2507 (2020)

- D. H. Zaitsau, R. Siewert, A. A. Pimerzin, M. Bülow, C. Held, M. Loor, S. Schulz, S. P. Verevkin
  Paving the way to solubility through volatility: Thermodynamics of imidazolium-based ionic liquids of the type [CnC1Im][I]
  Fluid Phase Equilibria, 522, 112767 (2020)

- H. Veith, E. Turan, C. Lübbert, G. Sadowski
  Hydrate formation in polymer-based pharmaceutical formulations
  Fluid Phase Equilibria, 112677 (2020)

- H. Veith, C. Lübbert, G. Sadowski
  Correctly Measuring and Predicting Solubilities of Solvates, Hydrates, and Polymorphs
  Crystal Growth & Design, 20, 723-735 (2020)

- F. Wolbert, J. Stecker, C. Lübbert, G. Sadowski
  Viscosity of ASDs at humid conditions
  European Journal of Pharmaceutics and Biopharmaceutics, 154, 387-396 (2020)

- F. Fischer, H.-D. Kühl
  Analytical model for an overdriven free-displacer thermos compressor
  Applied Thermal Engineering, 116251 (2020)

- D. Pabsch, C. Held, G. Sadowski
  Modeling the CO2 Solubility in Aqueous Electrolyte Solutions Using ePC-SAFT
  Journal of Chemical & Engineering Data, 65, 12, 5768-5777 (2020)

- C. Held
  Thermodynamic gE Models and Equations of State for Electrolytes in a Water-Poor Medium: A Review
  Journal of Chemical & Engineering Data, 65, 5073-5082 (2020)

- A. Reinhardt, N. Haarmann, G. Sadowski, S. Enders
  Application of PC-SAFT and DGT for the Prediction of Self-Assembly
  Journal of Chemical & Engineering Data, 65, 5897-5908 (2020)

2019

- Y. Sun, A. Schemann, C. Held, X. Lu, G. Shen, X. Ji
  Modeling thermodynamic derivative properties and gas solubility of ionic liquids with ePC-SAFT
  Industrial & Engineering Chemistry Research 58, 8401-8417 (2019)

- A. Wangler, C. Held and G. Sadowski
  Thermodynamic Activity-Based Solvent Design for Bioreactions
  Trends in Biotechnology 37, 1038-1041 (2019)

- H. T. Do, Y. Z. Chua, J. Habicht, M. Klinksiek, M. Hallermann, D. Zaitsau, C. Schick, C. Held
  Melting properties of peptides and their solubility in water. Part 1: dipeptides based on glycine or alanine
  RSC Advances, 32722–32734 (2019)

- C. H. J. T. Dietz, J. T. Creemers, M. A. Meuleman, C. Held, G. Sadowski, M. van Sint Annaland, F. Gallucci, M. C. Kroon
  Determination of the Total Vapor Pressure of Hydrophobic Deep Eutectic Solvents: Experiments and Perturbed-Chain Statistical Associating Fluid Theory Modeling
  ACS Sustainable Chemistry & Engineering 7, 4047-4057 (2019)

- C. H. J. T. Dietz, F. Gallucci, M. van Sint Annaland, C. Held, M. C. Kroon
  110th Anniversary: Distribution Coefficients of Furfural and 5-Hydroxymethylfurfural in Hydrophobic Deep Eutectic Solvent + Water Systems: Experiments and Perturbed-Chain Statistical Associating Fluid Theory Predictions
  Industrial & Engineering Chemistry Research 58, 4240-4247 (2019)

- C. H. J. T. Dietz, A. Erve, M. C. Kroon, M. van Sint Annaland, F. Gallucci, C. Held
  Thermodynamic properties of hydrophobic deep eutectic solvents and solubility of water and HMF in them: Measurements and PC-SAFT modeling
  Fluid Phase Equilibria 489, 75-82 (2019)

- J. Sauer, H.-D. Kühl
  Experimental Investigation of Displacer Seal Geometry Effects in Stirling Cycle Machines
  Energies 12, (2019)

- S. Körner, J. Albert, C. Held
  Catalytic Low-Temperature Dehydration of Fructose to 5-Hydroxymethylfurfural Using Acidic Deep Eutectic Solvents and Polyoxometalate Catalysts
  Frontiers in Chemistry, 7: 166 (2019)

- E. N. Tsurko, R. Neueder, C. Held, W. Kunz
  Guanidinium Cation Effect on the Water Activity of Ternary (S) Aminopentanedioic Acid Sodium Salt Solutions at 298.15 and 310.15 K
  Journal of Chemical & Engineering Data 64, 1256-1264 (2019)

- N. Haarmann, R. Siewert, A. A. Samarov, S. P. Verevkin, C. Held, G. Sadowski
  Thermodynamic Properties of Systems Comprising Esters: Experimental Data and Modeling with PC-SAFT and SAFT-γ Mie
  Industrial & Engineering Chemistry Research 58, 6841-6849 (2019)

- M. Knierbein, A. Wangler, T. Q. Luong, R. Winter, C. Held, G. Sadowski
  Combined co-solvent and pressure effect on kinetics of a peptide hydrolysis: an activity-based approach
  Physical Chemistry Chemical Physics 21, 22224-22229 (2019)

Publications 2020 - 2018

- M. Bülow, X. Ji, C. Held
  Incorporating a concentration-dependent dielectric constant into ePC-SAFT. An application to binary mixtures containing ionic liquids
  Fluid Phase Equilibria 492, 26-33 (2019)

- M. Schleinitz, D.Teschner, G. Sadowski, C. Brandenbusch
  Second osmotic virial coefficients of therapeutic proteins in the presence of excipient-mixtures can be predicted to aid an efficient formulation design
  Journal of Molecular Liquids 283, 575-583 (2019)

- M. Knierbein, M. Venhuis, C. Held, G. Sadowski
  Thermodynamic properties of aqueous osmolyte solutions at high-pressure conditions
  Biophysical Chemistry 253, 106211 (2019)

- M. Knierbein, C. Held, C. Hölzl, D. Horinek, M. Paulus, G. Sadowski, C. Sternemann, J. Nase
  Density variations of TMAO solutions in the kilobar range: Experiments, PC-SAFT predictions, and molecular dynamics simulations
  Biophysical Chemistry 253, 106222 (2019)

- N. Haarmann, A. Sosa, J. Ortega, G. Sadowski
  Measurement and Prediction of Excess Properties of Binary Mixtures Methyl Decanoate + an Even-Numbered n-Alkane (C6−C16) at 298.15 K
  Journal of Chemical & Engineering Data 6, 2816-2825 (2019)

- L. Schmolke, S. Lerch, M. Bülow, M. Siebels, A. Schmitz, J. Thomas, G. Dehm, C. Held, T. Strassner, C. Janiak
  Aggregation control of Ru and Ir nanoparticles by tunable aryl alkyl imidazolium ionic liquids
  Nanoscale 11, 4073-4082 (2019)

- K. Wysoczanska, G. Sadowski, E. A. Macedo, C. Held
  Toward Thermodynamic Predictions of Aqueous Vitamin Solubility: An Activity Coefficient-Based Approach
  Industrial & Engineering Chemistry Research 58, 7362-7369 (2019)

- K. Wysoczanska, E. A. Macedo, G. Sadowski, C. Held
  Solubility Enhancement of Vitamins in Water in the Presence of Covitamins: Measurements and ePC-SAFT Predictions
  Industrial & Engineering Chemistry Research 58, 21761-21771 (2019)

- J. Baz, C. Held, J. Pleiss, N. Hansen
  Thermophysical properties of glyceline–water mixtures investigated by molecular modelling
  Physical Chemistry Chemical Physics 21, 6467-6476 (2019)

- H. Veith, M. Schleinitz, C. Schauerte, G. Sadowski
  Thermodynamic Approach for Co-crystal Screening
  Crystal Growth & Design 19, 3253-3264 (2019)

- F. Wolbert, C. Brandenbusch, G. Sadowski
  Selecting Excipients Forming Therapeutic Deep Eutectic Systems A Mechanistic Approach
  Molecular Pharmaceutics 16, 3091-3099 (2019)

- C. Held, T. Stolzke, M. Knierbein, M. W. Jaworek, L. T. Quan Luong, R. Winter, G. Sadowski
  Cosolvent and pressure effects on enzyme-catalysed hydrolysis reactions
  Biophysical Chemistry 252, 106209 (2019)

- A. Wangler, R. Loll, T. Greinert, G. Sadowski, C. Held
  Predicting the high concentration co-solvent influence on the reaction equilibria of the ADH-catalyzed reduction of acetophenone
  The Journal of Chemical Thermodynamics 128, 275-282 (2019)

- A. Wangler, A. Hüser, G. Sadowski, C. Held
  Imultaneous Prediction of Cosolvent Influence on Reaction Equilibrium and Michaelis Constants of Enzyme-Catalyzed Ketone Reductions
  ACS Omega 4, 6264-6272 (2019)

- C. Choscz, C. Held, C. Eder, G. Sadowski, H. Briesen
  Measurement and modeling of lactose solubility in aqueous electrolyte solutions
  Industrial & Engineering Chemistry Research 58 , 20797-20805 (2019)

- C. Hölzl, P. Kibies, S. Imoto, J. Noetzel, M. Knierbein, P. Salmen, M. Paulus, J. Nase, C. Held, G. Sadowski, D. Marx, S. M. Kast, D. Horinek
  Structure and thermodynamics of aqueous urea solutions from ambient to kilobar pressures: From thermodynamic modeling, experiments, and first principles simulations to an accurate force field description
  Biophysical chemistry 254, 106260 (2019)

- A. Samarov, I. Prikhodko, N. Shner, G. Sadowski, C. Held, A. Toikka
  Liquid–Liquid Equilibria for Separation of Alcohols from Esters Using Deep Eutectic Solvents Based on Choline Chloride: Experimental Study and Thermodynamic Modeling
  Journal of Chemical & Engineering Data 64, 6049-6059 (2019)

2018

- Y. Z. Chua, H. T. Do, C. Schick, D. Zaitsau, C. Held
  New experimental melting properties as access for predicting amino-acid solubility
  RSC Advances 8, 6365-6372 (2018)

- N. Haarmann, S. Enders, G. Sadowski
  Heterosegmental Modeling of Long-Chain Molecules and Related Mixtures using PC-SAFT: 1. Polar Compounds
  Industrial & Engineering Chemistry Research 58, 2551-2574 (2018)

- Y. Sun, G. Shen, C. Held, X. Feng, X. Lu, X. Ji
  Modeling Viscosity of Ionic Liquids with Electrolyte Perturbed-Chain Statistical Associating Fluid Theory and Free Volume Theory
  Industrial & Engineering Chemistry Research 57, 8784-8801 (2018)

- A. Wangler, M. J. Bunse, G. Sadowski, C. Held
  Thermodynamic Activity-Based Michaelis Constants
  IntechOpen, DOI: 10.5772/intechopen.80235 (2018)

- A. Wangler, D. Böttcher, A. Hüser, G. Sadowski, C. Held
  Prediction and Experimental Validation of Co-Solvent Influence on Michaelis Constants: A Thermodynamic Activity-Based Approach
  Chemistry – A European Journal 24, 16418-16425 (2018)

- M. A. R. Martins, E. A. Crespo, P. V. A. Pontes, L. P. Silva, M. Bülow, G. J. Maximo, E. A. C. Batista, C. Held, S. P. Pinho, J. A. P. Coutinho
  Tunable Hydrophobic Eutectic Solvents Based on Terpenes and Monocarboxylic Acids
  ACS Sustainable Chemistry & Engineering 6, 8836-8846 (2018)

Publications 2020 - 2018

- N. Haarmann, S. Enders, G. Sadowski
  Modeling binary mixtures of n-alkanes and water using PC-SAFT
  Fluid Phase Equilibria 470, 203-211 (2018)

- V. N. Emel'yanenko, E. Altuntepe, C. Held, A. A. Pimerzin, S. P. Verevkin
  Renewable platform chemicals: Thermochemical study of levulinic acid esters
  Thermochimica Acta 659, 213-221 (2018)

- M. Voges, M. Herhut, C. Held, C. Brandenbusch
  Light-scattering data of protein and polymer solutions: A new approach for model validation and parameter estimation
  Fluid Phase Equilibria 465, 65-72 (2018)

- M. Lemberg, R. Schomäcker, G. Sadowski
  Thermodynamic prediction of the solvent effect on a transesterification reaction
  Chemical Engineering Science 176, 264-269 (2018)

- M. Hübner, C. Lodziak, H. T. Do, C. Held
  Measuring and modeling thermodynamic properties of aqueous lysozyme and BSA solutions
  Fluid Phase Equilibria 472, 62-74 (2018)

- C. Luebbert, M. Wessner, G. Sadowski
  Mutual Impact of Phase Separation/Crystallization and Water Sorption in Amorphous Solid Dispersions
  Molecular Pharmaceutics 15, 669-678 (2018)

- C. Luebbert, G. Sadowski
  In-situ determination of crystallization kinetics in ASDs via water sorption experiments
  European Journal of Pharmaceutics and Biopharmaceutics 127, 183-193 (2018)

- C. Luebbert, D. Real, G. Sadowski
  Choosing Appropriate Solvents for ASD Preparation
  Molecular Pharmaceutics 15, 5397-5409 (2018)

- K. Lehmkemper, S. O. Kyeremateng, M. Degenhardt, G. Sadowski
  Influence of Low-Molecular-Weight Excipients on the Phase Behavior of PVPVA64 Amorphous Solid Dispersions
  Pharmaceutical Research 35, 25 (2018)

- K. Lehmkemper, S. O. Kyeremateng, M. Bartels, M. Degenhardt, G. Sadowski
  Physical stability of API/polymer-blend amorphous solid dispersions
  European Journal of Pharmaceutics and Biopharmaceutics 124, 147-157 (2018)

- K. Wysoczanska, H. T. Do, C. Held, G. Sadowski, E. A. Macedo
  Effect of different organic salts on amino acids partition behaviour in PEG-salt ATPS
  Fluid Phase Equilibria 456, 84-91 (2018)

- K. Klauke, D. H. Zaitsau, M. Bülow, L. He, M. Klopotowski, T.-O. Knedel, J. Barthel, C. Held, S. P. Verevkin, C. Janiak
  Thermodynamic properties of selenoether-functionalized ionic liquids and their use for the synthesis of zinc selenide nanoparticles
  Dalton Transactions 47, 5083-5097 (2018)

- J. Sauer, H.-D. Kühl
  Analysis of unsteady gas temperature measurements in the appendix gap of a stirling engine
  Journal of Propulsion and Power 34, 1039-1051 (2018)

- S. E. E. Warrag, C. Pototzki, N. R. Rodriguez, M. van Sint Annaland, M. Kroon, C. Held, G. Sadowski, C. J. Peters
  Oil desulfurization using deep eutectic solvents as sustainable and economical extractants via liquid-liquid extraction: Experimental and PC-SAFT predictions
  Fluid Phase Equilibria 467, 33-44 (2018)

- C. Luebbert, C. Klanke, G. Sadowski
  Investigating phase separation in amorphous solid dispersions via Raman mapping
  International Journal of Pharmaceutics 535, 245-252 (2018)

- C. Held, J. Brinkmann, A.-D. Schröder, M. I. Yagofarov, S. P. Verevkin
  Solubility predictions of acetanilide derivatives in water: Combining thermochemistry and thermodynamic modeling
  Fluid Phase Equilibria 455, 43-53 (2018)

- H. B. Rose, T. Greinert, C. Held, G. Sadowski, A. S. Bommarius
  Mutual Influence of Furfural and Furancarboxylic Acids on Their Solubility in Aqueous Solutions: Experiments and Perturbed-Chain Statistical Associating Fluid Theory (PC-SAFT) Predictions
  Journal of Chemical & Engineering Data 63, 1460-1470 (2018)

- A. Wangler, R. Canales, C. Held, T. Q. Luong, R. Winter, D. H. Zaitsau, S. P. Verevkin, G. Sadowski
  Co-solvent effects on reaction rate and reaction equilibrium of an enzymatic peptide hydrolysis
  Physical Chemistry Chemical Physics 20, 11317-11326 (2018)

- A. Wangler, G. Sieder, T. Ingram, M. Heilig, C. Held
  Prediction of CO2 and H2S solubility and enthalpy of absorption in reacting N-methyldiethanolamine /water systems with ePC-SAFT
  Fluid Phase Equilibria, 461, 15-27 (2018)

- H.-D. Kühl
  Auxiliary Heating, Cooloing and Power Generation in Vehicles Based on Sterling Engine Technology
  2. ETA-Tagung-Energie- und Thermomanagement, Klimatisierung, Abwärmenutzunung (2018)

- A. Wangler, C. Schmidt, G. Sadowski, C. Held
  Standard Gibbs Energy of Metabolic Reactions: III The 3-Phosphoglycerate Kinase Reaction
  ACS Omega 3, 1783-1790 (2018)

- E. A. Crespo, L. P. Silva, M. A. R. Martins, M. Bülow, O. Ferreira, G. Sadowski, C. Held, S. Pinho, J. A. P. Coutinho
  The Role of Polyfunctionality in the Formation of [Ch]Cl-Carboxylic Acid-Based Deep Eutectic Solvents
  Industrial & Engineering Chemistry Research 57, 11195-11209 (2018)

SCIENTIFIC HIGHLIGHTS 2020

Impressum

Fakultät Bio- und Chemieingenieurwesen
TU Dortmund
www.bci.tu-dortmund.de

Redaktion: Prof. Joerg C. Tiller
Publication date: July 2021